University of Stavanger

Faculty of Science and Technology

MASTER'S THESIS

Study program/ Specialization: Petroleum Engineering / Well Engineering	Spring semester, 2015 Open / ~~Restricted access~~
Writer: Bisan El-fseis	..... (Writer's signature)
Faculty supervisor: Rune W. Time, University of Stavanger External supervisor(s): Tron Bjelland Helgesen, Wintershall Norge	
Thesis title: A feasibility study for drilling & completing ERD wells on the Brage field	
Credits (ECTS): 30	
Key words: ERD Drilling Completion ECD Wellplan™	Pages: 101 + enclosure: 8 Stavanger, .../...../2015 Date/year

Front page for master thesis
Faculty of Science and Technology
Decision made by the Dean October 30th 2009

Master Thesis
PETMAS

A feasibility study for drilling & completing ERD wells on the Brage field

Bisan El-fseis

University of Stavanger

June 12, 2015

Abstract

In this master thesis, the potential for drilling an ERD well from the Brage platform have been studied. ERD wells can help operators reach isolated reservoirs located far away from the drilling facility. For mature fields like Brage, tapping into new remote reserves can help increase the lifetime of the field.

A preselected well path with a TD at 9,390 mMD and horizontal displacement of 8,060 m was chosen as the basis for this study. The purpose for this study was to investigate the possibilities to drill this long well path from the Brage platform. It was investigated if it would be possible to drill and complete the well with the standard drill pipe already in use on the Brage platform. Afterwards it was investigated if it would be possible to do the same operations using a new type of composite drill pipe. An additional study was conducted by Reelwell for drilling the final well section (9 ½" hole) of the same well, using their technology. This was done to verify if it would be possible to drill the specific well section with their drilling method. All the results were compared and discussed, and limitations were be identified. At the end of the study it was investigated if there is new technology available on the marked that can help removing or reducing the identified limitations for drilling and completing this well.

Wellplan™ was used to simulate the drilling operation and running of liner and lower completion. Simulations were performed for two well sections, and the results were investigated. Based on the simulation for the given well path, it was concluded that it would be difficult to reach TD with the conventional drilling method. The main challenge was related to the high value of ECD in relation to the formation fracture pressure when drilling the final section to TD.

Acknowledgements

This master thesis has been written as part of my master degree in Petroleum Engineering at the Institute of Petroleum Technology, at the University of Stavanger. I would like to take opportunity to acknowledge the people who have helped me with this thesis.

First, I would like to express my appreciation to Wintershall Norge for allowing me to write this thesis about one of their fields, and providing me with material and support during my work. I would especially like to express my gratitude to Tron Bjelland Helgesen, my supervisor at Wintershall Norge, for his help and support with this thesis. His feedback and enthusiasm has been most valuable during my work, and I learned a lot during our discussions.

I would also like to thank the rest of the engineers in the Brage Drilling & Well team at Wintershall Norge for taking the time to assist me with my work. I am grateful for the knowledge, information and material you have provided me with during my work. Your help has been most valuable.

Finally, I would like to thank my faculty supervisor at the University of Stavanger, Professor Rune W. Time.

Bisan El-fseis

Table of Contents

1. The Brage field

The Brage field is located in the Norwegian North Sea, approximately 120 km west of Bergen, in blocks 31/4, 31/7 and 30/6. The sea depth is approximately 140 m. The field was discovered in 1980 by Norsk Hydro while drilling the discovery well 31/4-3. Brage was developed with a fixed integrated production, drilling and accommodation facility on a fixed steel jacket. The platform also has facilities for water and gas injection as well as gas lift. First oil was produced September 1993 from five predrilled wells tied back to the platform. The field has been operated by Wintershall Norge since 2013, and in November 2014 production from the first Wintershall-drilled well began. Another two sidetracks are planned to be drilled during 2015. The platform was designed with a total of 40 production well slots. Today, after over 20 years of drilling activities, these slots have all been used. All new wells drilled on Brage are therefore sidetracks from preexisting wells. Produced oil from Brage is transported to Oseberg, and from there it goes through the Oseberg Transport System (OTS) to the Sture terminal (Norway). The produced gas is exported via the Statpipe pipeline system (NPD, n.d.).

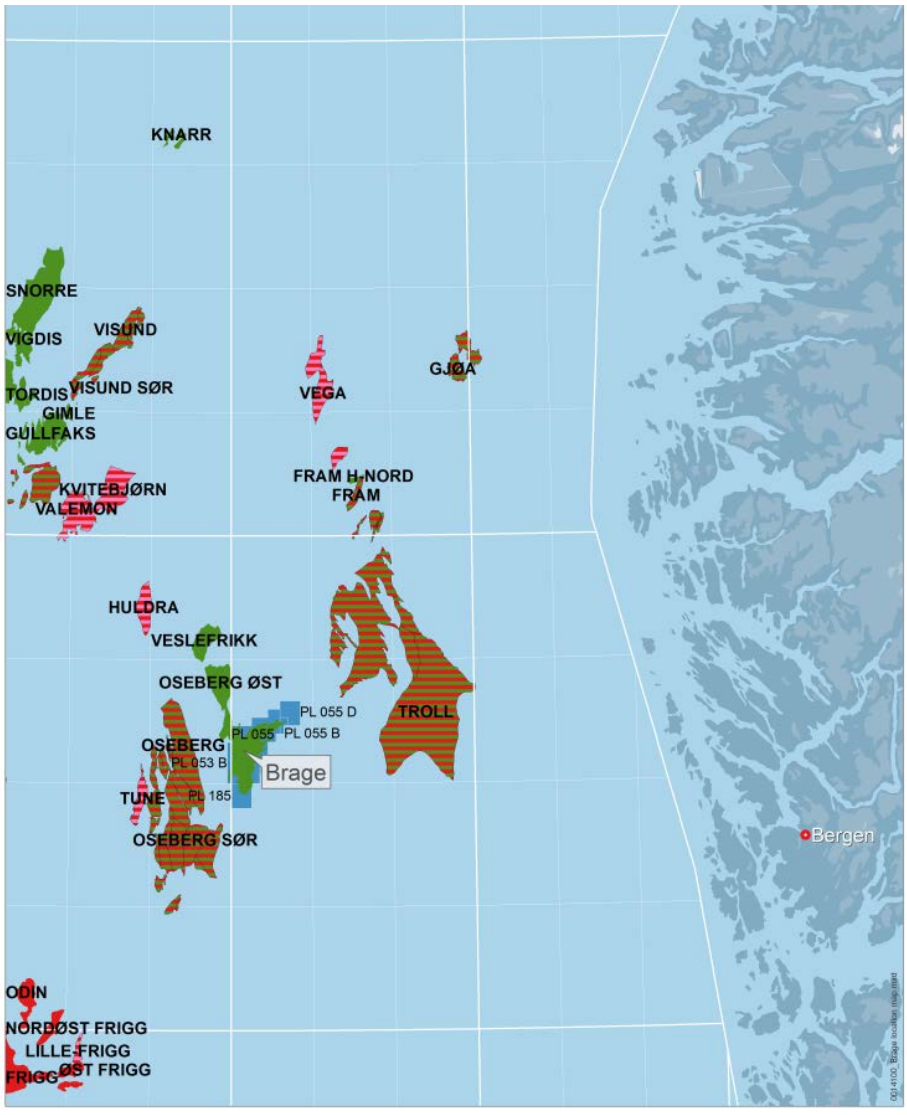

Figure 1.1: Brage field location in relation to the neighboring fields, courtesy of Wintershall Norge

The Brage area consists of four reservoirs with hydrocarbon-bearing sands, located at a depth varying from 2 000 – 2 300 m (Pajchel et al):

- Lower Jurassic Statfjord Formation: fluvial deposits
- Middle Jurassic Brent Group: deltaic to shore face deposits
- Middle to upper Jurassic Fensfjord Formation: shelf to shore face deposits. Stratified sandstone with calcite and highly permeable storm deposits.
- Upper Jurassic Draupne and Sognefjord Formation: shelf to shore face deposits

The Brage field has been in production since 1993 and is considered a mature offshore field. Production reached its peak in 1996, and since then the production has gradually declined due to reduction in reservoir volumes and reservoir pressure. To increase the lifetime of the field, and increase production, different injection strategies has been introduced. The main recovery strategy for the field is injecting water into the Statfjord and Fensfjord formations for pressure support. Water alternating gas (WAG) injection was also introduced to increase recovery (NPD, n.d.). Estimated reserves and oil in place volumes for the Brage field are listed in Table 1.1.

	Original recoverable	Remaining
Original recoverable oil [mill Sm^3]	60.70	4.30
Original recoverable gas [bill Sm^3]	4.30	0.90
Original recoverable NGL [mill ton]	1.40	0.10
Original recoverable oil equivalent [mill Sm^3 o.e]	67.66	5.39

Table 1.1 Reserves in the Brage field, updated 31.12.2014 (NPD, n.d.).

1.1 Brage north

The Brage North area is located in the northern part of the Brage field, as seen in figure 1. This area of the field was first discovered 1995, when Norsk Hydro drilled appraisal well 31/4-10. The purpose of this well was to verify the presence of hydrocarbons in the Sognefjord formation, and gather information about the reservoir properties. The well was drilled to 2325 mTVD and verified the presence of hydrocarbons in the encountered formations (NPD, n.d.).The Brage platform was put in place two years before the hydrocarbon discovery in well 31/4-10. Therefore, the platform's location was selected on the basis of the discovered reserves in the area surrounding the platform location. The hydrocarbons were verified in the northern part of the field, were therefore located outside the drilling range of the Brage platform. Individual development for this discovery was not feasible at the time, due to the small size of the reservoirs.

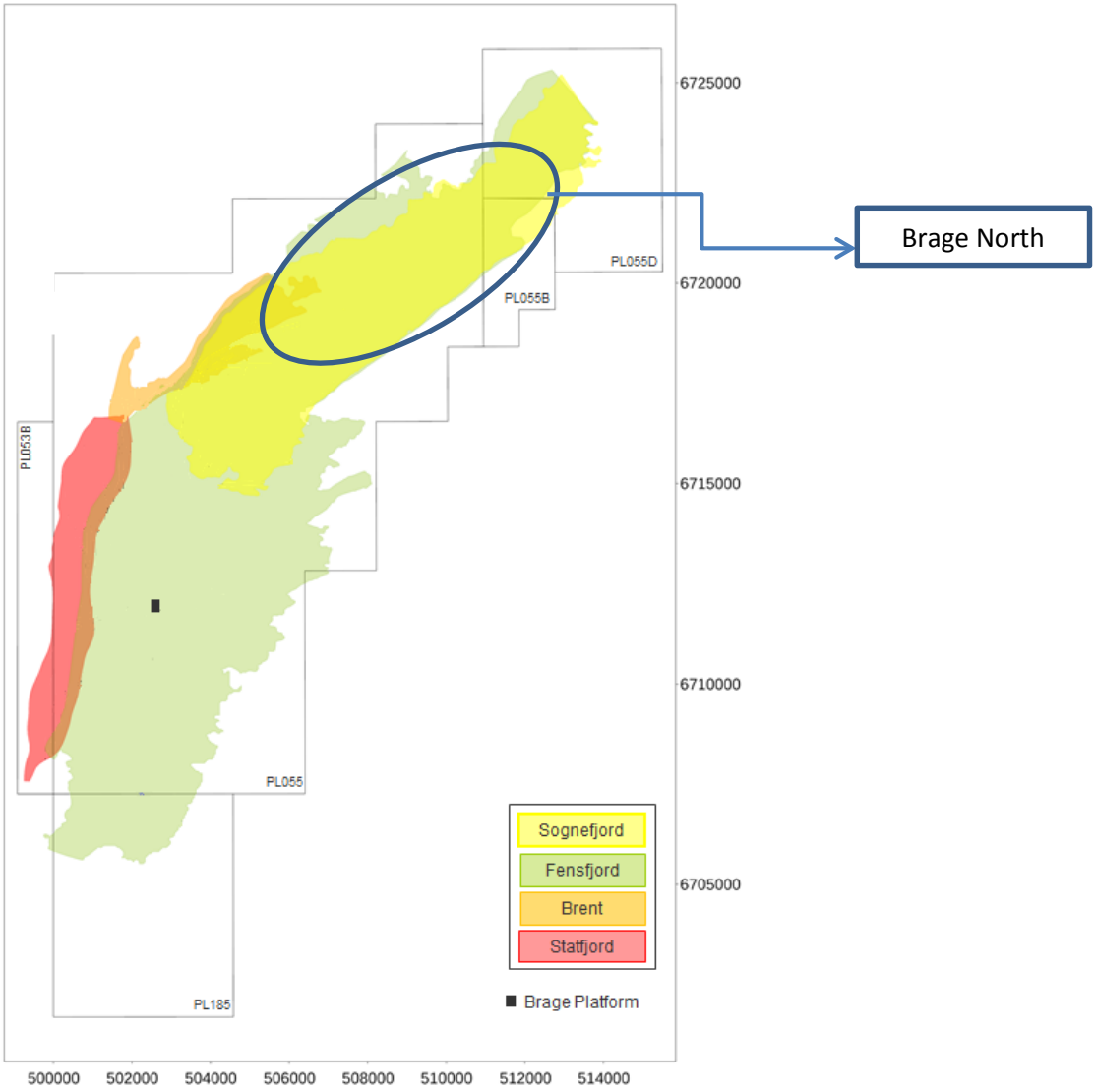

Figure 1.2: Brage reservoir map, courtesy of Wintershall Norge.

1.2 Geology & Reservoir

Further studies and new seismic surveys have been performed on the Brage North area to give a better understanding of the reservoir. Based on these studies the Brage North area has been divided into three hydrocarbon bearing segments, North, South and Bowmore. As shown in figure 1.2, the Brage North area consists of the Sognefjord and Fensfjord sandstone formations. The Sognefjord Reservoir is the uppermost of the Brage reservoirs, while the Fensfjord formation is below.

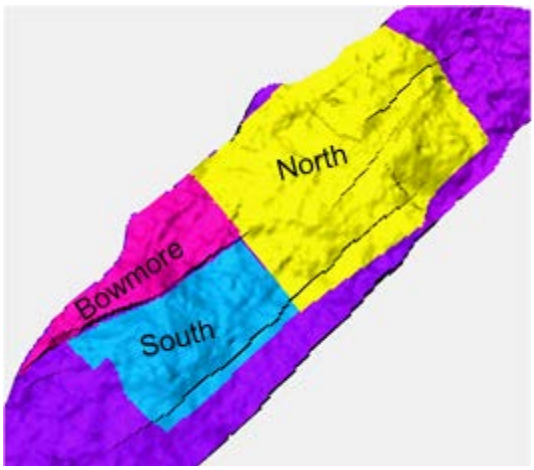

Figure 1.3: Geomodel of the three segments of the Brage North area, courtesy of Wintershall Norge.

1.3 Concept

Today there are technologies available that can make the development of Brage North a reality, and Wintershall Norge is considering developing the Brage North project. Wintershall Norge is looking into two development concepts for Brage North. The first considered concept is to develop the field using a subsea template, and tie back production to the Brage platform. A drilling rig (semi-submersible) will drill the needed wells through a template, and production will flow to the preexisting Brage platform for processing.

The alternative concept is to drill one or more extended reach wells from the Brage platform to the reservoir. The idea is then to use a pre-existing well, and drill a long horizontal well to reach the Brage North reservoirs. The economical potential for long reach wells is significant, as draining remote reservoirs is made possible from existing infrastructure. Both these concepts have their advantages and disadvantages, and the main drivers for which concept to select is cost and risk.

The concept of focus for this thesis is extended reach drilling (ERD) and completion from the Brage platform.

2. Drilling:

Wells drilled in the early 1980s with a horizontal displacement of 1 500 m from surface location was categorized as extended reach wells (Jerez et al. 2013). New technology and solutions have pushed the boundaries of drilling, allowing wells to reach much longer distances than before. In 2013 the operator at the Chayvo field managed to drill an ERD well with a horizontal reach of 11 739 m (Gupta et al. 2014). The characteristic difference between ERD wells and conventional directional wells makes drilling ERD wells more challenging. ERD wells are defined as wells with a horizontal displacement to true vertical depth ratio greater than two (Rubiandini, 2008). Long horizontal displacement and a high inclination angle will result in higher torque, drag and hook load force for an ERD well compared to a conventional well. These larger forces, in addition to rig specific limitations (e.g. pump limitations) makes drilling ERD wells more challenging than conventional wells (Rubiandini, 2008).

2.1 The ERD concept

Drilling from the Brage platform eliminates the extra cost related to a subsea field development, such as the template, subsea production system, pipeline(s), installation and topside modifications. On the other hand, when using the drilling equipment on the Brage platform to drill these long wells, other drilling operations has to be postponed. Delaying drilling operations that are supposed to increase production from the reservoirs closer to the platform is not an ideal option. Another important aspect to consider is if it's even possible to reach the Brage North reservoirs from the Brage platform. Does the platform have the capacity to drill and complete the necessary distance, and complete the well?

Extended reach wells are long wells drilled to reach reservoirs located at a distance that makes them unreachable from our infrastructure, with standard drilling technology. Before, these reservoirs could only be reached by placing a drilling infrastructure closer to them. Now we can use existing infrastructure located at a distance that previously was considered too far away, to reach these targets. Although these wells are more expensive and challenging to drill compared to standard wells, they make up for it by allowing us to reach reservoirs from already existing facilities. This will eliminate the cost associated with a subsea installation. The largest cost driver for an ERD well is the rig days. The rig is the largest expenditure for an offshore operation, and this expenditure will increase proportionally with number of days the operation will last. By increasing the length and complexity of a well, the number of operational days from start till finishing will also increase.

2.2 Drilling challenges

There are several challenges to consider during a drilling operation. As mentioned above, some of these challenges are greater for an ERD well, compared to a conventional well. Here are some challenges to consider:

2.2.1 Torque & Drag

When the drill string comes in contact with the borehole wall (formation or casing) during drilling, we experience torque and drag. Drag is the result of the friction caused by the movement of the pipe along the well bore, and torque is experienced while rotating the drill string. These loads limit the maximum length a well can be drilled, and excessive drag and torque can create problems for both drilling and completion operations (Wu and Wold, 1991).

The value of theses forces increase with the pipe/string weight, length, deviation angle, friction and reduction in buoyancy. Calculating torque and drag can be done using the 3-dimentional friction model. The following theory is taken from material from Modern Well Design (2010) by Bernt S. Aadnøy.

Drag for straight inclined wellbore without pipe rotation:

$$F_2 = F_1 + \beta \Delta L w(\cos\alpha \pm \mu sin\alpha) \quad (2.1)$$

±: + is used when hoisting while – is used when lowering the pipe.

Where F_2 and F_1 represents string forces, β is the buoyancy factor, ΔL is the pipe section length, w is the unit pipe weight, α is the wellbore inclination and μ is the friction coefficient.

Drag for curved wellbore sections without pipe rotation:

$$F_2 = F_1 e^{\pm\mu|\theta_2-\theta_1|} + \beta w \Delta L(\frac{sin\alpha_2 - sin\alpha_1}{\alpha_2-\alpha_1}) \quad (2.2)$$

±: + is used when hoisting while – is used when lowering the pipe.

θ is the absolute change in direction.

Torque for straight inclined wellbore without axial pipe motion:

$$T = \mu r \beta w \Delta L sin\alpha \quad (2.3)$$

Where T represents torque in string and r is the pipe/connection radius.

Torque for curved wellbore without axial pipe motion

$$T = \mu r N = \mu r F_1 |\theta_2 - \theta_1| \quad (2.4)$$

Where N represents the normal force.

Using these formulas, the friction for any wellbore shape can be computed, simply by dividing the well into section (curved and straight). Drag is calculated using equation 2.1 and 2.2, while torque is calculated using equation 2.3 and 2.4. Summing up these values gives the total torque and drag for the well.

Combined axial motion and rotation

A combined motion, axial motion and rotation, requires the consideration of the relation between axial velocity and tangential velocity. An increase in rotational speed will reduce axial drag. Therefore the angle between the axial and tangential velocity needs to be found:

$$\psi = tan^{-1}\left(\frac{V_h}{V_r}\right) = tan^{-1}(\frac{60 V_h(m/s)}{2\pi N_r(rpm) r(m)}) \quad (2.5)$$

Where ψ represents the angle between axial and tangential pipe velocities, V_h is the axial velocity, V_r is the tangential pipe speed, and N_r is the rotary pipe speed.

After the angle ψ is determined, the combined torque and drag can be calculated:
For straight sections:

$$F_2 = F_1 + \beta w \Delta L \cos\alpha \pm \mu\beta \Delta L sin\alpha \, sin\psi \quad (2.6)$$

$$T = r\mu\beta w \Delta L sin\alpha \, cos\psi \quad (2.7)$$

For curved pipe sections:

$$F_2 = F_1 + F_1(e^{\pm\mu|\theta_2-\theta_1|} - 1)sin\psi + \beta w \Delta L(\frac{sin\alpha_2 - sin\alpha_1}{\alpha_2 - \alpha_1}) \quad (2.8)$$

$$T = \mu r N = \mu r F_1 |\theta_2 - \theta_1| cos\psi \quad (2.9)$$

2.2.2 Hole cleaning & cuttings transport

Hole cleaning is of major concern during drilling, and is challenging for long deviated wells. It is important to transport the drilled cuttings out of the well. If the cuttings are not removed properly, they can lead to significant problems. According to experiences by Cameron (2001) deviated holes with angles from 40 to 65 degrees are most challenging to clean. Accumulation of cuttings in these deviated well sections tends to form beds that slide backwards in the hole, and can result in pack off. Cuttings in annulus may cause mechanical pipe sticking and can cause an increase in bottom hole pressure. This increase in bottom hole pressure may eventually lead to loss to the formation. Other problems caused by improper hole cleaning are excessive frictional torque and drag and casing landing difficulties (Nazari et al. 2010). Lou et al. (1994) points to a number of variables that affect hole cleaning in deviated wells (over 30°) and categorizes them as *controllable variables* and *uncontrollable variables*.

Controllable variables	*Uncontrollable variables*
• Mud flow rate • Rate of penetration (ROP) • Mud rheology • Mud flow regime • Mud weight • Hole angle • Hole size	• Drill pipe eccentricity • Cuttings density • Cuttings size

Table 2.1: Controllable and uncontrollable variables for hole cleaning.

Both Nazari et al. (2010) and Cameron (2001) describes flow rate as a key parameters for hole cleaning. Optimal hole cleaning can be achieved by using the maximum flow rate within the specific equivalent circulating density (ECD) limit. Increasing the flow rate will increase frictional pressure loss, which will increase the ECD. Exceeding the ECD limit can lead to fracturing of the formation and loss to formation. In addition to flow rate Nazari et al. (2010) lists pipe rotation as a key parameter for hole cleaning. Increasing pipe rotation can have a positive effect on hole cleaning. However, it will also increase the induced cyclic stresses on the pipe, which can lead to premature pipe fatigue failure.

2.2.3 ECD limitations

ECD is the effective density of the drilling fluid, combining both the actual mud density and the annular pressure drop. Long reach wells are characterized by their high ratio of horizontal displacement to TVD. The change in formation strength is relative to the TVD, while the annular pressure drop for horizontal and high deviated sections is related to the distance between the heel and toe. The increase in annular pressure drop is therefore not matched by the increase in formation strength. This limits the length a section can be drilled horizontally, especially in formations with a narrow fracture and pore pressure window. ECD limitations can also limit the pump rate, making it more difficult to achieve the necessary rates to ensure sufficient cuttings transport. ECD management is therefore of upmost importance when designing long reach horizontal wells. Minimizing ECD can be achieved by establishing a balance between minimum plastic viscosity and the requirements for transporting and suspending cuttings. As well as balancing the required flowrate, to minimize solid deposition (forming beds in annulus) without it leading to unnecessary ECD (Cameron, 2001).

2.2.4 Narrow drilling window

A safe drilling window is the window between pore and fracture pressure. During drilling it is important to keep the down hole pressure within this window. A section is drilled until down hole pressure reaches the boundaries of the safe window. To continue drilling, the previous section needs to be cased off. After installing the casing, the following section is drilled with a new mud density and a smaller diameter. This process continues until the well is drilled to TD. The narrower safe window there is, the more difficult it is to stay within it. This will therefore limit the length of the drilled section, and lead to installing the casing at a shallower depth. This can result in an increase in the number of sections before reaching TD. Increasing the number of sections, will reduce the final diameter at TD, and limit the maximum tubing diameter. Also, for conventional drilling with a narrow operating window, the rapid change in pressure during connections may cause the pressure curve to move outside the safe operating window.

2.2.5 WOB limitations

When drilling a vertical well, one of the forces helping the bit move downwards, is the gravitational force. The weight of the string is pulled in a downwards direction due to the gravity force. For horizontal sections, the same gravitational force will still pull the bit and string against the low side of the hole, while the intended path is horizontal. To be able to drill in the intended direction, the applied force along the string need to be large enough to overcome the gravitational pull. Using drill collars in the vertical section of the well, instead of drill pipe, is one way to increase the weight on bit (WOB). Gravity will act on the drill collars to provide the required downward force. For long horizontal wells with a shallow kick off point, the limited length of the vertical section is a challenge. Reducing the vertical section will reduce the number of drill collars providing downward force in the vertical section, limiting the WOB. A limited force to push the bit will subsequently limit the drillable distance.

2.2.6 Wellbore positioning

Inaccuracy in wellbore position can be caused by several sources of error, resulting in an uncertainty regarding the actual well trajectory. This uncertainty can be described as an ellipsoid around the wellbore. The actual borehole position is located somewhere in the ellipsoid, with a given certainty. The area of the ellipsoid, which is the same as the area of

uncertainty, increases as the length of the well increases. This is related to the data uncertainty related to the well positioning data (MD, inclination and azimuth). An ERD well will therefore have a bigger uncertainty related to its position. For a multiwell platform (like Brage), the limit of error is smaller due to the large number of adjacent wells (Inglis, 1987).

2.2.7 Hole diameter – ECD vs. Buckling

The selection of the correct hole size is important. By minimizing the gap between the drill string and wellbore (Δd), the chance of buckling the string is reduced. The backside of a small Δd is the negative effect on the ECD. Reducing Δd will result in an increase in annular friction pressure drop, and increase ECD. It is therefore important to find a compromise in hole diameter that takes into consideration both these issues. Equation 2.10 is for single phase flow, and shows how changing the value of the denominator will affect the final ΔP_f value.

$$\Delta P_f = \frac{4f\rho V^2 L}{D_o - D_i} = \frac{4f\rho V^2 L}{\Delta d} \tag{2.10}$$

Where ΔP_f is the frictional pressure drop, f is Fanning friction factor, ρ is the mud density, V is the flow velocity, L is the section length and Δd is the gap between inner and outer diameter. For a multiphase flow, the equation is a bit different, but Δd is still the denominator, and will have same effect on the friction pressure drop.

3. Completion:

New solutions and technology in the field of drilling allows us to drill longer horizontal wells, compared to just a few years ago. At the same time, the advance in completion technology has not evolved at the same pace. The completion phase for an open hole completion starts after the final section of the well has been drilled and evaluated. For a cased hole completion, completion starts after the final section is drilled, evaluated, cased and cemented. According to (Bellarby, 2009) "Completions are the interface between the reservoir and surface production", and the objective of the completion is to transform our drilled well into a safe and efficient producer or injector. The main goal for the completion is to recover as much of the original oil in place (OOIP) as possible, at a reasonable cost, in a safe and controlled manner (SLB 2011/2012). As we drill longer wells and in more challenging environments, our well design are getting more complex. New challenges emerges and completions, by necessity, become more complex (Bellarby, 2009).

3.1 General

Wells are drilled and completed for production or injection purposes, and the completion design is decided by the purpose of the well. Produced fluids from a production well are usually oil, gas and water. For an injection well the completions can be designed for injecting gas, water, steam and waste products. A well can also be used for more than one of these purposes. Example of a simultaneously multipurpose well is a well producing hydrocarbons from the tubing, while injecting gas down the annulus. Another example is to transform one well from its original purpose to have a new purpose, like transforming a hydrocarbon producer into a water injector (Bellarby, 2009).

Completion can be divided into two parts; upper and lower completion. Upper completion is related to well control, housing tools like the downhole safety valve (DHSV). The lower completion is related to the part of the well located in the production zone, and its main goal is to maximize production (for a production well). In this thesis the main focus will be on the lower completion design.

For the lower completion there are many design concepts available, and they can be classified into two categories; (1) cased hole completions and (2) open hole completions. Under each of these two categories there are different completions concepts, as listed in figure 3.1. According to Bellarby (2009) the major decisions related to the selection of lower completion solution are:

- Well trajectory and inclination
- Open hole or cased hole
- Need of sand control, and if so, what kind?
- Proppant or acid for stimulation
- Commingled or selective production

The selection of the specific completion design is driven by cost. The goal is to select a completion design that will maximize the production potential, and at the same time keep the cost as low as possible to maximize profit.

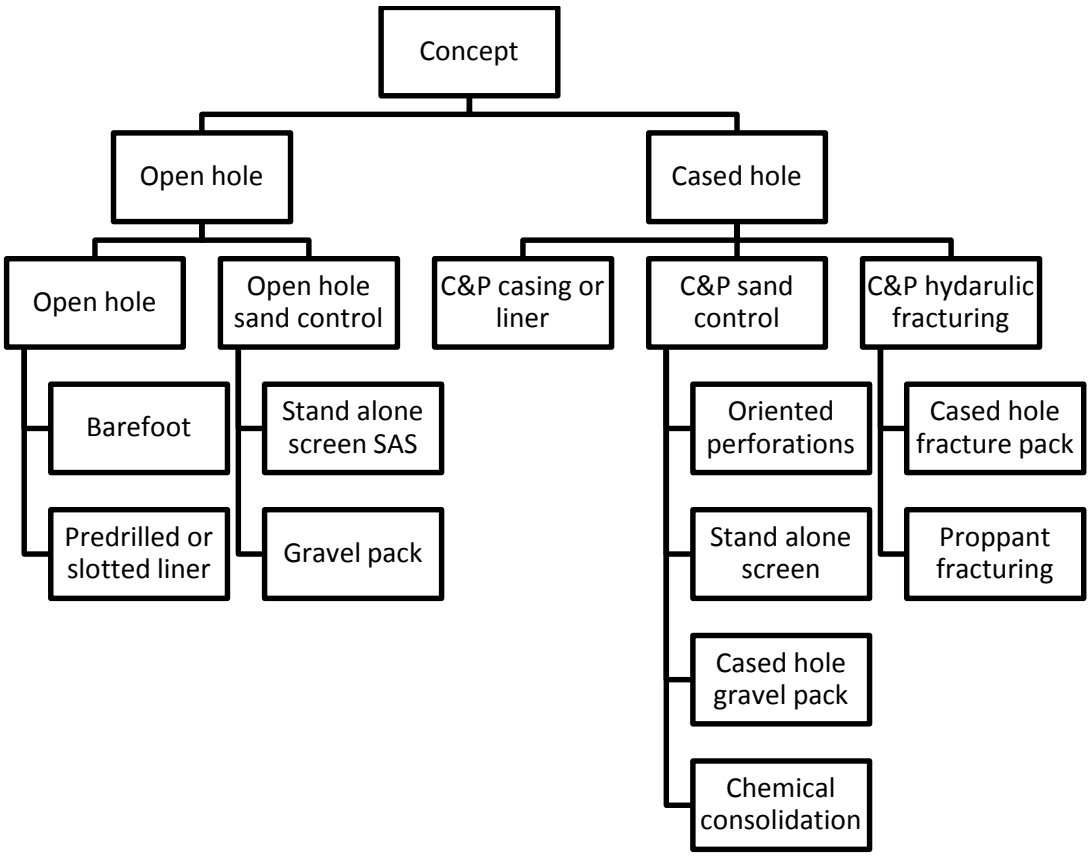

Figure 3.1: Various types of concepts for lower completion design.

3.2 Horizontal wells and challenges

3.2.1 Pressured drop

Pressure drop from the toe to the heel of the horizontal section is of great concern for long sections. The pressure drop is affected by numerous factors, and the distance from toe to heel is one of them. The following theory is based on Multiphase Flow Compendium (2009) by Rune W. Time

On a general basis, the pressure gradient dP/dx in a pipe depends on the following factors; *Pipe diameter, fluid viscosity, fluid density, flow velocity, pipe roughness, inclination and flow regime.* The total pressure gradient can be presented as a composition of three gradients:

$$(a)\left(\frac{dp}{dx}\right)_f, (b)\left(\frac{dp}{dx}\right)_h, (c)\left(\frac{dp}{dx}\right)_a \tag{3.1}$$

(a)Frictional pressure gradient, (b) hydrostatic pressure gradient, (c) acceleration pressure gradient.

The type of flow regime is determined by the Reynolds number, *Re*.

$$Re = \frac{\rho U D}{\mu} \tag{3.2}$$

Where ρ represents the fluid density, U is the flow velocity, D is the pipe diameter and μ is the viscosity of the fluid.

The flow regime can be determined by using the Reynolds number and table 3.1.

Re ≤ 2000:	Laminar flow
2000 < Re ≤ 4000:	Transition flow
4000 < Re	Turbulent flow

Table 3.1: Flow regimes in relation to Reynolds number.

For ***single phase flow***, the frictional pressure drop gradient can be given by

$$\left(\frac{dp}{dx}\right)_f = \frac{4}{D} * f * \frac{1}{2}\rho U^2 \quad (3.3)$$

f represents the friction factor. The friction factor for laminar flow is $f = \frac{16}{Re}$ (Fanning), while $f = C*Re^{-n}$ for turbulent flow (Power law). For the power law the values for *C* and *n* are given in table 3.2.

Type	*C*	*n*
Blasius	0.079	0.25
Dukler	0.046	0.2

Table 3.2: Values for turbulent friction factor (Blasius and Dukler).

The *frictional pressure drop gradient* is as a function of the wall shear stress:

$$\left(\frac{\mathrm{dp}}{\mathrm{dx}}\right)_\mathrm{f} = \frac{4}{\mathrm{D}} * \tau_\mathrm{W}$$

$$\tau_\mathrm{W} = \mathrm{f}\frac{1}{2}\rho\mathrm{U}^2$$

$$\left(\frac{\mathrm{dp}}{\mathrm{dx}}\right)_\mathrm{f} = \frac{4}{\mathrm{D}} * \mathrm{f}\frac{1}{2}\rho\mathrm{U}^2 \quad (3.4)$$

The *hydrostatic pressure gradient* is the pressure of fluid as a function of depth. With inclination β relative to the perpendicular direction, the hydrostatic pressure gradient can be presented as:

$$\left(\frac{\mathrm{dp}}{\mathrm{dx}}\right)_\mathrm{h} = \rho g \cos\beta \quad (3.5)$$

Where g is the gravitational acceleration and β is the inclination in degrees.

Acceleration pressure gradient is related to the pressure variations in a stationary single phase flow, if the flow velocity is altered due to pipe expansion or contraction of the pipe.

$$\left(\frac{\mathrm{dp}}{\mathrm{dx}}\right)_\mathrm{a} = -\rho\mathrm{U} * \frac{\mathrm{dU}}{dx} \quad (3.6)$$

Calculating the pressure gradients for a **two-phase flow** is more complex. To simplify the process, some assumptions can be made. The new fluid mixture from the two fluids can be assumed to be homogeneous. Density calculated by multiplying the percentages of each fluid with the specific fluid density, and adding them up. Same procedure is done to calculate the

viscosity. This method for calculating the pressure drop is called *the homogenous two phase pressure drop model*. The *frictional pressure drop* gradient is shown below:

$$\left(\frac{\mathrm{dp}}{\mathrm{dx}}\right)_{\mathrm{f}} = \frac{4}{D} * f * \frac{1}{2}\rho_m {U_m}^2 \tag{3.7}$$

Where $f = C\,(Re_m)^{-n}$, and the letter *m* is short for *mixture*. This model is realistic in turbulent well flow, and uses Dukler's values for turbulent flow.

The *hydrostatic pressure gradient* is similar for the one for single phase flow. The only alteration is that ρ_m has been inserted instead of ρ.

$$\left(\frac{\mathrm{dp}}{\mathrm{dx}}\right)_{\mathrm{h}} = \rho_m \mathrm{g}\cos\beta \tag{3.8}$$

Note that if the well is horizontal (β=90°) this equation can be neglected, since cos90° is equal to zero.

The *acceleration pressure gradient* is similar for the one for single phase flow. The only alteration is that ρ_m and U_m has been inserted instead of ρ and U.

$$\left(\frac{\mathrm{dp}}{\mathrm{dx}}\right)_{\mathrm{a}} = -\rho_m U_m * \frac{\mathrm{d}U_m}{dx} \tag{3.9}$$

The total pressure gradient can than be calculated with the following equation:

$$\frac{dp}{dx} = \left(\frac{dp}{dx}\right)_f + \left(\frac{dp}{dx}\right)_h + \left(\frac{dp}{dx}\right)_a \tag{3.10}$$

In long horizontal wells the pressure drop from the toe to the heel is significant. This change is pressure have a direct impact on the gas density, hence changing the gas velocity during transportation in the horizontal section. Furthermore, during hydrocarbon production separation of gas from oil will increase the gas flow velocity. Increase in gas flow velocity indicates a higher pressure drop, resulting in a larger amount of gas evaporation from the oil. This shows how increasing the distance from the toe to the heel affects the total flow velocity. Other factors that must be considered, especially for a hydrocarbon producer, are the temperature profile along the well and heat conductivity from the surroundings. Using the total pressure gradient from the previous section, total pressure drop over length L can be calculated using: $\Delta P = \int_0^L \frac{dp}{dx}(x, U_{LS}, U_{GS}, \alpha)dx$ where α characterizes all non-flow rate related parameters while U_{LS} and U_{GS} represent superficial velocities for liquid and gas. Superficial velocity is the flow *q* divided by the cross sectional area *A*.

3.2.2 Zonal isolation

Accomplishing zonal isolation in a well is important when producing from a multi zone reservoir. For long horizontal wells there might be zones containing water or gas, in addition to the oil bearing zones. Isolating the unwanted zones in a well is required for several reasons, like preventing cross-flow between zones and reduce gas (or water) migration into the produced oil. For open hole completions, zonal isolation is usually achieved using swell packers. For cased hole completions cement can be used to isolate specific zones.

Nevertheless, these methods have their limitations, especially in long horizontal sections. For instance, swell packers are not suitable for HTHP environments. High temperature and pressure will reduce the packer's integrity, limiting the sealing capability. Change in differential pressure across the packers during the wells lifetime can also reduce the packer integrity. For zonal isolation with cement, the ECD requirement can limit the cement interval. The ECD during cementation must be within the operational window (between fracture/pore curve), to avoid an unsuccessful cement job (Bardsen et al. 2014).

3.2.3 Sand control

Sand production is a concern when producing hydrocarbons from sandstone reservoirs. Between 25-30% of all wells drilled in sandstone reservoirs experience some sort of sand production throughout their lifespan (Walton et al., 2001). Produced sand can lead to surface equipment failure, erosion, plugging of slots and loss in revenue. These problems can eventually result in loss of the whole well. Therefore it is important to select a sand control method that will minimize the sand production during the lifetime of the well. On the other hand, installing sand control equipment without actually needing it is an unnecessary expenditure. Should the reservoir be completed with sand control equipment? If so, what type of sand control equipment? Both these questions can be answered by predicting when the sand production will start in the reservoir. According to Bellarby (2009) the production of sand depends on three key mechanisms:

I. *Rock strength* is the stress limit for a rock, exceeding this limit will result in rock failure. Rock strength refers to tensile strength, compressive strength, shear strength and impact strength. These strengths are not equal. A rocks tensile strength is generally 10% of the compressive strength. (Aadnøy and Looyeh, 2011). The strength of the rock is determined by how the grains are cemented together, and what condition the rock has been exposed to. Older rocks are usually stronger than younger, since the older rock has had more time to be exposed to the elements of nature (diagenesis). The physical, chemical and biological changes of the sediments are referred to as diagenesis. During this phase, sediments are compressed and buried. The magnitude and amount of diagenesis which a sedimentary rock is exposed to, determines the rocks strength. Rock strength can be derived from both core samples and logs (Bellarby, 2009).

II. *Regional stresses* are the various stresses that rocks below surface are exposed to. These stresses are referred to as far-field or in-situ stresses. Usually, three principal stresses exist at any point in below surface. Vertical (overburden) stress σ_V, maximum horizontal stress σ_H and minimum horizontal stress σ_h. Vertical stress represents the weight of the overburden formation and fluids. In areas like the North Sea with no horizontal tectonic forces acting on an area, vertical stresses can create horizontal stresses. These horizontal stresses are usually not equally related to σ_V, resulting in a maximum σ_H and minimum horizontal stress σ_h.

III. *Local* loads. After defining the formations strength and stresses, the next step is to predict the effects of the local loads. Unlike the formations strength and stresses, the local loads are not only affected by previous geological processes. The local loads are the result of the disturbance caused by the drilling and production activities. The magnitude of the local loading is influenced by the geological structure and the type of disturbance. These disturbances are related to the effects of drilling, perforating, flowing and depleting the reservoir (Bellarby, 2009).

3.3 Lower completion – Sand control

The lower completion is the part of the completion placed in the pay zone and is designed to maximize the production potential. As pointed out in table 3.3, there are two main completion categories, open and cased hole completions. The selection of lower completion concept is influenced by several factors, like cost, previous experience and type of formation. Listed under the two main categories of completions concepts, are several designs concepts. Each of these lower completion options have their respective advantages and disadvantages.

Open hole completion		**Cased hole completion**	
Some advantages	Some disadvantages	Some advantages	Some disadvantages
• Avoid cost (perforations, casing +++) • Avoid complex cement job • Good productivity in hard rock formations compared to C&P	• Limited zonal isolation • Productivity is sensitive to drilling damage • Not optimal for predrilled wells • Higher completion fluid cost • Challenging chemical treatment	• Exceptional zonal isolation • Can bypass drilling damaged zone • Can perforate new zones during the wells lifetime	• Larger completion cost related to open hole completion • Limited options regarding sand control, compared to open hole completion.

Table 3.3: Completion advantages and disadvantages (Bellarby, 2009).

The selected completion design for most of the previous production wells drilled on the Brage field in Sognefjord formation, has been open hole completions, with stand alone screens (SAS). The overall cost savings in addition to good track record has made open hole completions the preferred completion on Brage. The focus of this thesis will therefore be on the various open hole completion designs. The different designs for an open hole completion is described in the next section.

3.3.1 Open hole completion

Open hole completions are the types of completions were the last casing is usually placed above the reservoir section. Occasionally casing or liner can be landed in the reservoir sections. With this design the reservoir is exposed during the completion process of the well. Advantages with this completion design are lower cost, and avoiding complex cement and perforation jobs. In addition to the cost savings, it results in better productivity from hard rock formations, compared to cased and perforated (C&P) completion design (Bellarby). For an open hole completion, as seen in Figure 3.1, there are two options for the completion design, (1) open hole and (2) open hole sand control. Each of the different subcategories for these two solutions is described below.

3.3.1.1 Barefoot

Barefoot usually have no casing or liner in the reservoir section of the well, and is the cheapest completion option available. In cases were there is a gas cap on the top a casing can be run to overlap the oil-gas interface. The same applies for situations where there is a water bearing bed near the top a casing can be run over the water-oil interface. Then the upper part is sealed, while the reservoir section below is left open (Wan Renpu, 2008). The fluids can

flow unrestricted into the reservoir part of the wellbore, and continue to surface. Some of the advantages with this completion, beside the low cost, are according to Bellarby (2009):

1. Increasing the length of well and performing sidetracks is easy to perform since there are no restrictions in the reservoir section.
2. Simplifies the drilling of multiple wells from the reservoir section (multilaterals).
3. Problems with water and/or gas shut-off are easier to deal with in this well, then a well with a liner. Running an open hole bridge plug followed by cement is not a complicated operation.

The disadvantages by selecting this simple completion are related to hole collapse, sand control and zonal isolations issues. To avoid these issues, this completion design requires competent formations, with sufficient formation strength. Barefoot completions are common in onshore wells producing from competent limestones and dolomites (Jahn et al. 2008)).

According to Wan Renpu (2008) there are two types of procedures to create an open hole barefoot completion.

1. The well is drilled to the top of the reservoir, then cased and cemented. After the cement has set, and been tested and approved, a bit with a smaller diameter is run into the casing to drill through the cement plug and continue drilling to TD. After the bit reaches TD, the string is tripped out, and the well is completed. This is the most common of the two design.
2. The well is drilled to through the reservoir to TD. Afterwards the casing is run to the top of the reservoir section and cemented. One of the solutions to avoid cement contamination is to have an external casing packer and cement stinger at the lower part of the casing. This procedure is much more complicated and not applied during normal conditions.

3.3.1.2 Pre-drilled or slotted liners

This completion design is a bit more advanced, compared to the barefoot solution. Pre-drilled and slotted liners are simply liners with holes in them. The holes in the liner are created before installation, and are there to allow reservoir fluids to flow into the well. The difference between them is that a pre-drilled liner has round holes in it, while a slotted liner has thin long open slots instead, as illustrated in figure 3.2.

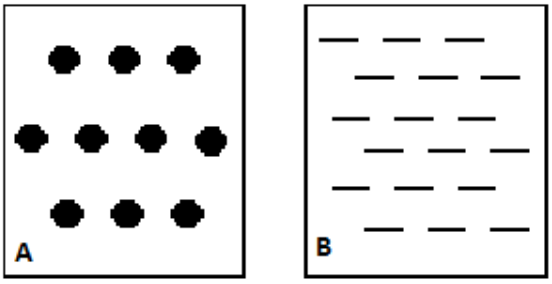

Figure 3.2: Sketch of the different holes/slots in the two liners. A- Pre-drilled liner. B- Slotted liner

The advantages of using these liners in an open hole compared to a barefoot solution are related to preventing hole collapse. The liner will work as a support structure around the

wellbore, stopping it from totally collapsing. An intact wellbore makes it is easier to run in with intervention and logging tools. Also, choosing liners in an open hole completion allows the application of open hole packers in order to isolate water or gas zone (Jahn et al. 2008). Since pre-drilled liners have larger inflow area and can handle larger collapse and torque loads than slotted liners, they are usually the preferred option. It is important to note that pre-drilled and slotted liners are not a type of sand control tool. The slots in the liners are usually too large to stop the sand from flowing through. Slots can be created with smaller openings, but small openings can result in plugging of the slots (Bellarby, 2009).

3.3.1.3 SAS – Stand alone screen

When there is a risk of sand production from a well, it is important to have measures to reduce the sand production. For open hole completions installing SAS for sand control is simple and quick, compared to the available sand control alternatives. After drilling the reservoir section, the screen assembly is installed in the pay zone. Usually the mud in the well is either replaced or conditioned, before running in with the screens. After installation, the screen is in contact with the formation and acts like a filter. The goal for this completion concept is for the screens to allow hydrocarbons through and stop sand grains from passing through (Furgier et al. 2013). Sand screens can be installed both in open hole and cased hole completions.

The way the screen retains the sand from entering through with the fluid is by forming sand bridges around the slots in the screen. The bridging theory implies that large sand particles will bridge around the slot opening and filter out smaller sand particles while allowing hydrocarbons to pass. The slots sizes are designed so that the largest 10% of the formation sands will bridge. The bridge formed by the largest sands will work as a filter, stopping the remaining sands (the other 90%) from passing through (Carlson et al. 1992). Figure 3.3 shows this process. Before sand bridge is formed small sands pass through (A). When the 10% largest sand reaches the slot the bridging process begins (B).Bridge is formed and smaller sands are stopped from entering the slot (C).

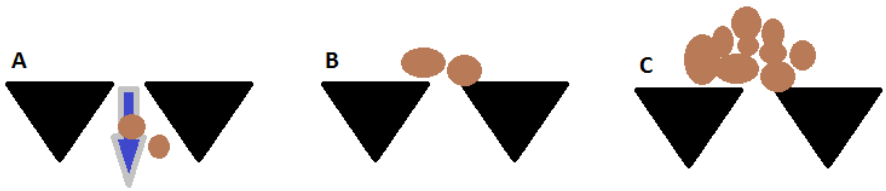

Figure 3.3: Bridging process

Numerous case studies show that the main cause for SAS failure is related to erosion aggravated by screen plugging. Arukhe et al., (2005) mentions several reasons why a screen may fail; Plugging and improper cleanup, burst and collapse, corrosion, inappropriate screen selection and trouble installing screen. The screen may also be damaged during installation (mechanical damage) if wrong load is applied. The failure rate for pre-packed and conventional screens in the Gulf of Mexico and elsewhere is over 25% (Bennett et al., 1997). BP and Shell's regionally extensive databases for sand control failures show that SAS completed wells perform poorly (Bellarby, 2009). BP's database is the result of an inter-and intra-company cooperation with sand control failure data from more than 2000 wells in 2003 SAS completed wells. From the compiled data in the database, SAS completed wells show a

higher failure rate compared OHGP and frac packs (King et al., 2003). Shell reported (Arukhe et al., 2005) a high failure rate for SAS completions. Completely plugged wells or wells with considerable reduced production represented an overall failure rate of nearly 20%.

One important factor that affects the reliability of SAS is flow between screen and formation (annular flow). Since the annular flow velocity will increase from toe to heel, the formation sands will be transported towards the heel, and backfill the annulus. If the formation sands traveling with the annular flow gradually starts to plug the screens, it will result in a higher flow rates over the remaining open screen slots. This will eventually create hot spots over the screens that may cause screen erosion (Bennett et al., 1997). To cope with problems relating annular flow in these long horizontal sections, operators use isolating equipment like external casing packers (ECP) and swellable elastomer packers. To deal with crossflow and get a uniform flow through the produced section, inflow control devices (ICDs) are deployed in combination with swell packers. ICDs can reduce the annular flow velocity, and therefore increase the screen reliability (Ellis et al., 2009/2010)

ICDs were originally developed to cope with water coning problems in long horizontal wells, and have been used with success since 1994 (Aadnoy and Hareland, 2009). If the distance between the heel and toe is very long, there is a significant pressure drop is experienced in the tubing. The oil at the toe needs to overcome this pressure drop to be produced, while oil at the heel is not affected by the pressure drop. The oil at the heel will be produced with a higher flow rate, (more oil will be produced from this area), leading to water or gas coning around the heel. Water production will increase, creating water disposal issues and limiting the production from the formation near the toe. This problem can be avoided by equalizing and maintaining the horizontal drawdown in the well. By normalizing the flow in the sections around the heel, better reservoir drainage can be achieved. This is done by installing ICDs in the production string. With ICDs the production flow from the horizontal section is controlled. ICDs reduce the fluid flow rate at the heel while increasing the inflow rate near the toe of the well. By avoiding the high flow rate near the heel, the screens reliability will increase, while water and gas coning is delayed.

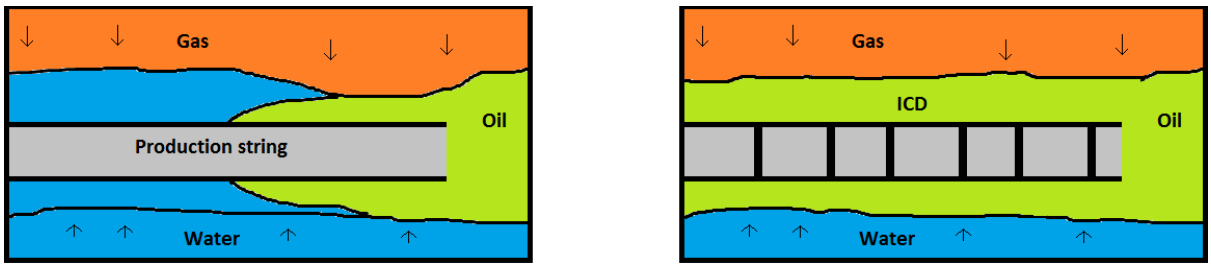

Figure 3.4: Production without and with an ICD. .

There are four types of screen on the marked today, (1) Wire-wrapped, (2) Pre-packed, (3) Premium and (4) Expandable.

(1) Wire-wrapped: These screens are the most basic sort of screens. The screen is composed by longitudinal rods on a pre-drilled base pipe. Wrapped around the rods is a single keystone-shaped wire. This wire is spot-welded to the rods. The wires keystone shape is good for two reasons. It ensures that the sand particles will bridge around the wire gap, or pass through if they are small. Also, if the wire is eroded, the inflow area will increase, reducing the chance of plugging the gap. The inflow area on

wire-wrapped screens is small, and depends on wire thickness, distance between the wire (gaps/slots) and amount of blank pipes (Bellarby, 2009). Figure 3.5 shows an illustration of the keystone shaped wire wrapping before (A) and after (B) erosion. .

Figure 3.5: Keystone shaped wire wrapping.

(2) Pre-packed: These screens can be described as two screens with gravel between. The construction is similar to the one for wire-wrapped screens, but with two screens and gravel between. The gravel between the screens is usually consolidated. By selecting consolidated gravel, the likelihood of voids to develop between the screens is reduced. The screens are designed both to keep sand out of the well, and to keep the gravel in place. The inflow area for this sort of screen is limited. Pre-packed screens can be designed with an outer shroud for installation and jetting protection. This does however increase the screens thickness, and may not always be possible due to size limitations. Keep in mind that pre-packed screen consists of two screens and gravel, and are already considered thick, before installing the shroud. Though this screen has built-in gravel, does not mean it gives the same advantages as a gravel pack (more on gravel pack in next section). The annulus between screen and formation is present for pre-packed screen, and so is the risk of sand failure and sand transport in annulus (Bellarby).

(3) Premium: This type of screen is also called mesh screen, and comes in various designs from different manufacturers. Premium screens have multiple woven non-uniform layers surrounding the base pipe. The multiple layers allow sand bridges to form in two directions over the wedges, instead of in one direction, resulting in better sand control (Figure 3.6). The outer layer is a shroud to protect the filter layers underneath. This makes this screen type more robust, and it is therefore applicable in harsh environments and long horizontal wells. This type of screen has an inflow area around 30% (Bellarby, 2009). Figure 3.6 shows a wire bridge overlapping in one direction (A) and a wire bridge overlapping in two directions (B9).

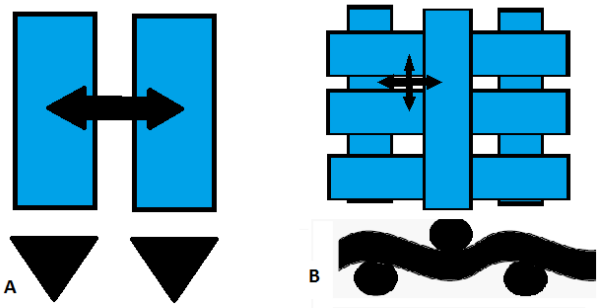

Figure 3.6: Wire bridges overlapping.

(4) Expandable screen: This is the newest screen design concept of the four mentioned in this thesis, and the first commercial application for an expandable sand screen was in

1999. The idea behind expandable screens was to eliminate the annulus between the screen and wellbore without the deployment of a gravel pack. By eliminating the annulus, the risk of sand transport in annulus is removed, improving downhole sand control. The expanded screen will support the wellbore, stabilizing sand particles in unconsolidated reservoirs (Ismail and Geddes, 2013). According to Bellarby (2009) there are basically two types of expandable screens in use. The first case has an expandable metal base pipe surrounded by the screen mesh. The mesh is protected with an expandable outer shroud. The screen mesh is packed to overlap when the screen is unexpanded. While expanding the base pipe and shroud, the mesh is pushed out to cover the new area of the pipe. The alternative is to have a screen where the mesh can expand. Warp wires are fixed while weave wires are expanded tangentially, creating filtration gaps between the weave wires, as seen in figure 3.7. After running in the hole with the screen, different methods can be used to expand it. Some methods used are expansion with weight from drill pipe and expansion with pressure cycles. The technology was initially developed for application in openhole completed wells, but has also been used for cased holes applications. Several papers have been written about expandable screens being deployed in cased holes, for example in the Niger Delta (Ayoola et al., 2008) and in Nigeria (Innes et al., 2007).

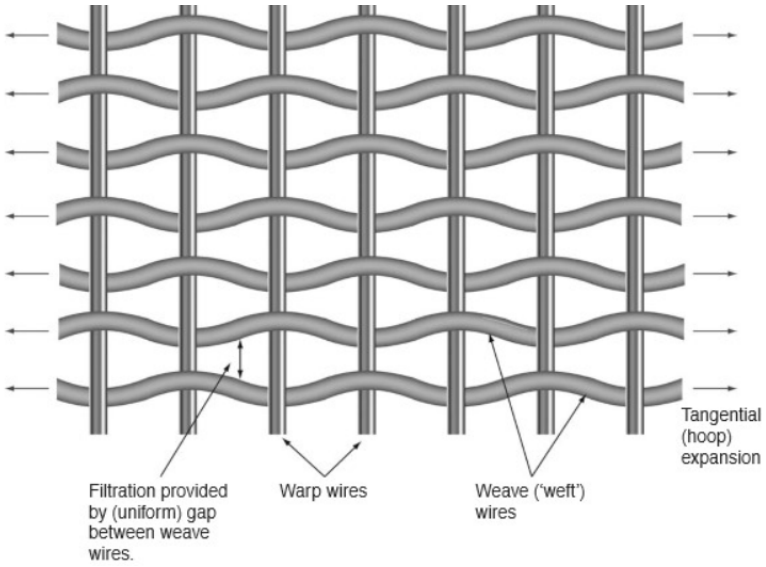

Figure 3.7: Woven mesh for expandable screens (Bellarby, 2009).

3.3.1.4 Gravel pack

Open hole gravel pack (OHGP) is a robust sand control method. The application of OHGP in horizontal wells has a good track record. The goal with an OHGP operation is to pack off annulus between screen and wellbore with gravel. This is done by mixing gravel and gravel pack fluid into a slurry, and pump into the well. This will support and stabilize the formation, reducing the risk of formation collapse. In addition, the gravel minimizes the potential of annular flow and sand transport in annulus. Bridging theory mentioned previously for sand screens, applies for gravel packs. The bridges are formed over pathways in the gravel and work as a filtering medium. The filter allows formation fluids to pass through, while filtering out smaller sand particles. It is important that the selected screen slots and gravel size are

compatible, so that the gravel can't escape through the screens slots. Gravel used for the job needs to be clean, round and small enough to exclude formation sands (Schlumberger, 2007).

A lot of work has been done to determine the optimal size for the gravel. Coberly and Wagner (1938) suggested using gravel 10 times D_{10} of the formation sand. D_{10} represents the effective particle size of the formation sands, meaning that 10% of the sands are finer than this size, while the remaining 90% are coarser. D50 is the median. After many failures, Hill (1941) suggested reducing the size to 8 times D_{10}. Even after the introduction of this reduction in gravel size, failures continued to happen. Saucier (1974) and other authors focused on the fine balance between excluding formation sands and plugging the gravel. Based on laboratory tests, Saucier conclude that using gravel 5-7 times the D_{50} of the formation sands would give highest ratio of gravel pack to sand permeability. The selection of 6 times D_{50} was afterwards used widely with good results (Bellarby, 2009).

Installing OHGP is more complex compared to installing SAS, and have a higher installation cost. Important limitations to consider during a gravel packing operation are ECD and fracture pressure of the formation. Similar to drilling operations, it is important to have an ECD within the operational window between the pore and fracture pressure curves. Pumping gravel in long horizontal wells will increase the frictional pressure loss from heel to toe, increasing the ECD. If the pressure increase is greater than the fracture pressure limit, gravel pack fluid will enter the formation. The pressure required to transport the gravel will increase with the length of the horizontal section, limiting the maximum length of the gravel slurry interval. On the other hand, if the wellbore pressure goes below pore pressure, formation fluids will enter the well. It is therefore important to design a gravel pack fluid with a density compatible with both formation pressures.

The two most common methods for OHGP in use today are (1) circulating packs and (2) alternate path gravel packs (shunt tubes) (Bellarby, 2009).

(1) In horizontal wells the gravel will be transported and displaced in annulus in two parts; the alpha wave and the beta wave. During the alpha wave phase, gravel slurry is pumped down the work string, into the crossover tool and through gravel pack ports. Gravel then starts to settle on the low side of the annular space, between wellbore and screen. The gravel will form a bed in the annulus, and as it grown, the annular volume will decrease. Gravel slurry velocity will increase as the annular volume decreases. The gravel dune will increase in height until the transport velocity of the slurry is greater than the minimum velocity needed to transport gravel over the gravel bed top. At this equilibrium the gravel stops settling on top of the bed and the bed cease from growing. Now the gravel slurry is transported over the dune, reaching the next part of annulus, and continues the process of forming the bed. This deposition process continues towards the toe of the well. (P. Nguyen et al. 2001). The next wave front is the beta wave, and starts right after the alpha wave. The beta wave starts when the alpha wave reaches the end of the workstring, the toe of the well, a gravel bridge or a collapsed formation (Edment et al., 2005). During the beta wave the gravel will start to backfill the annular space above the bed, from the toe to towards the heel of the well.

    Premature packing is when the beta wave phase starts before the alpha wave has reached the toe of the well. If the pump rate and the ECD are too high, and the formation fractures, backfilling of gravel will start before the alpha wave has reached

the target destination. This would result in a shorter gravel packed interval. It is not only staying below fracture pressure that effects premature packing. There are other elements to pay attention to, like keeping the filter cake intact, having a uniform wellbore diameter (Bellarby, 2009), gravel concentration, fluid properties and to have relatively low fluid-loss rates (P.Nguyen et al. 2001)

(2) For a circulating pack, it is a fundamental requirement to have a hydraulically isolated formation. That is however not the case for alternate path gravel packs (shunt tubes). Shunt tubes are installed when encountering formations where losses are expected. The shunts are installed outside the gravel pack screen or integrated under the gravel screen (Bellarby, 2009).

A gravel pack operation with shunt tubes starts like a circulating gravel pack operation. Gravel slurry is pumped down the work string, and gravel fills up the annulus. In the event of a screen out, pressure in the well will increase. A screen out is a blockage caused by bridging of the gravel in the annulus. The increase in pressure then pushes the gravel slurry through the shunt. The gravel slurry will then exit through the first available nozzle and bypass the blockage. The gravel slurry will continue packing the annular space behind the bridge until final screen out (Schlumberger, 2007).

4. Stresses and Stress Analysis

This chapter presents some background theory on the various stresses to consider during well design. It also includes some general theory on stress analysis in a well. These stresses will be simulated and analyzed later in this thesis.

4.1 Purpose of Stress Analysis

Tubing stress analysis is a fundamental part of a completion design. Today, most completion designs require a well and tubing stress analysis. NORSOK D-010 specifies:

> "All completions, liners and tie-back strings shall be designed to withstand all planned and/or expected stresses, including those induced during potential well control situations. The design basis and margins must be known and documented. All components of the completion string including connections shall be subject to load verification. Weak points shall be identified and documented."

By simulating the different load cases, and quantifying the value of them, engineers can design the string to withstand these loads. The aim is to find the worst case potential loads a string can be subjected to during its lifetime and see if the load is within the selected safety limits. Reasons for performing a stress analysis include (Bellarby, 2009):

1. Define the completions weight, grade and size
2. Ensure that the selected tubing and casing will withstand all projected loads (installation and service) for the life of the well.
3. Ensure that the tubing and casing can be run into the well, eventually pulled out (for tubing).
4. Define the loads for casing stress analysis.

4.2 Stress, Strain and Grades

A fundamental part of stress analysis is to understand the behavior of metals during loading and the limitations of the specific material. There are multiple sources of loading, which include pressure, temperature and pipe weight. These loads act axially (tension and compression) or radially (burst and collapse), and the quantification of these loads comes from stress. Stress is defined as force per unit area:

$$\sigma = \frac{F}{A_x} \tag{4.1}$$

Where σ represents the stress, F is the force and A_x is the unit area.

A casing or tubing subjected to stress will elongate or compress, depending on the direction of the stress. This phenomenon is described as strain. Strain is dimensionless and defined as:

$$\varepsilon = \frac{\Delta L}{L} \tag{4.2}$$

Where ε represents the strain, ΔL is the length change of the material and L is the initial length of the material.

Figure 4.1 show the behavior of a material when experiencing loading. Here it is shown that the stress-strain relation is approximately linear in the start of the loading. This straight lines slope is called the modulus of elasticity, or Young's modulus (Bellarby, 2009). The relation between stress and strain in the linear slope is described in Eq. 4.3. The elastic limit is where the non-permanent deformation ends, and the permanent (plastic) deformation of the material begin. The yield point is where a small increase in stress results in a larger increase in strain.

$$E = \frac{\sigma}{\varepsilon} \tag{4.3}$$

E is the modulus of elasticity or Young's modulus.

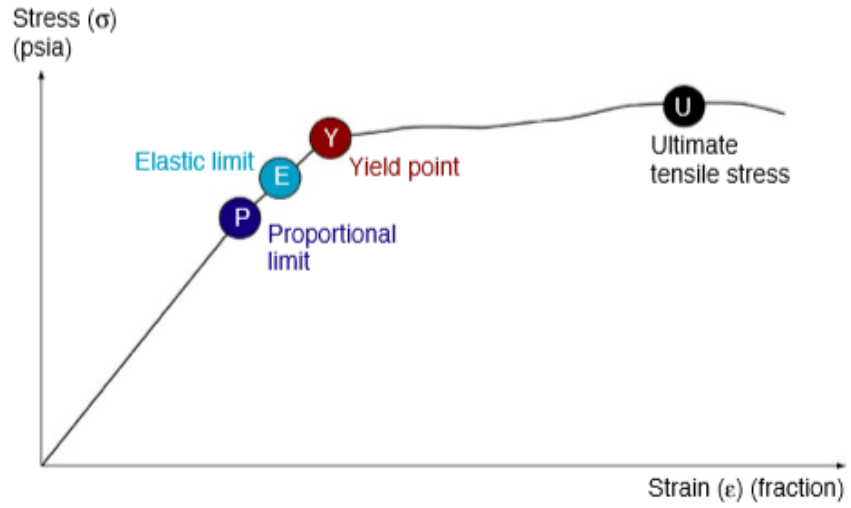

Figure 4.1: Typical tubing stress-strain relation (Bellarby, 2009).

4.3 Axial Loads

Loads along the length of the casing or tubing are referred to as axial loads, and is affected by pressure, temperature and the weight of the casing or tubing. Axial loads can be tensile (positive) or compressive (negative) (Bellarby, 2009). The axial load must not exceed the axial strength of the pipe, otherwise it can fail. The axial strength can be calculated with the following formula:

$$F_{a,max} = A_x Y_p \tag{4.4}$$

Where F_a represents the maximum axial strength, A_x is the pipe cross-sectional area and Y_p is the yield stress.

Axial loads caused by pressure on a casing or tubing cross section are referred to as piston forces. These piston forces can come from buoyancy effect, expansion devices and crossovers (Bellarby, 2009). Though tubing is loaded in axial tension and generates axial strain, it also generates a radial compressive strain. This is referred to as ballooning, and is observed when

pressure is applied to tubing (Bellarby, 2009). Ballooning is affected by the pressure difference between the inside and outside of the tubing.

Temperature effects on the metal in a pipe, tubing or casing have a major consequence on the metals strength. The strength of metals decreases as the temperature increases (Aadnøy, 2010). Also, metals will expand when heated. Metal expansion is calculated in eq. 4.5. Heating a casing or tubing that is fixed in both ends will cause compressive force, and cooling will cause a tensile force. Heating of a well occurs in general during production of hot fluid, and the cooling occurs during injection of a cooler fluid (Bellarby, 2009).

$$\Delta L_T = C_T \Delta T L \tag{4.5}$$

Where ΔL_T represents the metal expansion, C_T is the coefficient of thermal expansion, ΔT is the average change in temperature and L is the length.

Other loads defined as axial loads, according to Bellarby (2009), are bending stress, fluid drag and buckling. Aadnøy (2010) lists other tension loads for casing that are caused by axial loading:

1. Dynamic forces or shock loads
2. Movements to free differential sticking
3. During pressure testing
4. Bending loads
5. Drag forces

4.4 Burst

A pipe will burst when the pressure differential between the internal and external pressure is larger than the pipes mechanical strength. Burst is a tensile failure that results in a rupture along the axis of the pipe. Equation 4.6 is used to describe the burst rating, if the tangential stress is equal to the tensile material strength (Aadnøy, 2010).

$$P_{burst} = 2\sigma_{\text{tensile}}\left(\frac{t}{D_o}\right) \tag{4.6}$$

Where P_{burst} represents the burst rating, σ_{tensile} is the yield strength of the pipe, t is the pipe thickness and D_o is the pipe outer diameter. In addition it is normal to add on a safety factor in the equation. According to NORSOK D-010 the design factor for the burst parameter is 1.10. This implies that the value of the calculated P_{burst} needs to be multiplied with 1.10, and that the new value is the acceptable burst rating. There are many situations where pressure conditions can cause a pipe to burst. Although there are many different situations, the pressure picture is similar for several operations. Therefore, from a design point of view, three main categories can be a considered for burst rating (Aadnøy, 2010):

1. Gas filled casing
2. Leaking tubing
3. Maximum gas kick

4.5 Collapse

Collapse occurs when the external pressure acting on the pipe exceeds the internal pressure. During collapse, a pipe will change shape from its original circular shape to an elliptical or a non-circular shape. This causes problems for equipment and tools that may no longer fit in through the pipe. For casing collapse, the external pressure is caused by pore pressure, drilling fluid pressure or temperature expansion. The internal pressure is equal to the hydrostatic pressure of the mud or water column. Since collapse leads to material deformation, it is considered a geometric failure (Aadnøy, 2010). Calculating the collapse rating depends on the diameter and thickness, and properties such as pipe ovality (Bellarby, 2009). According to both Bellarby (2009) and Aadnøy (2010) collapse is divided into four categories:

1. Yield collapse
2. Plastic collapse
3. Transitional collapse
4. Elastic collapse.

The diameter/wall thickness (D/t) ratio is different for each of the collapse categories. It is the D/t ratio that decides which category the specific collapse belongs to. Yield collapse has the smallest D/t ratio, and elastic collapse has the largest D/t ratio. More on the different collapse categories and their formulas can be found in Appendix A.

There are many situations that can cause a pipe to collapse. Since the pressure picture is similar for several of these situations, the following two main categories can be considered for collapse rating (Aadnøy, 2010):

1. Mud loss to a thief zone
2. Collapse during cementing

4.6 Triaxial Analysis

When performing a stress analysis, it is not sufficient to analyze the different loadings separately. A pipe can experience multiple loadings simultaneously. It is therefore important to understand the effect these loads have on the pipe when occurring at the same time. A three-dimensional stress analysis includes the axial stress, the radial stress, and the hoop/tangential stress (Aadnøy, 2010). Figure 4.1 show how these stresses act on a pipe wall.

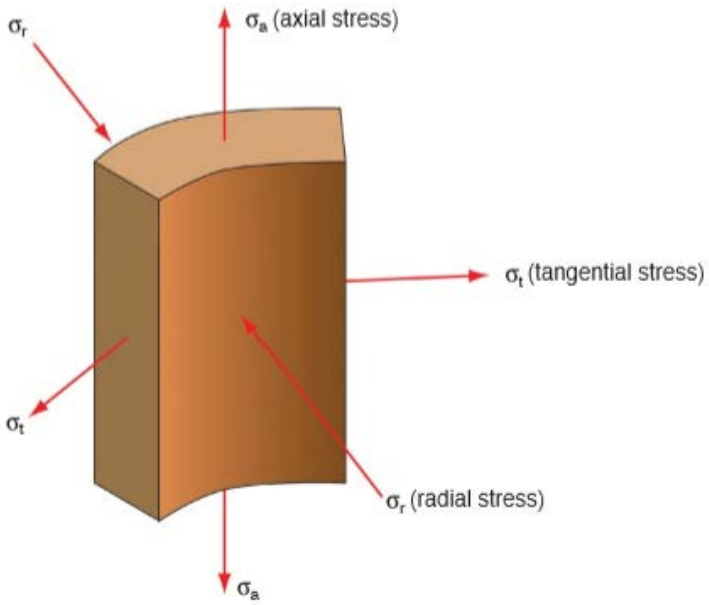

Figure 4.2: Stress components of triaxial analysis (Bellarby, 2009).

The combination of these three stresses is referred to as triaxial stress. These three stresses can be combined into a single stress, σ_{VME}, using the Von Mises equivalent (VME). The Von Mises equivalent is widely used, and is based on the maximum distortion energy theorem. The material will start to yield when the VME stress becomes larger than the materials yield stress.

4.7 Safety Factors and Design Factors

If the various loads a pipe will be exposed to during its lifetime are known and the pipe rating is provided, it is possible to decide if the design is acceptable. The ratio between the pipe rating and load is referred to as the safety factor (SF). SF larger than 1 represents a rating larger than the load. Each of the failure mechanisms mentioned earlier (axial, burst, etc.) have their own rating and loading, hence their own SF.

$$SF = \frac{Rating}{Loading} \tag{4.7}$$

A SF value larger than 1 implies that the pipe should stay intact. However, there is uncertainty in the loading calculations, pipe behavior under downhole conditions and the downhole conditions themselves. It is therefore normal that the required SF is larger than 1. The minimum safety factor is called a design factor (Bellarby, 2009). Table 4.1 lists the minimum design factors during drilling and well operations according to NORSOK D-010.

Parameter	**Design factor**
Burst	1,10
Collapse	1,10
Axial	1,25
Triaxial	1,25

Table 4.1 Design factors according to NORSOK D-010.

4.8 Buckling

Buckling is a phenomenon that may occur in oil and gas wells. All pipes run in the well have the potential of experiencing buckling. Buckling is related to the deformation of elements that are thin compared to their length, like drill pipe and tubing. For pipes and tubing, buckling is affected by the compression forces as well as the internal and external pressures. For deviated wells there are additional factors that have an effect on buckling (Bellarby, 2009). There are two modes of buckling in oil and gas well, sinusoidal and helical buckling.

The first buckling phase is the sinusoidal mode of deformation. The name is due to the sinusoidal shape the pipe or tubing gets when this occurs. Sinusoidal buckling is achieved when the loading exceeds the critical, or sinusoidal, buckling load limit. The second phase is the helical buckling mode of deformation, which is the more critical of the two modes. When the loading is increased to exceed the helical buckling limit, the pipe or tubing will form a helical shape inside the well. Helical buckling is considered more critical due to the occurrence of "lock up". When the pipe or tubing has formed a helical shape, pushing it will transfer the force from the string to the wellbore wall. This will increase the wall contact forces. Increase in wall contact forces will increase the friction with the wellbore. This results in a stuck pipe situation, where the pipe or tubing is "locked up" with the wellbore wall (Belayneh, 2006). Figure 4.3 illustrates the two buckling modes.

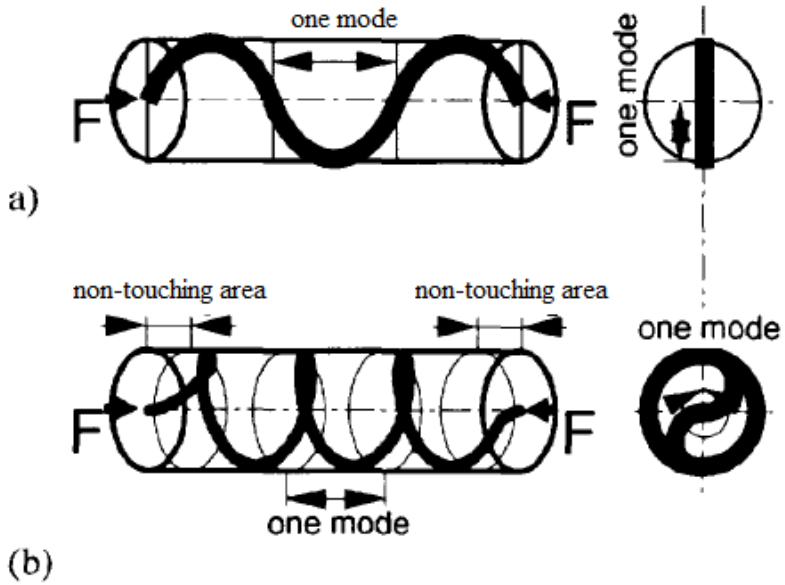

Figure 4.3: a) Sinusoidal buckling b) Helical buckling (Hishida, et al. 1996)

5. Results and simulations:

Due to the location of the Brage platform in relation to the Brage North reservoirs, a long horizontal well is required to reach the oil bearing formations. Drilling and installation of sand screen will be simulated using Wellplan™. A pre-existing Brage well is used as a base case for these simulations. The previous well path has been permanently plugged below the kick off point of our new simulated well path.

The $13^{3}/_{8}$" casing in the old well has been cut and pulled, and a bridge plug has been installed inside the $18^{5}/_{8}$" casing. The plan is to install a whipstock on the bridge plug and kick off in the $18^{5}/_{8}$" casing. The kick off point of the new well path is located at to 1050 mMD. The plan is to drill a $16^{1}/_{4}$" x $17^{1}/_{2}$" hole from kick off to 3969 mMD. A $13^{3}/_{8}$" x 14" intermediate casing is run into the hole afterwards. Next section is the $12^{1}/_{4}$" x $13^{1}/_{2}$" hole, which runs from the previous casing shoe to 6380 mMD. This section is then isolated from the formation with a $10^{3}/_{4}$" Liner. The final section of the well is the $8^{1}/_{2}$" x $9^{1}/_{2}$" hole, reaching TD at 9,390 mMD. More information on the various sections can be found in Appendix C. After the drilling phase the plan is to run $6^{5}/_{8}$" screens down to TD.

WellPlan™ is the tool used to simulate the drilling and completion running operation. The length of the selected well path is 9,390 mMD, with a horizontal displacement of 8,060 mMD. The highest inclination in the well is 92,21°, and the final section of the well have a 90° inclination. All data used in this study was provided by Wintershall Norge.

In addition to the generated Wellplan™ simulations, a study was conduced by Reelwell on drilling the 9 ½" hole. Reelwell looked at drilling the $9^{1}/_{2}$" hole with their technology. The results from their drilling method will later be compared to the results from the conventional drilling method. Reelwell's simulation results can be found in Appendix B.

The aim for this study is to see if it is possible to drill and complete the proposed well using a conventional method. The aim is to design a functioning long reach well.

5.1 Well simulations

The two sections that will be investigated in this study are the $13^{1}/_{2}$" and the $9^{1}/_{2}$" hole sections. The aim is to see if these two sections can be drilled using a conventional drilling method, and check if the selected completion string can be run down to TD. Rig capacity and specifications can be found in Appendix D. The drilling mud selected for these two sections are oil based drilling fluid. The Herschel-Buckley rheology model is used to show the specific properties of the mud. A list with the fluid specifications and can be found in Appendix C.

Two separate studies have been conducted for drilling the selected well sections and installing the completion. The first study was performed with the standard drill pipe used on Brage today, while the second study was performed with a new type of composite drill pipe. The second study was performed to see what benefits the use of composite drill pipe would have, compared to conventional pipe. Both studies were performed with the same BHA setup and components. The various BHA's was built up with components and tools previously used

on Brage. The specific results for each section can be found in the section below. During the simulation process, various string designs were tested to find the optimal design for each section and operation. The criterion for the conventional string design was to only use standard Brage pipe (drill pipe and heavy weight). The drilling setup for the specific sections is listed in Appendix C, while the drilling simulation results are listed in Appendix E.

The selected lower completion design for this well is open hole lower completion with stand alone screen (SAS). The reason for this selection is based on previous experience from other wells producing from the same type of sand (Sognefjord). Due to low sand strength in the reservoir, sand production is to be considered very probable for this well. The well will therefore be completed with a 6 5/8" 250µ premium screens. Swellpackers will be installed in selected intervals of the completion string. There are two main reasons for installing the swellpackers. First, the selected intervals are either intervals with water or intervals expected to have water breakthrough during the wells production life. The second reason is to deal with crossflow in annulus during production.

5.2 Simulations–Conventional Drill Pipe

12 ¼" x 13 ½" hole:

	mMD	mTVD
Section Start	3969	2040
Section TD	6380	2078

	mMD	mTVD
Section Length	2411	38
Casing Shoe	6380	2078

Table 5.1: Section data for the 12 ¼" x 13 ½" hole section.

Drilling:

The section is drilled with a 1.430 sg oil based mud, and the drill strings upper part is built with a mix of 6 5/8" and 5 1/2" drill pipe. For the selected string design in Appendix C, simulations show that the well section could be drilled. Simulations show that hook load, tension load and torque were all within the set limitations. For torque and tension the critical area is around the section TD. The safety margin between the limit and these two loads is small, but acceptable. The minimum flowrate simulations for cuttings transport show that the selected flowrate was acceptable. Stress simulations show that the various stresses, including Von Mises, are within the acceptable limit.

The critical part drilling this section is related to the ECD. As shown in figure D.5, the fracture gradient drops at the end of the section from approximately 1.81 sg to approximately 1.36 sg. The simulated fracture gradient of 1.36 sg is lower than the ECD at that depth, which likely will result in fracturing the formation and loss of mud. The drop in fracture gradient is due to the change in formation. A thin layer of Draupne shale is located on top of the targeted Draupne Sandstone. The goal is to drill through the Draupne shale and reach section TD in top of the Draupne Sandstone (6380 mMD). This will allow the 10 ¾" liner to seal off the Draupne shale. Loss in the sandstone section is an acceptable risk, and preferred over risking shale collapse in the shale section above.

Liner running:

The liner length is 2511 m and is run on 6 5/8” heavy weight drill pipe. Simulations show that the liner can be run down to section TD. Simulations also show that hook load and tension load were acceptable. For tension load, simulations show that the load while tripping in will not cross the helical buckling limit, and is therefore considered to be acceptable. Stress simulations show that the various stresses, including Von Mises, are within the acceptable limit. The critical aspect of this operation is related to the low fracture gradient, as was for the drilling operation. Pumping during a liner installation is a contingency used if the liner experiences problem running to section TD. Once mud starts flowing at bottom, the ECD will increase. If the installation goes as planned, pumping should not be required to get the liner to section TD. An alternative contingency, to avoid the ECD problem, is rotating the liner to get the liner to section TD. The main risk rotating the liner is related to the torque limitations of the downhole equipment. It is important that the generated torque required to rotate the liner, do not exceed the torque limit.

8 ½” x 9 ½” hole:

	mMD	mTVD
Section Start	6380	2078
Section TD	9390	2078

	mMD	mTVD
Section Length	3010	0
Screen Shoe	9390	2078

Table 5.2: Section data for the 9 ½” x 8 ½” hole section.

Drilling:

The section is drilled with a 1.18 sg oil based mud, and the drill strings upper part is built with a mix of 6 5/8” and 5 1/2" drill pipe. Simulations show that the well section will be challenging to drill to TD. Hook load, tension load and torque were all within the set limitations. For tension loading, the critical area is around 6200 mMD. Here the safety margin between buckling and tripping in is small, but acceptable. The minimum flowrate simulations for cuttings transport show that the selected flowrate was less than the minimum required flowrate. Excessive cuttings and debris can be handled when tripping out of hole, since it is possible to wash the hole when tripping out. Also, a lower flowrate will have a positive impact on ECD. Stress simulations show that the various stresses, including Von Mises, are within the acceptable limit.

The challenge drilling this section is related to the ECD. Simulations show that while ECD increases with distance drilled, the fracture gradient is stable. This is mainly caused by the selected horizontal well path. ECD will increase as the horizontal distance increases. The fracture gradient for the formation drilled will however stay constant. The result is an ECD exceeding the fracture gradient.

Screen running:

The screen section (including packers) is 1898 m and is run on a mix of 6 5/8” and 5 1/2" heavy weight drill pipe and 6 5/8” drill pipe. Simulations show that hook load might be a problem if trying to trip out after 9200 mMD. Running into hole is however not a problem for

the hook load capacity. Tension load simulations show that the safety margin between tripping in and helical buckling is very small at two specific points. Stress simulations show that the various stresses, including Von Mises, are within the acceptable limit.

5.3 Simulations–Composite Drill Pipe

12 ¼" x 13 ½" hole:

	mMD	mTVD
Section Start	3969	2040
Section TD	6380	2078

	mMD	mTVD
Section Length	2411	38
Casing Shoe	6380	2078

Table 5.3: Section data for the 12 ¼" x 13 ½" hole section.

Drilling:

The section is drilled with a 1.430 sg oil based mud, and the drill strings upper part is built with 5 7/8" composite drill pipe. For the selected string design in Appendix C, simulations show that the well section might not be drilled with the selected string. Simulations show that hook load and torque are within the set limitations. The safety margin for torque is small at around TD, but acceptable. The tension load simulations show that for rotating on bottom, the tension generated will be equal to or just over the helical buckling limit. The simulation shows that drilling this well section will potentially result in helical buckling. The minimum flowrate simulations for cuttings transport show that the selected flowrate was sufficient for cuttings transport. Stress simulations show that the simulated stresses are within the acceptable limit. As for drilling this section with conventional pipe, the low fracture gradient and high ECD is still a great challenge. Simulation results can be found in Appendix C.

Liner running:

The liner length is 2511 m and is run on 5 7/8" composite drill pipe. Simulations show that running the liner on composite drill pipe instead of conventional pipe, would not be possible due to multiple factors. Hook load simulation show that the string will go over the minimum helical buckling limit when tripping in. Tension simulation shows that tripping in to well will be less than the acceptable minimum limit. This results in helical buckling. Stress simulations show that the Von Mises stress will be larger than the pipes stress limit when tripping in to the hole. The low fracture gradient and high ECD is challenging, as it was for the conventional pipe run.

8½" x 9 ½" hole:

	mMD	mTVD
Section Start	6380	2078
Section TD	9390	2078

	mMD	mTVD
Section Length	3010	0
Screen Shoe	9390	2078

Table 5.4: Section data for the 9 ½" x 8 ½" hole section

Drilling:

The section is drilled with a 1.18 sg oil based mud, and the drill strings upper part is made up with 5 7/8” composite drill pipe. Simulations for hook load and torque show that loads are within the set limitations. For tension load the critical depth is between 6200 and 6300 mMD. Here the tension load when tripping is close to the helical buckling limit. The safety margin is small, but the tension load does not cross the helical buckling limit. The minimum flowrate simulations show that the selected flowrate is less than the minimum required flowrate. Excessive cuttings and debris can be handled when tripping out of hole, since it is possible to wash the hole when tripping out. Also, a lower flowrate will have a positive impact on ECD. Stress limitations show that the simulated stresses are within the acceptable limit.

The challenge with drilling this section is the same as it was for drilling it with conventional pipe, the ECD. The low fracture gradient and the high ECD poses a great challenge when drilling this section.

Screen running:

The screen section (including packers) is 1898 m and is run on 5 7/8” composite drill pipe. Hook load simulations show that minimum helical buckling limit is crossed when tripping in to the well. Also the tension simulations show that the tension when tripping in is below the minimum helical buckling limit. Stress simulations show that the simulated stresses are within the acceptable limit.

6. Discussion

The basis of this study was to investigate if the planned well could be drilled and completed. A preselected well path was the starting base for this study, and Wellplan™ was used as the simulation software to investigate this. After performing the simulations, the result was investigated.

6.1 Results discussion

6.1.1 Drilling 12 ¼" x 13 ½" Section

For the 12 ¼" x 13 1/2" hole, simulations performed for drilling with conventional and composite pipe showed different results. The hook load was drastically reduced with composite pipe. Maximum trip out load was reduced from around 164 ton to around 44 ton. Torque values were also reduced when simulating with the composite pipe. Maximum torque was reduced from 61 kNm to 20 kNm. For stress simulations composite pipe showed a drastic reduction in stresses. The maximum stress for conventional pipe, Von Mises stress, was around 395 MPa during trip in and around 470 MPa during trip out. Maximum Von Mises stress during trip in with composite pipe was around 60 MPa, and around 70 during trip out. This was as expected, since the effective weight of the conventional pipe was 23.1 ppf, and the effective weight of the composite pipe was 14.25 ppf. The weight reduction had a positive impact on the mentioned simulations, but it also important to mention that the maximum limits for conventional and composite pipes are different. The torque simulations results show that the torque limit for conventional pipe is much higher than for composite pipe. The same applies for the stress limit for conventional pipe, which is much higher than for composite pipe. Though composite pipe gives smaller maximum load values, the pipe also have smaller load limit compared to conventional pipe. This needs to be acknowledged to ensure that the loading values for composite pipe are within the new and reduced limits.

The tension simulation for composite pipe showed that the maximum compression was approximately the same as the pipes' minimum helical buckling limit. Simulations with the conventional pipe showed that the maximum compression was larger than the minimum helical buckling limit. The results for the composite pipe show that tension in top of the string has been reduced for all the tension loads. Tension load at TD is pretty much similar for both pipes. For drilling with conventional pipe, the largest compression (rotating on bottom) is greater than the minimum helical buckling limit. It is worth mentioning that the margin between the limit and the maximum compression is small. For the composite pipe, the minimum buckling limits were larger (shifted to the right) than for the conventional pipe. Simulations show that the largest compression (rotating on bottom) for composite pipe was approximately the same as for the conventional pipe. Simulation showed a maximum compression for composite pipe that is approximately the same as the minimum helical buckling limit. This shows that drilling the selected well section, with the selected composite pipe, will have a great risk of helical buckling, which is not acceptable.

The reason for the change in minimum helical buckling limit for composite pipe, compared to conventional pipe, was investigated using equation A.11 in Appendix A. At first, the assumption was that the reduction in minimum helical buckling limit for composite pipe was

caused by a smaller E-modulus *E* than for conventional pipe. However, drill pipe data from Appendix D showed that the connection torsional yield was larger for the composite pipe than for the conventional drill pipe used in the same section. Next assumption was that the moment of inertia *I* was smaller for the composite pipe. Using the diameter data provided in Appendix D, calculations revealed that *I* was larger for composite pipe than for the conventional pipes. By eliminating the effect of these two factors, the last assumption was that the change in minimum helical buckling limit was caused by the weight reduction. Reducing the effective pipe weight to 14.25 ppf was identified as the main cause. Calculations showed that increasing the effective pipe weight above 14.25 was necessary to keep the maximum tension from exceeding the minimum helical buckling limit. In addition, the buoyancy effect of the mud plays a part. The heavier the mud is, the better is the buoyance effect that it provides the drill pipe. Lowering the mud weight from 1.430 sg (the selected mud weight) will therefore result in a reduced buoyancy effect on the drill pipe, which again will have a positive impact on the helical buckling limit.

There is also the issue change in the minimum helical buckling limit at the end of the 12 ¼" x 13 1/2" hole section. For the tension simulations, the minimum helical buckling limit shifts to the left, at approximately 6150 mMD. This occurs in the simulations for both the conventional and the composite drill pipe. This is caused by a drop in the well path that starts in the end of the section. As shown in the helical buckling equations in Appendix A, inclination have an effect on the helical buckling limit. The tension simulations with conventional drill pipe show good clearance between maximum compression load and the minimum helical buckling limit. From approximately 6150 mMD, the clearance is reduced due to the change in inclination.

6.1.2 Drilling 8 ½" x 9 ½" Section

As for the previous section, simulations for drilling the 8 ½" x 9 ½" hole was performed for both conventional and composite pipe. As previously experienced, the weight of the composite pipe has a positive effect on hook load, torque and stresses. Simulations show that the maximum loads are reduced when replacing the conventional drill pipe with the lighter composite pipe. The effective weight of the conventional string, for the 8 ½" x 9 ½" hole, was 24.34 ppf, and the effective weight of the composite pipe was 14.25 ppf. Unlike the tension simulations for the previous section, the simulations for this sections show that there are no problems related to helical buckling, for either one of the simulations. Simulations show that hook load, torque and stress are much less for composite pipe, and increase the margin between maximum load and the limit. For tension load, the margin between the maximum load and the minimum helical buckling limit is larger for conventional pipe, than for composite pipe. Still, the mentioned simulations show that both drill pipes can be used to drill the selected well section.

For this section, unlike the previous section, there was a significant variation in maximum ECD for conventional and composite pipe. This was not the case for the 12 ¼" x 13 1/2" hole section, where the maximum ECD was pretty much the same for both types of pipe. Maximum ECD for the conventional pipe was approximately 1.425 sg, and approximately 1.450 sg for composite pipe. Equation 2.10 was used to investigate this. Both simulations had

the same horizontal section length, flow velocity and mud density. The assumption was therefore that the reduction in annular area between pipe and wellbore wall, Δd, was the reason for the increase in ECD for composite pipe. The conventional pipes OD is 5 ½" in the lower part of the string, while the composite pipes OD is 5 7/8". By recalculating ECD for the composite pipe, while assuming the same pipe OD as for conventional pipe, it was verified that it was the different OD size that caused the increase in ECD. By changing the OD input to 5 ½" for composite pipe, the simulated ECD values were similar to the values for the conventional pipe.

Looking at the simulation results for the two types of pipe, it seems like both pipes can handle the various loadings, and both will struggle with ECD. Composite pipe will generate much lower loads compared to the conventional pipe, while the conventional pipe will generate a smaller ECD. Since ECD, as shown in the simulations, is the biggest challenge for this well, the preferred pipe should be the one that generates the lowest ECD. An alternative could be a composite pipe with a smaller ID that would reduce the ECD. However, it is important to remember that by reducing the ID of the pipe, it will have a negative effect on the buckling limit. As shown in the simulations, the distance between maximum compression for helical buckling with the composite pipe, and the minimum helical buckling limit is small. A reduction in pipe ID could therefore cause the maximum compression load of the pipe to exceed the minimum helical buckling limit.

6.1.3 Running 10 ¾" Liner

Simulations for running the 10 ¾" on conventional pipe show that it would be possible to run the liner to section TD. Loading simulations for hook load and tension show that even though the maximum loads do not exceed the set limits, the margins are small. Due to these small margins, simulations for running the liner with the lighter composite pipe were conducted. The composite pipe used for the simulations was the same that was used for the drilling simulations. The main application for this type of composite pipe is drilling, not liner running. Still, simulations were conducted to verify if it was possible or not. The new simulation results showed that it would not be possible to run the liner on the composite pipe. As expected, the reduction in pipe weight reduced the maximum hook load and tension load. On the other hand the reduction in pipe weight and strength resulted in helical buckling. Also, the stress simulation showed that Von Mises stress would exceed the pipes stress limit. The length and weight of the 10 ¾" liner, in addition the inclined well path, was simply too great for the composite pipe to handle. The installation of the 10 ¾" liner could therefore only be performed with string made up of conventional pipe.

6.1.4 Running 7" x 6 5/8" Screen

The final set of simulations were performed for running the screen section down to TD. Hook load simulations show that running into the hole with the screen is not a problem. For tripping out there might me a problem after going past 9200 mMD. After this point, the hook load will be approximately equal to the maximum weight yield limit. This means that if a situation occurs where the screen section needs to be pulled after reaching 9200 mMD, it may not be possible to pull it. This risk is categorized as acceptable due to the short interval left to run in after the critical depth, compared to the entire screen section. Tension simulations

show that the compression load does not exceed the minimum helical buckling limit, but margins were small. The loading when tripping in almost crosses the helical buckling limit at around 6300 mMD. Stress simulations showed that the maximum stress was less than the stress limit. As for the 10 ¾" liner, a simulation for running the screen section on composite pipe was performed. This was done to see if a load reduction would give the screen running operation better margins between loads and limitations. It was confirmed from simulations that it would not be possible to run the screen section on the composite pipe, due to problems with helical buckling. Therefore, the screen section could only be run on the string made up of conventional pipe. Since the application area for composite pipe is drilling, the results for the 10 ¾" liner and the 7 x 6 5/8" screen run on composite were anticipated.

6.1.5 Reelwell Simulations

Simulations performed by Reelwell for drilling the final section to TD showed better results than simulation performed in this study. Reelwell's hook load simulations (Appendix B) show that with their technology the hook load is lower than for running with conventional pipe. Comparing the simulation results also reveled that Reelwell's simulation for maximum torque at surface was lower than for drilling with conventional pipe. The main reason why Reelwell's simulations for hook load and torque generated lower loads was the "Heavy over light" solution proposed by Reelwell. By having a lighter fluid inside the strings and a heavier fluid in the outer annulus, an increase in buoyancy is achieved. This reduces the effective weight of the pipe, resulting in a reduction in hook load and torque. As simulations in Appendix E show, drilling to TD with the conventional drill string resulted in too high ECD. According to Reelwell, using their method will allow drilling the well section, without generating an ECD that will exceed the fracture gradient limit.

6.2 ECD Challenge

As mentioned earlier, there are multiple challenges related to drilling and completing an ERD well. For long horizontal wells there will always be fundamental factors limiting the maximum reach of the well. In chapter 2, under drilling challenges, some of them are listed. Simulations for this particular well show some of the fundamental challenges related to long horizontal wells. The main challenge for this specific well is the ECD. Based on theory, and previous drilled wells, it was anticipated that ECD would be the biggest challenge for drilling and completing this well. This was primarily due to the long horizontal displacement. Due to this challenge, and the diameter restrictions set by the previous casing for each section, it was decided to use a reamer to enlarge the hole sections OD. This would be performed while drilling. By applying this technique, a reduction in ECD can be accomplished. By increasing the clearance between the drill string and the wellbore wall, Δd, the frictional pressure drop is reduced. This had a positive effect on the generated ECD. An additional benefit of enlarging the hole diameter is related to running the following liner and screen section. A larger diameter gives a better clearance between the wellbore and the pipe that is run in hole. The application of the reamer on the drill string reduced the ECD. Unfortunately the simulated ECD was still too high, and exceeded the fracture pressure curve.

6.2.1 ECD for 12 ¼" x 13 1/2" hole

Drilling the 12 ¼" x 13 1/2" hole section with composite pipe was not possible according to simulations, due to problems with helical buckling. For the conventional drill string, simulations showed that the challenge was related to the ECD near section TD. Simulations show that the sudden reduction in formation fracture gradient near TD will cause the ECD to exceed the fracture gradient. Investigation into the geological data of the field revealed the source for this change in formation properties. The sudden drop in fracture gradient is due to a thin layer of Draupne shale located in this section. Below the Draupne shale is a thin layer of Draupne Sandstone. Both these layers have a lower fracture gradient than the previous Shetland Group interval. Since the collapse gradient in shale is low, shale collapse is a concern when drilling into shale. The collapse gradient for the shale is in this case larger than the fracture gradient is for the sandstone below. Therefore, when entering the Draupne Sandstone, the fracture gradient curve will shift more to the left. However, previous wells drilled in the same formation show higher fracture strength for the Draupne Sandstone. It is therefore most likely that the simulated fracture gradient of the Draupne Sandstone is underestimated in the top part of the sand. To avoid later problems with the Draupne shale the section TD was set below the shale (in the sandstone below). This would allow the 10 ¾" liner to seal off the Draupne shale section. Loss in the sandstone section is an acceptable risk, and preferred over risking shale collapse in the section above. One possible mitigation method to cope with the losses near section TD is pumping a LCM (lost circulation material) pill into the well to reduce the loss. The material in the pill will bridge over and seal the fractured zones.

6.2.2 ECD for 8 ½" x 9 ½" hole

Simulations for drilling the 8 ½" x 9 ½" hole showed that ECD would be a great challenge in this section. For both the conventional and the composite pipe, ECD simulations showed that the maximum ECD would exceed the fracture gradient. As mentioned earlier, the simulated ECD was higher for the composite pipe. This was due to the larger pipe OD for composite pipe, compared to the conventional pipe is the lower section. For the best case (conventional pipe) the difference between maximum ECD and the fracture gradient is approximately 0.065 sg (1.425 – 1.360). The drop in the formation fracture gradient starts from around 7200 mMD. From around 7200 mMD to 7300 mMD, the fracture gradient drops from around 1.785 to 1.360. Looking into the fields geological data, and comparing it with the selected well path, gave a better understanding to the change in formation properties. As shown in Appendix C, the final section drop (drop in inclination) is followed by a section build-up. The build-up stage starts around 6600 mMD. The plan is to build-up angle, until reaching the reservoir sand section, located in the layer above. The geological data show that during this section build up, a thin layer of Draupne shale will be encountered at approximately 7200 mMD. After exiting the thin shale, the bit will reach the reservoir sand, and continue drilling till TD. The main challenge here is that both the shale layer and the reservoir sand have a low fracture gradient. A low fracture gradient for a long horizontal well is not ideal. This results in an ECD exceeding the fracture gradient, potentially resulting in loss to the formation.

The selected flowrate for drilling the 8 ½" x 9 ½" hole section was less than the required minimum flowrate. The main reason for the low flowrate was the ECD limitation. Selecting a higher flowrate would have a negative impact on ECD. Since ECD is already too high, it is best not to increase flowrate more. At the same time, not using optimal flowrate would leave cuttings and debris in the hole, which can cause problems. One of these problems is related to the screen installation. Cuttings accumulations, especially in the inclined sections of the well, can reduce the effective well ID. A reduction in well ID can result in the screen not passing, which poses a great challenge for the lower completion installation. According to the flow simulation in Appendix E, the critical area that requires the highest flowrate is located around the 13 3/8" shoe. The well path figure in Appendix C show that the 13 3/8" shoe is located in the end of build section. Simulations show that the build section from around 1100 mMD to the 13 3/8" shoe requires a flowrate higher than the actual flowrate, to achieve sufficient cuttings transportation. If the cuttings transportation in this section is insufficient, cuttings will accumulate in the lower part of the slope and form a bed. With the selected flowrate and RPM, cuttings transport could be acceptable in the horizontal section below the 13 3/8" shoe. The accumulated cuttings in the inclined section can be handled by washing the well during trip out. The success for this procedure depends on the amount of cuttings left in the well. The maximum amount of cuttings can not exceed the operational limit. The operational limit indicates the amount of cuttings that can be left in the hole, without preventing the bit from reaching TD. With a manageable amount of cuttings in the inclined section, washing while tripping out is normally the preferred solution to this sort of problem. The simulation provides information about where there will be insufficient cuttings removal. During trip out, the drill string is stopped at the locations where cuttings accumulations are expected. The combination of a high RPM to lift the cuttings and sufficient flowrate to transport the cuttings out is used to transport the remaining cuttings out of the well. This procedure is performed in each area where it is assumed to be cuttings located.

An alternative solution to improve wellbore cleaning is installing one or multiple circulation subs in the drill string. A circulation sub can be used to redirect the flow through circulation valves, instead of the bit nozzles. When needed, the circulation sub can be opened to allow flow through. When the circulating sub is at the desired depth (where there are cuttings) the valve is shifted from closed to open position. This redirects flow circulation valve, and improves hole cleanup around the circulation sub. After sufficient hole cleaning has been achieved, the circulation sub is closed, and drilling continues. Weatherford have developed a new type of circulation sub. Unlike most circulating subs, which require a ball drop mechanism, their tool is activated using radio-frequency identification (RFID) tags. A ball drop activated circulation sub has a limited opening and closing capability. The RFID activated circulation sub have unlimited opening and closing capability. An RFID tag is circulated through the sub, and gives open/close commands to the antenna located in the circulating sub (Weatherford n.d.).

6.3 New Technology

There is technology available today that can help operators drill and complete longer and more complex wells. Looking at the challenges and limitations experienced in the simulations

for this well, it was investigated if there is technology and tools available to cope with these issues. One example of new technology is provided by Reelwell, and is mentioned earlier in this study. Their technology has the potential to improve the drilling process, helping us reaching TD. There are also other solutions available, addressing the other challenges related to ERD wells.

Hook load and tension load simulations for the 10 ¾" liner installation shows that the margin between the largest load and limit is not large. This meant that if the 12 ¼" x 13 ½" hole was longer, the 10 ¾" might not have reached section TD. This can pose a limitation for longer ERD wells drilled from the Brage platform, by limiting the liner setting depth. One way to address this challenge is to reduce the effective weight of the liner. Effective weight can be reduced by increasing the mud weight. However, increasing mud weight will not only increase the buoyancy effect. An increase in mud weight can result in exceeding the fracture gradient limit. One way to reducing the effective weight, without increasing the mud weight, is floating the liner. Instead of running in hole with an open liner where the same mud is present on inside and outside the liner, the idea is to run in with a closed or "sealed" liner. By isolating the liner, the inner part of it can be filled with a lighter mud, nitrogen or air. The effect of a light fluid/air on the inside is a reduction in effective liner weight. An added benefit with reducing the effective weight is a reduction in friction between liner and wellbore, which reduces drag. This technology have been developed and successfully deployed in offshore Norway. Floating the 10 ¾" liner helped Statoil drill a 10 km+ long well in 2006. The Gullfaks well A-32 C was in 2006 the longest well planned from an offshore installation. During the planning phase simulations revealed that it would not be possible to run the 10 ¾" liner to planned TD with conventional methods. Simulations showed that drag and buckling limits were exceeded by the generated loads. The vast weight of the 4660 m liner was the main reason for this. With the floatation method simulations showed that the liner would overcome the drag and buckling restrictions. A reduction in torque was also achieved. Buoyancy calculations reveled that the buoyant weight of the liner was reduced greatly. By using this technology, Statoil were able to run the 10 ¾" liner to section TD (Eck-Olsen et al. 2007). Applying this technology on the Brage field could help increasing the maximum length of the 10 ¾" liner interval, increasing the total length for future wells.

Similar floating technology has also been used for running sand screens. As for the 10 ¾" liner, simulations for the sand screen section show that the margins between load and limit for hook load and tension load are small (see Appendix E). One of the main challenges floating a sand screen, compared to a solid liner, is all the openings in the sand screen. These opening needs to be temporarily sealed to prevent flow to create a closed pressure-tight system. There are different methods to achieve this. In 2008 Baker Hughes developed a hydro-mechanical delay opening valve, to eliminate operational limitations and risks associated with the other methods. The basis of their technology was to have a valve system that works in combination with the sand screens to control the fluid flow into the liner. The fluid flow would enter through a filter container and sent through the valve system before entering the liner. This valve is closed during installation, not allowing fluid to pass through. Once the sand screen is installed, pressure is increased in the liner (to a preselected pressure).

This will activate a sequence that will open up the temporary closed valve, allowing the production of reservoir fluid (Bowen and Coronado, 2008). This technology shows that it is possible to overcome challenges related to hook load and buckling, for sand screen installation in longer sections.

The simulations for running the sand screen in Appendix E show that the margins before entering the helical buckling are small. For long completions and challenging well paths helical buckling is a great challenge. One way to improve margins when running the sand screen section is to install the lower completion in two runs. The combination of more drill pipe and less sand screens on the string will improve the helical buckling margins when running in hole. This solution has been developed and is in use today. When Statoil wanted to run a deep sidetrack on the Troll field, they had a challenging well path and long lower completion section. Simulations for running this long completion showed a potential for helical buckling. Halliburton's solution to this problem was to run the lower completion in two runs. The first sand screen section would be run to TD. The second section would then be run in hole, and stung into the first screen section (Smith et al. 2013).

7. Conclusion

The goal for this thesis was to investigate the potential for drilling and completing an ERD well from the Brage platform. Wellplan™ was used to investigate the drilling and completion of two well sections. Results were presented and challenges and limitations were identified and investigated based on theory. This work resulted in the following conclusion:

- Simulations results for drilling and completing the selected well were not promising.
- The biggest challenge drilling this well with a conventional method is related to the ECD exceeding the fracture gradient.
- According to Reelwell, the ECD problem in the final well section can be managed using their technology
- There is technology available that can have a positive impact on drilling and completing this and other ERD wells.

References

Aadnoy, B.S. *Modern Well Design.* CRC Press/Balkema, second edition, 2010. ISBN 978-0-415-88467-9

Aadnoy, B.S. and Hareland, *G. Analysis of Inflow Control Devices.* SPE 122824. Presented at the SPE Offshore Europe Oil & Gas Conference & Exhibition, Aberdeen, U.K. 8-11 September 2009.

Aadnoy, B.S and Looyeh, R. *Petroleum rock mechanics: Drilling Operations and Well Design.* Gulf Professional Publishing, first edition, 2011. SBN: 978-0-12-385546-6

Arukhe, J., Uchendu, C. and Nwoke, L. *Horizontal Screen Failures in Unconsolidated, High-Permeability Sandstone Reservoirs: Reversing the Trend*. SPE 97299. Presented at the SPE Annual Technical Conference and Exhibition held in Dallas, Taxas, USA. 9-12 October 2005.

Ayoola, O., Nnanna, E., Osadjere, P. and De Landro, W. *Expandable Sand Screen Deployment in Cased Hole Completions: SPDC Experience.* SPE 128601. Presented at the 33rd Annual SPE International Technical Conference and Exibithion in Abuja, Nigeria, August 3-5, 2008.

Bardsen. J., Hazel, P., Vasques, R.R.R., Hjorteland, O. and Eikeskog, O. *Improved Zonal Isolation in Open Hole Applications.* SPE 169190. Presented at the SPE Bergen One Day Seminar, Bergen, Norway. 2 April 2014.

Belayneh, A. *A Review of Buckling in Oil Wells.* Shaker Verlag, 2006. ISBN 3832250387

Bellarby, J. *Well Completion Design*. Elsevier B.V., first edition, 2009. ISBN 978-0-444-53210-7

Bennett, M.R., Montagna, J.M. and Penberthy, W.L. *Stand-alone Screens Vary In Effectiveness.* Oil & Gas Journal 1997. http://www.ogj.com/articles/print/volume-95/issue-32/regular-features/ogj-newsletter/stand-alone-screens-vary-in-effectiveness.html (accessed 01.06.15)

Bowen, E.G. and Coronado, M.P. *Providing Floating Capabilities in Latest-Generation Sand Screens.* SPE 117615. Presented at the International Thermal Operations and Heavy Oil Symposium, Calgary, Alberta, Canada. 20-23 October 2008

Cameron, C. *Drilling Fluids Design and Management for Extended Reach Drilling*. SPE 72290. Presented at the IADC/SPE Middle East Drilling Technology Conference, Bahrain, 22-24 October 2001

Carlson, J., Gurley, D., King, G., Price-Smith, C. and Waters, F. *Sand control: Why and How?* Schlumberger Oilfield review October 1992. Page 41-43.

Coberly, C. J. and Wagner, E. M. *Some considerations in the selection and installation of gravel packs for oil wells*. SPE 938080. Presented in Los Angeles, USA, 1937.

Eck-Olsen, J., Sletten, H. and Loklingholm, G. *Floating of 10 ¾" liner - A Method Used to Reach Beyond 10 km.* SPE 105839. Presented at the SPE/IADC Drilling Conference and Exhibition, Amsterdam, The Netherlands, 22-24 February 2007

Edment, B., Elliott, F., Gilchrist, J., Powers, B., Jansen, R., McPike, T., Onwusiri, H., Parler, M., Twynam, A. and van Kraneburg, A. *Improvements in Horizontal Gravel Packing*. Schlumberger Oilfield Review, Spring 2005. Page 50-60.

Ellis, T., Erkal, A., Goh, G., Jokela, T., Kvernstuen, S., Leung, E., Moen, T., Porturas., Skillingstad, T., Vorkinn, P.B. and Raffn, A.G. *Inflow Control Devices – Raising Profiles*. Schlumberger Oilfield Review Winter 2009/2010: 21, no.4. Page 30-37. https://www.slb.com/~/media/Files/resources/oilfield_review/ors09/win09/03_inflow_control_devices.pdf (accessed 01.06.15)

Furgier, J., Viguerie, B., Aubry, E. and Rivet, P. Stand Alone Screens: *What Key Parameters are Really Important for a Successful Design?* SPE 165170. Presented at the SPE European Formation Damage Conference and Exibithion in Noordwijk, The Netherlands, 5-7 June 2013.

Gupta, V.P., Yeap, A.H.P., Fischer, K.M., Mathis, R.S. and Egan, M.J. *Expanding the Extended Reach Envelope at Chayvo Field, Sakhalin Island.* SPE 168055. Presented at the IADC/SPE Drilling Conference and Exhibition, Fort Worth, USA. 4-6 March 2014.

Hill, K. E. *Factors Affecting the Use of Gravel in Oil Wells*. API-41-134. 1941

Hishida, H., Ueno, M., Higuchi, K. and Hatakeyama, T. *Prediction of Helical / Sinusoidal Buckling.* SPE 36384. Presented at the IADC/SPE Asia Pacific Drilling Technology Conference, Kuala Lumpur, Malaysia. 9-11 September 1996.

Inglis, T.A. *Petroleum engineering and development studies. Vol. 2: Directional Drilling.* Springer Science Business Media, LLC, 1987. ISBN 0 86019 716 7

Innes, G., Lacy, R., Neumann, J. and Guinot, F. *Combining Expandable & Intelligent Completions to Deliver a Selective Multizone Sandface Completion, Subsea Nigeria*. SPE 108601. Presented at Offhore Europe in Aberdeen, Scotland, U.K., 4-7 September 2007

Ismail, M. and Geddes, M.W. *Fifteen Years of Expandable Sand Screen Performance and Reliability*. SPE 166425. Presented at the SPE ATCE held in New Orleans, USA, 30 September -2 October 2013.

Jahn, F., Cook, M. and Graham, M. *Hydrocarbon Exploration & Production.* Elsevier, second edition, 2008. ISBN 978-0-444-53236-7

Jerez, H., Dias, R. and Tilley, J. *Offshore West Africa Deepwater ERD: Drilling Optimization Case*. SPE 163485. Presented at the SPE/IADC Drilling Conference and Exhibition, Amsterdam, The Netherlands, 5-7 March 2013.

King, G.E., Wildt, P.J. and O'Connell, E. *Sand Control Completion Reliability and Failure Rate Comparison With a Multi-Thousand Well Database*. SPE 84262. Presented at the SPE Technical Conference and Exhibition held in Denver, Colorado, USA. 5-8 October 2003.

Landmark A. Wellplan™ - https://www.landmarksoftware.com/Pages/WELLPLAN.aspx (accessed 03.06.2015)

Luo, Y., Bern, P.A. and Chambers, B.D. *Flow-Rate Predictions for Cleaning Deviated Wells*. SPE 23884. Presented at the IADC/SPE Drilling Conference, New Orleans, Louisiana, USA. 18-21 February, 1992

Nazari, T., Hareland, G. and Azar, J.J. SPE 132372. *Review of Cuttings Transport in Directional-Well Drilling: Systematic Approach.* Presented at the SPE Western Regional Meeting, Anaheim, California, USA. 27-29 May 2010.

Nguyen, P., Sanders, M., McMechan, D., Gibson, R. and Lord, D. *Tests expand knowledge of horizontal gravel packing*. Oil & Gas Journal. 2001. http://www.ogj.com/articles/print/volume-99/issue-34/drilling-production/tests-expand-knowledge-of-horizontal-gravel-packing.html (accessed 01.06.15)

NPD, n.d. Norwegian Petroleum Directory Facts Page. http://factpages.npd.no/ReportServer?/FactPages/PageView/field&rs:Command=Render&rc:Toolbar=false&rc:Parameters=f&NpdId=43651&IpAddress=80.239.24.2&CultureCode=en (accessed 01.06.2015).

Pajchel, B.S., Hansen, M.D., Galta, S., Thorsen, A.K. and Kurz, G. *Petrophysical Interpretation Using Magnetic Resonance In North Sea Horizontal Wells.* SPWLA-2011-U. Presented at the SPWLA 52nd Annual Logging Symposium, Colorado Springs, Colorado, USA. May 14-18, 2011

Pelfrene, G., Sellami, H. and Gerbaud, L. *Mitigating Stick-Slip In Deep Drilling Based On Optimization Of PDC Bit Design*. SPE 139839. Presented at the SPE /IADC Drilling Conference and Exhibition, Amsterdam, The Netherlands, 1-3 March 2011.

Renpu, Wan. *Advanced Well Completion Engineering*. Gulf Professional Publishing, third edition, 2011. ISBN 978-0-12-385868-9.

Rubiandini, R.S. *Extended Reach Drilling (ERD) Design in Deepwater Application.* SPE 115286. Presented at the IADC/SPE Asia Pacific Drilling Technology Conference and Exhibition, Jakarta, Indonesia. 25-27 August 2008.

Saucier, R. J. *Considerations in Gravel Pack Design*. SPE 4030, 1947.

Schlumberger, 2007. *Frac Packing: Fracturing for Sand Control*. Middle East &Asia Reservoir Review nr.8, 2007. Page 38-49. http://www.slb.com/~/media/Files/resources/mearr/num8/37_49.pdf (accessed 01.06.15)

SLB 2011/2012. *The science of oil and gas well construction*. Oilfield Review Winter 2011/2012:23, no. 4. Page 50-51.

Smith, P.E., Dahle, B.O., Prebeau-Menezes, L.J. and Gjelstad, G. *Case History: First Intelligent Well with Feed-Through Zonal Isolation in a Multilateral Sidetrack Completion in the Troll Field.* SPE 166657. Presented at the SPE Offshore Europe Oil and Gas Conference and Exhibition, Aberdeen, U.K. 3-6 September 2013.

Time, R.W. *Multiphase Flow Compendium 2009.* Chapter 2, page 11-40. Downloaded from Its Learning.

Vestavik, O.M., Syse, H. and Hole, O. *New Approach to Improve the Horizontal Drilling.* SPE 137821. Presented at the Canadian Unconventional Resources & International Petroleum Conference, Calgary, Alberta, Canada. 19-21 October 2010.

Vestavik, O., Egorenkow, M., Schmalhorst, B. and Falcao, J. *Extended Reach Drilling - new solution with a unique potential.* SPE 163463. Presented at the SPE/IADC Drilling Conference and Exhibition, Amsterdam, The Netherlands, 5-7 March 2013.

Weatherford n.d.– *JetStream™ RFID Actuated Drilling Circulation Sub.* http://www.weatherford.com/doc/wft233343 (accessed 01.06.2015).

Wu, J. and Wold, H.C.J. *Drag and Torque Calculations for Horizontal Wells Simplified for Field Use.* Oil & Gas Journal 1991. http://www.ogj.com/articles/print/volume-89/issue-17/in-this-issue/drilling/drag-and-torque-calculations-for-horizontal-wells-simplified-for-field-use.html
(accessed 01.06.15)

Abbreviations

BHA	Bottom hole assembly
C&P	Cased & Perforated
DHSV	Downhole safety valve
ECD	Equivalent circulating density
ECP	External casing packer
ERD	Extended reach drilling
HTHP	High temperature high pressure
ICD	Inflow control device
MD	Measured depth
OHGP	Open hole gravel pack
OOIP	Original oil in place
RFID	Radio-frequency identification
RDM	Reelwell drilling method
RPM	Revolutions per minute
SAS	Stand alone screen
TD	Target depth/Total depth
WAG	Water alternating gas
WOB	Weight on bit

List of Figures

Appendix E

List of Tables

Appendix A – Stress analysis

A.1 Burst

To calculate burst in a pipe or casing, the string is assumed to be a thin walled vessel. The vessel is made up by a tube that is closed at both ends. If this tube is pressurized on the inside, stresses will propagate in in the tubing wall, axially and tangentially. For tangential stress, Figure A.1a, the force acting on the plane is the sum of internal pressure multiplied with the internal area. The area that absorbs this force is the wall thickness on both sides. Tangential stress is then:

$$\sigma_t = \frac{F_t}{A_t} = \frac{PD_iL}{2tL} = \frac{1}{2}P\left(\frac{D_i}{t}\right) \quad \text{(A.1)}$$

Where σ_t represents the tangential stress, F_t is the tangential force acting on plane, A_t is the area absorbing the force, P is the pressure, D_i is the inner diameter, L is the length and t is the wall thickness.

For axial stress, Figure A.1b, the following equation is used:

$$\sigma_a = \frac{F_a}{A_a} = \frac{P\pi {D_i}^2}{4\pi Dt} = \frac{1}{4}P\left(\frac{D_i}{t}\right) \quad \text{(A.2)}$$

Where σ_a represents the axial stress, F_a is the axial force acting on plane, and A_a is the area absorbing the force.

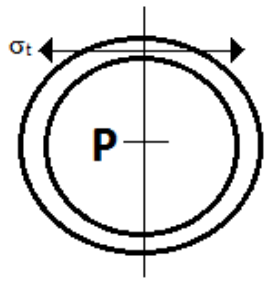

Figure A.1a: The tangential stress.

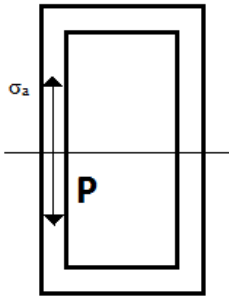

Figure A.1b: The axial stress

The ratio between the previous two stresses are $\sigma_t = 2\sigma_a$. This show that tangential stress, in a thin-walled vessel pressurized from within is twice the size of the axial stress. This implies that burst failure for this kind of vessel usually occurs in the tangential direction (Aadnøy, 2010).

The formula to calculate the API burst rating is based on Barlow's formula for thin walled pipe, eq. A.3. Unlike collapse and axial failure, burst failure only needs to experience failure in a very small piece of the pipe. The effect of change in the minimum wall thickness will have a direct impact on the burst rating. Most common mechanism that affects the wall thickness are casing wear for casing and corrosion for tubing (Bellarby, 2009).

$$P_b = Tol(\frac{2Y_p t}{D}) \quad \text{(A.3)}$$

Where P_b represents the burst pressure, *Tol* is the wall thickness tolerance correction (fraction), Y_p is the minimum yield strength, *t* is the pipe thickness and *D* is the outer pipe diameter.

A.2 Collapse

Collapse occurs in different modes, and each mode has its own formula. There are four collapse modes and the correct mode is selected using the pipes D/t ratio (outside diameter divided on the thickness). The four collapse modes are (Bellarby, 2009):

1. Elastic
2. Transitional
3. Plastic
4. Yield

Grade (ksi)	Elastic Collapse (*D*/*t*)	Transitional Collapse (*D*/*t*)	Plastic Collapse (*D*/*t*)	Yield Collapse (*D*/*t*)
40	>42.64	27.01–42.64	16.40–27.01	<16.40
55	>37.21	25.01–37.21	14.81–25.01	<14.81
80	>31.02	22.47–31.02	13.38–22.47	<13.38
90	>29.18	21.69–29.18	13.01–21.69	<13.01
95	>28.36	21.33–28.36	12.85–21.33	<12.85
110	>26.22	20.41–26.22	12.44–20.41	<12.44
125	>24.46	19.63–24.46	12.11–19.63	<12.11
140	>22.98	18.97–22.98	11.84–18.97	<11.84
155	>21.70	18.37–21.70	11.59–18.37	<11.59

Table A.1: Collapse modes (Bellarby, 2009).

Elastic collapse:

$$p_e = \frac{46.95*10^6}{{}^{D}/_{t}[({}^{D}/_{t})-1]^2} \quad \text{(A.4)}$$

Where p_e represents the elastic collapse rating, *D* is the outer diameter of the pipe and *t* is the pipe thickness.

Plastic collapse:

$$p_p = Y_p\left(\frac{A}{{}^{D}/_{t}} - B\right) - C \quad \text{(A.5)}$$

Where p_p represents the plastic collapse rating. *A*, *B* and *C* are values supplied from API 5C3 via formula or table A.2.

Grade (ksi)	*A*	*B*	*C*
40	2.95	0.0465	754
55	2.991	0.0541	1206
80	3.071	0.0667	1955
90	3.106	0.0718	2254
95	3.124	0.0743	2404
110	3.181	0.0819	2852
125	3.239	0.0895	3301
140	3.297	0.0971	3751
155	3.356	0.1047	4204

Table A.2: Plastic collapse factors (Bellarby, 2009).

Transitional collapse:

$$p_t = Y_p \left(\frac{F}{D/t} - G \right) \tag{A.6}$$

p_t represents the transitional collapse rating. *F* and *G* are values supplied from API 5C3 or from Table A.3.

Grade (ksi)	*F*	*G*
40	2.063	0.0325
55	1.989	0.036
80	1.998	0.0434
90	2.017	0.0466
95	2.029	0.0482
110	2.053	0.0515
125	2.106	0.0582
140	2.146	0.0632
155	2.188	0.0683

Table A.3: Transitional collapse factors (Bellarby, 2009).

Yield collapse:

Equation A.7 shows that the external pressure generates a stress equivalent to the minimum yield stress on the inside of the pipe.

$$p_y = 2Y_p \left[\frac{(D/t) - 1}{(D/t)^2} \right] \tag{A.7}$$

Where p_y represents the yield collapse rating and Y_P is the yield stress.

There are further complications related to yield collapse recognized by the API. For both the tension and the internal pressure the API derates collapse resistance. The equivalent external pressure (p_e) is given by the outer pressure (p_o) minus the internal pressure (p_i) in equation A.8.

$$p_e = p_o - \left(1 - \frac{2}{D/t}\right) p_i \quad \text{(A.8)}$$

The equivalent pressure can be affected if there is pressure being applied from the inside of the pipe or by the increase in hydrostatic pressure with depth. This can cause the differential pressure to remain stable with depth, while the collapse loads would increase (Bellarby, 2009).

A.3 Triaxial Analysis

The most commonly used criterion for yielding is the Von Mises (VME) yield condition. This criterion is based on the maximum distortion energy theorem. The material will yield if the Von Mises stress is larger than the yield stress limit. Not including torque, the yielding criterion is calculated using the axial, radial and hoop/tangential stress, as in equation A.9 (Bellarby, 2009).

$$\sigma_{VME} = \frac{1}{\sqrt{2}} [(\sigma_a - \sigma_t)^2 + (\sigma_t - \sigma_r)^2 + (\sigma_r - \sigma_a)^2]^{0.5} \quad \text{(A.9)}$$

Where σ_{VME} represents the triaxial stress, σ_a is the axial stress, σ_r is the radial stress and σ_t is the hoop/tangential stress.

A.4 Buckling

Buckling limits used for calculations are based on the theory of two buckling modes, sinusoidal and helical buckling. When a pipe is compressed inside the wellbore, the string will first go into the sinusoidal buckling mode. After exceeding the limit of sinusoidal buckling, the string will move into the helical buckling zone. Once this limit has been exceeded, the string may go into lockup. This occurs because the wall force is increased due to the helical buckling. Since buckling is a state of compression, the calculated buckling limits are negative. The following theory has been composed from Belayneh (2006).

An equation (A.10) for sinusoidal buckling in inclined wellbores has been derived by Dawson and Paslay in 1984. Their equation for sinusoidal buckling is widely accepted in the oil and gas industry.

$$F_{sin} = 2\left(\frac{EI\, w \sin\alpha}{r}\right)^{0.5} \quad \text{(A.10)}$$

$$I = \frac{\pi(d_o{}^4 - d_i{}^4)}{64}$$

Where F_{sin} represents the sinusoidal buckling load, E is the E-modulus, I is the axial moment of inertia of tubing, w is the buoyant weight per unit length of pipe/tubing, α is the angle of inclination and r is the radial clearance.

From equation A.10, researchers later derived formulas to be applied for helical buckling loads. The Dawson and Paslay's critical load equation was the starting point, and using it other researcher derived their own equations for helical buckling loads. One example is the

model of Chen et al. They derived the following equation for helical buckling in an inclined well:

$$F_{hel} = 2\sqrt{2(EI)^{0.5} * (wsin\alpha)^{0.5} * (1/r)^{0.5}} \quad (A.11)$$

Where F_{hel} is the helical buckling load.

Buckling in wells with curvature is a bit more complex. Robert F. Mitchell derived formulas for both sinusoidal and helical buckling.

$$F_{sin} = \frac{2EI\ k}{r} * \left[1 + \sqrt{\frac{wsin\alpha\ r}{EI\ k^2}}\right] \quad (A.12)$$

$$k = 1/R$$

Where R is the radius of curvature.

$$F_{hel} = 2.83 * F_{sin} \quad (A.13)$$

There are other factors besides inclination and curvature that affect the buckling loads. For example the presence of torque and friction will have an effect on the buckling loads. More theory and other models for buckling can be found in Belayneh (2006).

Appendix B –Reelwell

B.1 The Reelwell Drilling Method

Reelwell conducted a study for drilling the 9 ½" hole using the Reelwell Drilling Method (RDM). They were provided with the well path and well data used in this study, and asked to simulate results for drilling the section using their technology. The goal for this was to see if the RDM could get better simulation results for drilling the well.

The theory in the following section is composed from Vestavik et al. (2010), Vestavik et al. (2013) and www.reelwell.no. More details about the technology can be found there.

Unlike conventional drilling, RDM is based on the use of a dual drill pipe. Drilling fluid is transported to bit in the drill string annulus, while returns are taken back through the inner string. The idea was to see if their technology would provide better simulated results, compared to conventional drilling. Some challenges addressed by RDM related to ERD are:

1. Hole cleaning
2. ECD limitations
3. Torque and drag

1. Hole cleaning is an important factor when drilling long horizontal wells. Cuttings accumulation in annulus increases the risk for plugging the hole, and may lead to a stuck pipe situation. This is specially a problem for inclined sections. The RDM addresses this problem by transporting the cuttings from the bottom of the well through the inner string. No cuttings are transported in well annulus, eliminating the risk for cuttings accumulation in annulus.

2. For conventional drilling it is important to keep the well pressure within the safe pressure window to ensure hole stability. For long horizontal wells, this pressure window can be very small. As the horizontal distance increases, dynamic ECD will increase, limiting the length possible to drill. The RDM addresses this problem by eliminating the difference between annulus well pressure in the beginning and the end of the horizontal section. The pressure differential can be eliminated due to the short distance between bit and the dual float valve. The flow in the well annulus behind the dual float valve is usually very small (sometimes there is no flow), which results in eliminating the ECD for the horizontal section.

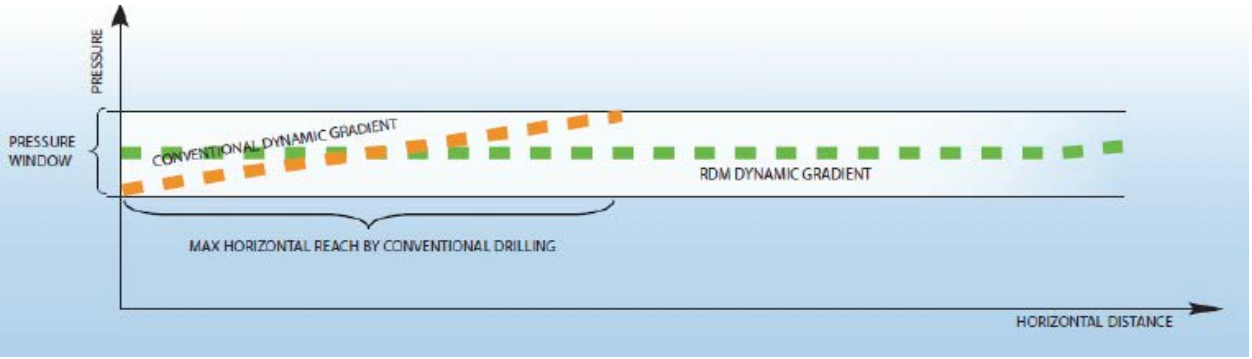

Figure B.1: Pressure gradients in horizontal well with the RDM (Vestavik et. al. 2010).

3. Torque and drag are two challenges that pose limitations when drilling long horizontal well sections. Drag is created due to friction between drill pipe and wellbore wall when the pipe is moving up and down. Torque comes from friction when rotating the pipe inside the well. Curved and horizontal sections will increase friction between drill string and wellbore. Cuttings in the annulus will increase the friction even more, increasing torque and drag during drilling. The RDM method eliminates the increase in friction due to cuttings in annulus by transporting cuttings through the inner string. A technique called “Heavy over light” has been developed to reduce torque and drag even more. The purpose with the “Heavy over light” concept is to increase the pipes’ buoyancy. By displacing a heavier fluid in the outer annulus, and drilling with a light fluid, the drill string will experience a positive buoyancy effect. It is the density difference between the two fluids that contributes to the buoyancy effect. Increasing the density difference will increase the buoyancy effect. This will result in a reduction in friction between the drill string and the well bore. This will ultimately have a positive impact on torque and drag.

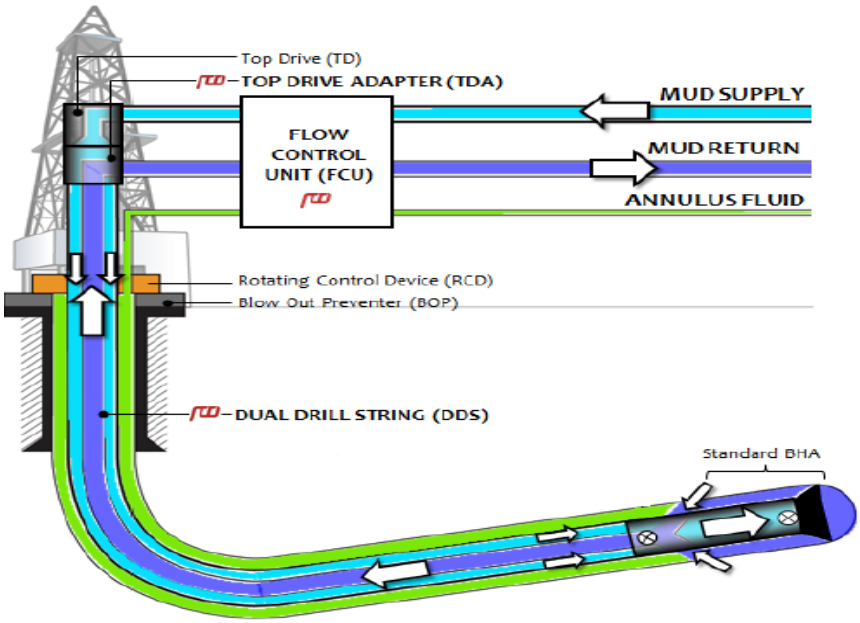

Figure B.2: Schematic of the proposed RDM arrangement, courtesy of Reelwell.

B.2 Simulations performed by Reelwell with the RDM.

Simulations performed by Reelwell show that the considerable reduction torque compared to the conventional simulations. Requiered flow rates for cuttings transport were also reduced. Constant downhole pressure resulted in stable ECD when drilling the horizontal section. Below are figures showing the simulations results provided by Reelwell.

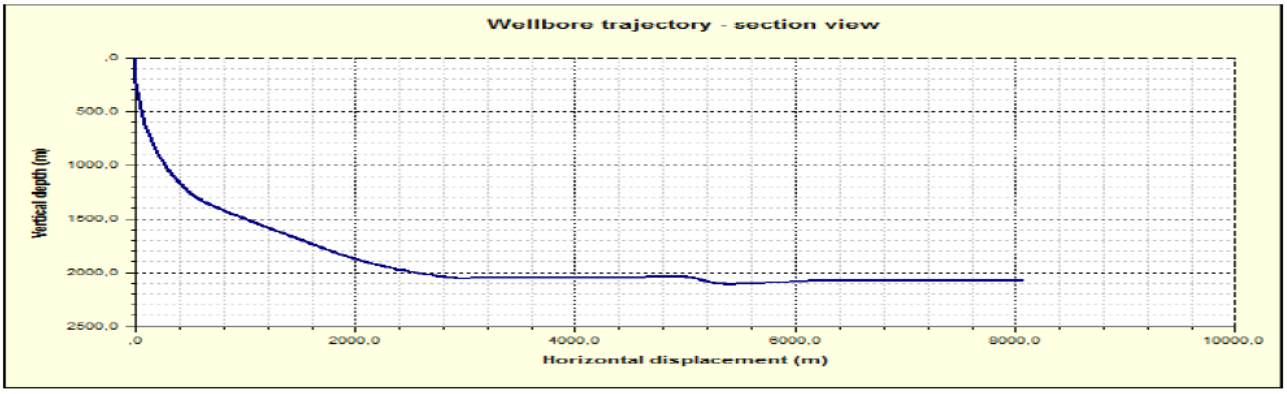

Figure B.3: Wellbore trajectory used for simulations, courtesy of Reelwell

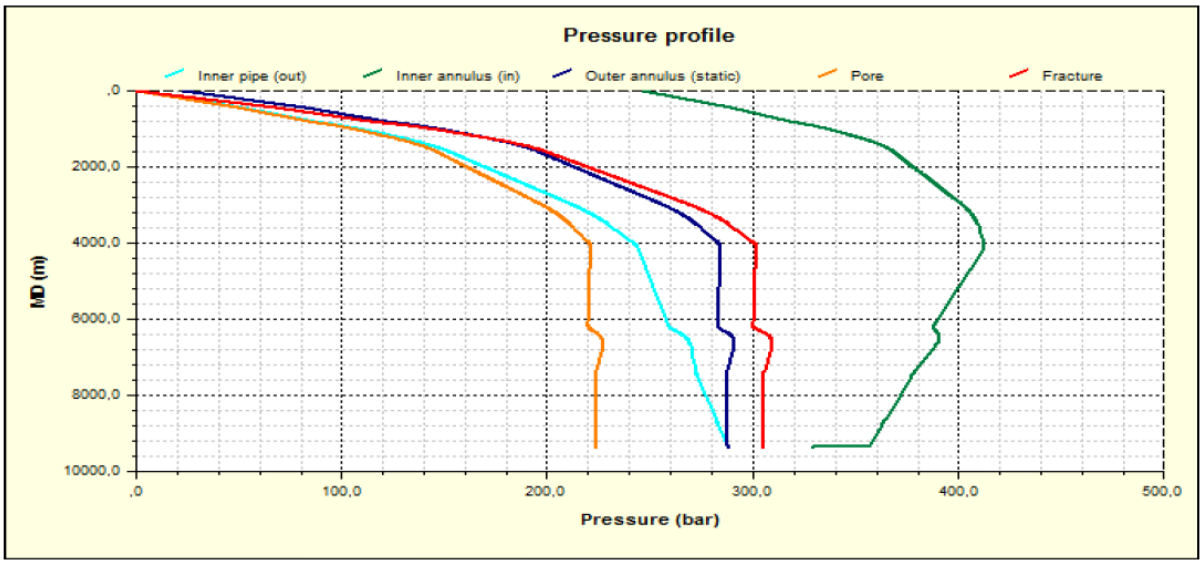

Figure B.4: Pressure profile drilling with the RDM, courtesy of Reelwell

Where the blue line represents pressure from 1.30 sg fluid in well annulus, the red line is pressure fracture pressure and the orange line is the pore pressure. The teal and green line are internal pressures in the dual drill string that are not seen by the formation.

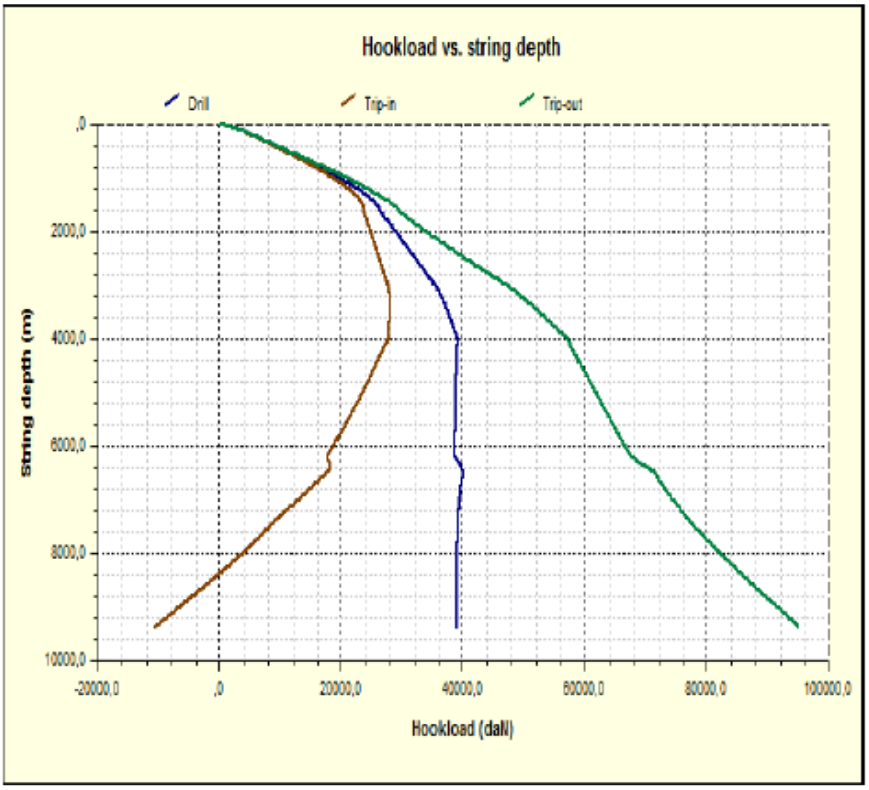

Figure B.5: Drag profile for drilling with the RDM, courtesy of Reelwell

Figure B.5 show a reduction in hook load for all three scenarios, compared to the hook load values for the conventional drilling simulation. Simulations for conventional drilling showed a maximum hook load of 186 ton (181423 daN) for trip-out, and 101 ton (93163 daN) for drilling. Drilling simulations can be found in Appendix E.

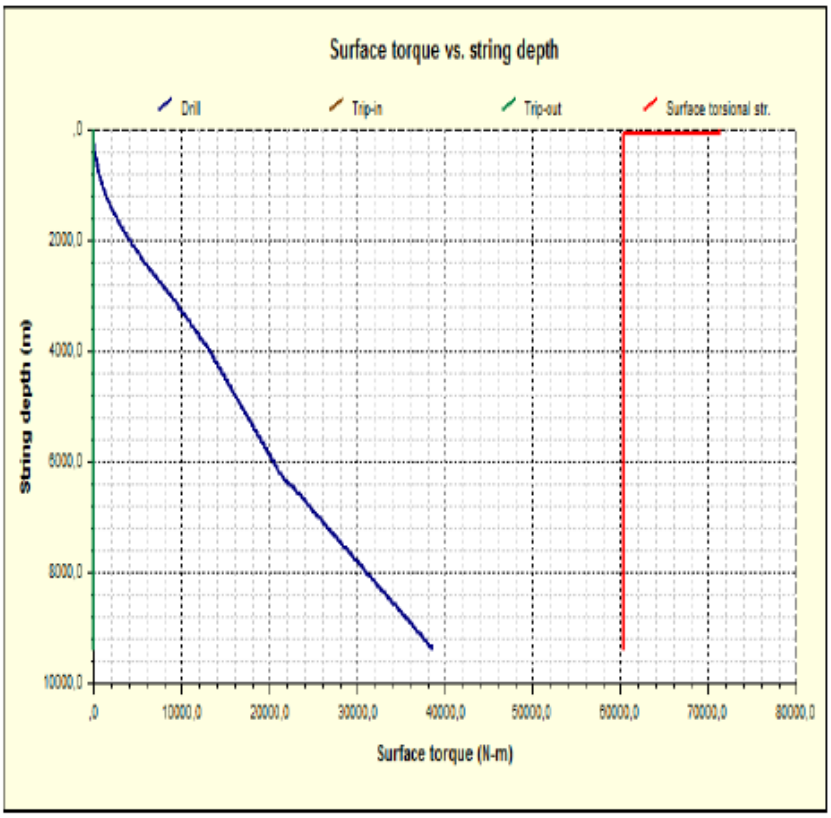

Figure B.6: Torque profile for drilling with the RDM, courtesy of Reelwell

Figure B.6 show that the simulated value of the torque for drilling with the RDM is about 38 kNm. Simulations performed in Wellplan™ for the conventional drilling showed a maximum torque at about 56 kNm. Drilling simulations can be found in Appendix E.

The RDM has a “built-in” Managed Pressure Drilling (MPD) system, which improves ECD control by preventing pressure differences during pump start and stop. A backpressure is introduced from surface to keep the pressure downhole constant. This backpressure can be altered to deliver an ECD that is less than the fracture gradient. This, in addition to the possibility to alter the active circulating fluid, can deliver an ECD that will stay within the safe drilling window. To generate an ECD value that is below the fracture gradient, Reelwell proposed the following parameters to cope with the ECD problem, using their technology:

- Flowrate above 800 l/min
- 1.30 sg fluid in well annulus
- 1.05 sg active circulation fluid

With these parameters, it would be possible to keep ECD below the fracture gradient.

Appendix C – Setup

The setup in Appendix C was composed using data from well previously drilled from the Brage platform. The proposed well design is similar to the standard well design concept on Brage. Sections lengths and setting depths were set before starting the study. The setup for the various drill strings and completion strings was created to fit this particular well.

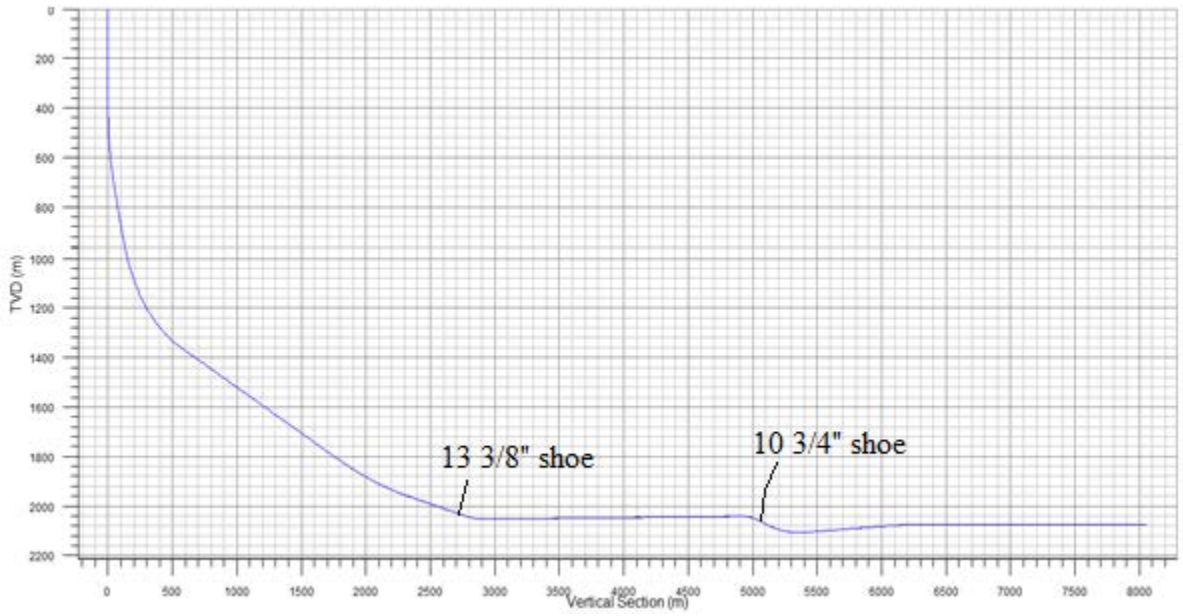

Figure C.1: The selected well path for the investigated well.

Hole Size	Casing Type	Interval	[m]
24”	18 5/8” Surf. (Preinstalled)	39-1050	MD
17 ½”	13 3/8”	36 – 1025	MD
17 ½”	14	1025-1050	MD
17 ½”	13 3/8”	1050-3800	MD
17 ½”	14	3800-3934	MD
17 ½”	13 3/8”	3934 3969	MD
13 ½”	10 3/4” Liner	3919-6380	MD
8 ½” x 9 ½”	6 5/8” Screen	6330 - 9390	MD

Table C.1: Hole and casing data for the well

Drilling Fluid			
Hole Section	**Base Fluid**	**Type**	**Density [SG]**
12 ¼” x 13 ½”	Oil	Versatec	1.43
8 ½” x 9 ½”	Oil	Versatec	1.18
Running screens in 8 ½”	Oil	Versapro	1.18

Table C.2: The selected mud for the two sections.

12 ¼" x 13 ½" hole - Conventional Pipe - WellPlan™ Setup

	Section Type	Measured Depth (m)	Length (m)	ID (in)	Drift (in)	Effective Hole Diameter (in)	Friction Factor	Linear Capacity (L/m)	Item Description
1	Casing	3969,00	3969,000	12,347	12,258	17,500	0,20	77,28	13 3/8 in, 72 ppf, P-110 (XH),
2	Open Hole	6329,00	2360,000	13,500		13,500	0,30	92,35	10 3/4 in, 60.7 ppf, P-110,
3	Open Hole	6380,00	51,000	12,250		12,250	0,30	76,04	
4									

Table C.3: Hole section data for 12 ¼" x 13 ½" hole (Copy from WellPlan™).

	Section Type	Length (m)	Measured Depth (m)	OD (in)	ID (in)	Weight (ppf)	Item Description
1	Drill Pipe	1309,640	1309,64	6,625	5,901	31,54	Drill Pipe 6 5/8 in, 27.70 ppf, S (XH), FH, P
2	Drill Pipe	4980,000	6289,64	5,500	4,778	26,33	Drill Pipe 5 1/2 in, 21.90 ppf, S, FH, P
3	Heavy Weight	9,000	6298,64	5,000	3,000	49,99	Heavy Weight Drill Pipe, 5,000 in, 74,40 kg/m, 1340 MOD, NC 50
4	Sub	1,000	6299,64	5,400	2,160	45,24	Cross Over, 5,400 in, 67,32 kg/m, 4130-80, 4 1/2 REG
5	Heavy Weight	18,000	6317,64	5,000	3,000	49,99	Heavy Weight Drill Pipe, 5,000 in, 74,40 kg/m, 1340 MOD, NC 50
6	Jar	9,330	6326,97	6,500	2,750	143,00	Hydraulic Jar, 6,500 in, 212,81 kg/m, 4145H MOD, 4 1/2" IF
7	Stabilizer	2,000	6328,97	4,500	2,000	43,43	Integral Blade Stabilizer 6 3/4" FG, 4 1/2 x2 in
8	Heavy Weight	9,000	6337,97	5,000	3,000	49,99	Heavy Weight Drill Pipe, 5,000 in, 74,40 kg/m, 1340 MOD, NC 50
9	Stabilizer	2,000	6339,97	4,500	2,000	48,11	Integral Blade Stabilizer 6 3/4" FG, 4 1/2x1 1/2 in
10	Sub	0,800	6340,77	7,000	2,812	110,00	Non-Mag Crossover Sub 6 3/4" Stop Sub, 6 3/4" in
11	MWD	7,300	6348,07	6,750	2,813	113,51	Logging While Drilling TesTrak, 6 3/4 in
12	Sub	2,100	6350,17	6,875	2,813	105,00	Non-Mag Crossover Sub, 6,875 in, 156,26 kg/m, SS07, NC 50 x 6 3/4" T2
13	MWD	2,380	6352,55	6,750	2,264	167,84	Logging While Drilling, 6,750 in, 249,77 kg/m, SS07, 8 1/4" T2
14	MWD	3,020	6355,57	6,750	1,875	175,18	Logging While Drilling, 6,750 in, 260,70 kg/m, SS07, 6 3/4" T2
15	Sub	2,100	6357,67	6,960	2,340	78,91	Non-Mag Crossover Sub, 6,960 in, 117,43 kg/m, 1340 MOD, 5 1/2 REG
16	MWD	4,950	6362,62	6,750	2,281	160,17	Pulser Sub, 6,750 in, 238,36 kg/m, SS07, 6 3/4" T2
17	Stabilizer	1,310	6363,93	6,750	2,250	84,00	Non-Mag Integral Blabe Stabilizer, 6,750 in, 84,00 ppf, SS07 (XH), 6 3/4" T2
18	MWD	5,000	6368,93	6,750	2,281	178,04	MWD Tool, 6,750 in, 264,95 kg/m, SS07, 6 3/4" T2
19	MWD	2,200	6371,13	6,750	2,281	168,43	MWD Tool, 6,750 in, 250,65 kg/m, SS07, 6 3/4" T2
20	Stabilizer	1,700	6372,83	6,750	2,299	117,29	Non-Mag Integral Blabe Stabilizer, 6,750 in, 117,29 ppf, SS07 (XH), 6 3/4" T2
21	MWD	6,590	6379,42	9,625	2,375	192,18	MWD Tool, 9,625 in, 192,18 ppf, 15-15LC MOD (1) [SH], 7 5/8" Reg
22	Bit	0,580	6380,00	12,250		739,17	Polycrystalline Diamond Bit, 1,210 in²

Table C.4: String and BHA specifications for 12 ¼" x 13 ½ " hole (Copy from WellPlan™).

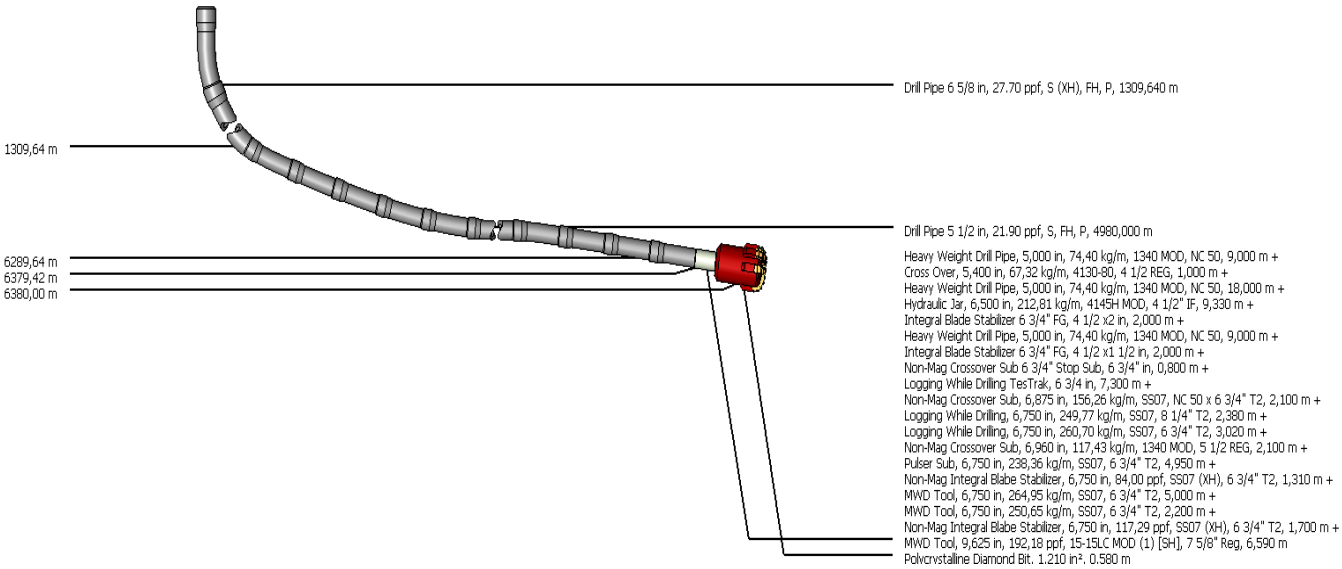

Figure C.2: String and BHA specifications for 12 ¼" x 13 ½" hole (Copy from WellPlan™).

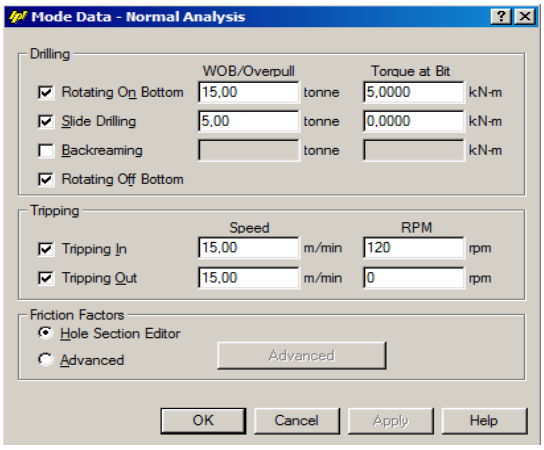

Figure C.3: Run parameters for 12 ¼" x 13 ½ " string (Copy from WellPlan™).

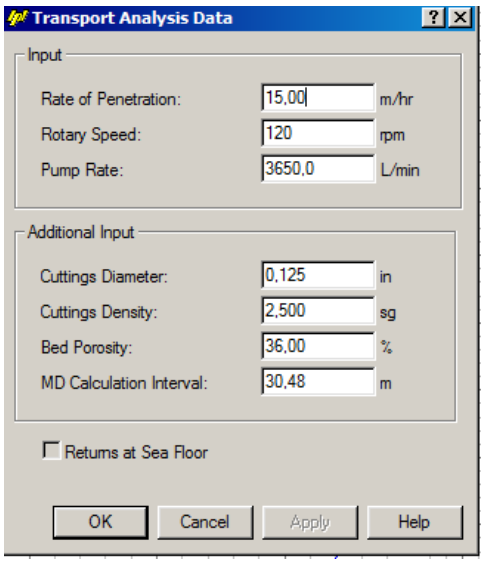

Figure C.4: Transport analysis data for 12 ¼" x 13 ½ "hole (Copy from WellPlan™).

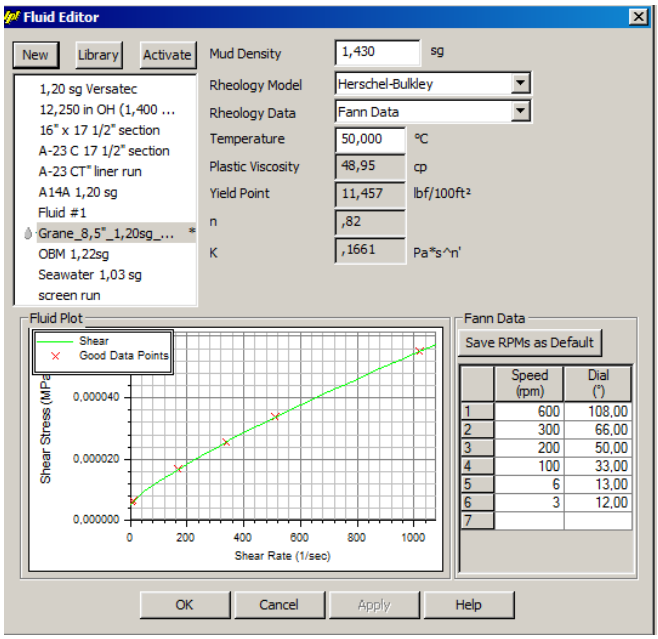

Figure C.5: Fluid data - 12 ¼" x 13 ½ " hole (Copy from WellPlan™).

10 ¾ " Liner - Conventional Pipe - WellPlan™ Setup

	Section Type	Measured Depth (m)	Length (m)	ID (in)	Drift (in)	Effective Hole Diameter (in)	Friction Factor	Linear Capacity (L/m)	Item Description
1	Casing	3969,00	3969,000	12,347	12,250	17,500	0,20	77,25	13 3/8 in, 72,000 ppf, P-110, 13 3/8" Vam T
2	Open Hole	6329,00	2360,000	13,500		13,500	0,30	92,35	13,5 in
3	Open Hole	6380,00	51,000	12,250		12,250	0,30	76,04	
4									

Table C.5: Hole section data running 10 ¾ " Liner (Copy from WellPlan™).

	Section Type	Length (m)	Measured Depth (m)	OD (in)	ID (in)	Weight (ppf)	Item Description
1	Drill Pipe	5,000	5,00	6,625	5,000	32,42	Drill Pipe, 6,625 in, 32,42 ppf, S (XH), FH Vam Eis
2	Heavy Weight	3099,000	3104,00	6,625	4,500	71,34	Heavy Weight Drill Pipe, 6,625 in, 71,34 ppf, 1340 MOD (XH), 6 5/8 FH
3	Heavy Weight	765,000	3869,00	6,625	4,500	71,34	Heavy Weight Drill Pipe, 6,625 in, 71,34 ppf, 1340 MOD, 6 5/8 FH
4	Casing	2511,000	6380,00	10,750	9,660	60,70	10 3/4 in, 60,700 ppf, P-110 (ACTIVE), Vam TOP
5							

Table C.6: String specifications for 10 ¾ " Liner (Copy from WellPlan™).

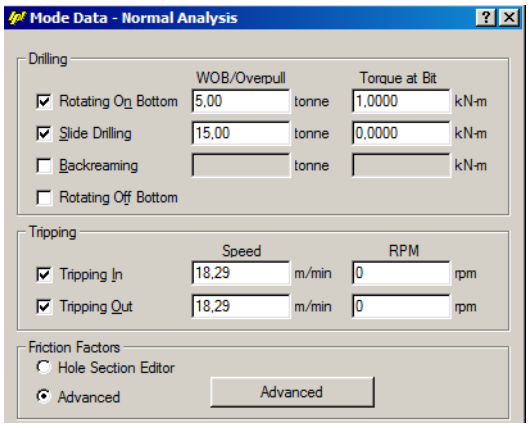

Figure C.6: Run parameters for 10 ¾ " Liner (Copy from WellPlan™).

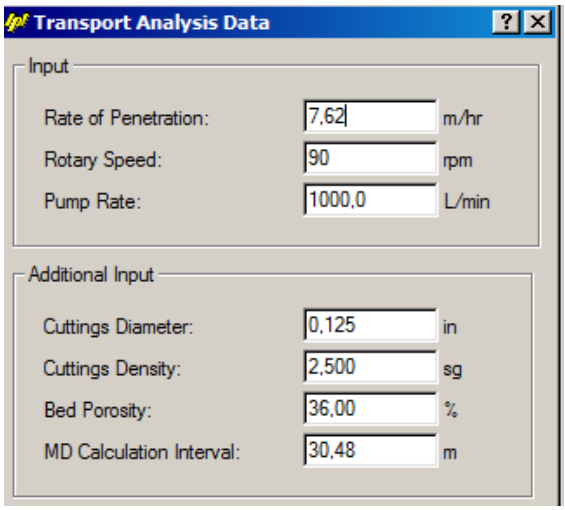

Figure C.7: Transport analysis data for 10 ¾" Liner (Copy from WellPlan™).

8 ½” x 9 ½ “ hole - Conventional Pipe - WellPlan™ Setup

	Section Type	Measured Depth (m)	Length (m)	ID (in)	Drift (in)	Effective Hole Diameter (in)	Friction Factor	Linear Capacity (L/m)	Item Description
1	Casing	3969,00	3969,000	12,347	12,258	17,500	0,20	77,28	13 3/8 in, 72 ppf, P-110 (XH).
2	Casing	6380,00	2411,000	9,660	9,504	13,500	0,25	47,28	10 3/4 in, 60.7 ppf, P-110.
3	Open Hole	9350,00	2970,000	9,500		9,500	0,30	45,73	
4	Open Hole	9400,00	50,000	8,500		8,500	0,30	36,61	
5									

Table C.7: Hole section data for 8 ½” x 9 ½” hole (Copy from WellPlan™).

	Section Type	Length (m)	Measured Depth (m)	OD (in)	ID (in)	Weight (ppf)	Item Description
1	Drill Pipe	3914,210	3914,21	6,625	5,901	31,54	Drill Pipe 6 5/8 in, 27.70 ppf, S (XH), FH, P
2	Drill Pipe	5400,000	9314,21	5,500	4,778	26,33	Drill Pipe 5 1/2 in, 21.90 ppf, S, FH, P
3	Heavy Weight	9,000	9323,21	5,000	3,000	49,99	Heavy Weight Drill Pipe, 5,000 in, 74,40 kg/m, 1340 MOD, NC 50
4	Sub	1,000	9324,21	5,400	2,160	45,24	Cross Over, 5,400 in, 67,32 kg/m, 4130-80, 4 1/2 REG
5	Heavy Weight	18,000	9342,21	5,000	3,000	49,99	Heavy Weight Drill Pipe, 5,000 in, 74,40 kg/m, 1340 MOD, NC 50
6	Jar	9,330	9351,54	6,500	2,750	143,00	Hydraulic Jar, 6,500 in, 212,81 kg/m, 4145H MOD, 4 1/2" IF
7	Stabilizer	2,000	9353,54	4,500	2,000	43,43	Integral Blade Stabilizer 6 3/4" FG, 4 1/2x2 in
8	Heavy Weight	9,000	9362,54	5,000	3,000	49,99	Heavy Weight Drill Pipe, 5,000 in, 74,40 kg/m, 1340 MOD, NC 50
9	Stabilizer	2,000	9364,54	4,500	2,000	48,11	Integral Blade Stabilizer 6 3/4" FG, 4 1/2x1 1/2 in
10	Sub	0,800	9365,34	7,000	2,812	110,00	Non-Mag Crossover Sub 6 3/4" Stop Sub, 6 3/4" in
11	MWD	7,300	9372,64	6,750	2,813	113,51	Logging While Drilling TesTrak, 6 3/4 in
12	Sub	2,100	9374,74	6,875	2,813	105,00	Non-Mag Crossover Sub, 6,875 in, 156,26 kg/m, SS07, NC 50 x 6 3/4" T2
13	MWD	2,380	9377,12	6,750	2,264	167,84	Logging While Drilling, 6,750 in, 249,77 kg/m, SS07, 8 1/4" T2
14	MWD	3,020	9380,14	6,750	1,875	175,18	Logging While Drilling, 6,750 in, 260,70 kg/m, SS07, 6 3/4" T2
15	Sub	2,100	9382,24	6,960	2,340	78,91	Non-Mag Crossover Sub, 6,960 in, 117,43 kg/m, 1340 MOD, 5 1/2 REG
16	MWD	4,950	9387,19	6,750	2,281	160,17	Pulser Sub, 6,750 in, 238,36 kg/m, SS07, 6 3/4" T2
17	Stabilizer	1,310	9388,50	6,750	2,250	84,00	Non-Mag Integral Blabe Stabilizer, 6,750 in, 84,00 ppf, SS07 (XH), 6 3/4" T2
18	MWD	5,000	9393,50	6,750	2,281	178,04	MWD Tool, 6,750 in, 264,95 kg/m, SS07, 6 3/4" T2
19	MWD	2,200	9395,70	6,750	2,281	168,43	MWD Tool, 6,750 in, 250,65 kg/m, SS07, 6 3/4" T2
20	Stabilizer	1,700	9397,40	6,750	2,299	117,29	Non-Mag Integral Blabe Stabilizer, 6,750 in, 117,29 ppf, SS07 (XH), 6 3/4" T2
21	Stabilizer	2,200	9399,60	6,750	3,000	246,65	Adjustable Stabilizer, 6,750 in, 246,65 ppf, 1340 MOD (XH), 6 3/4" T2
22	Bit	0,400	9400,00	8,500		200,00	0x11, 0,778 in²

Table C.8: String and BHA specifications for 8 ½” x 9 ½” hole (Copy from WellPlan™).

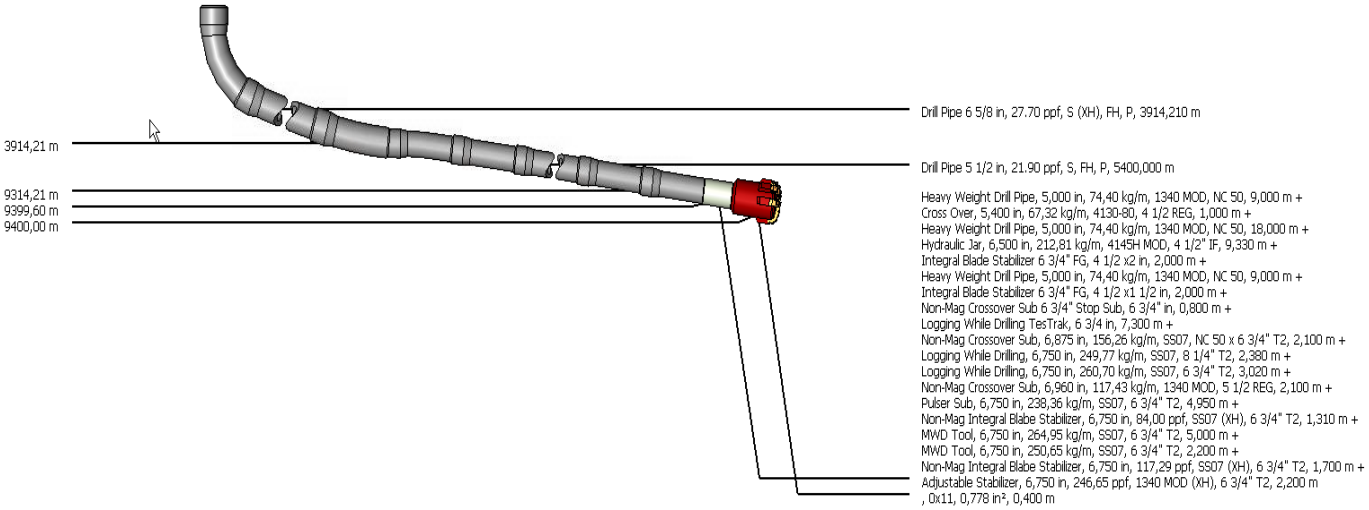

Figure C.8: String and BHA specifications for 8 ½” x 9 ½” hole (Copy from WellPlan™).

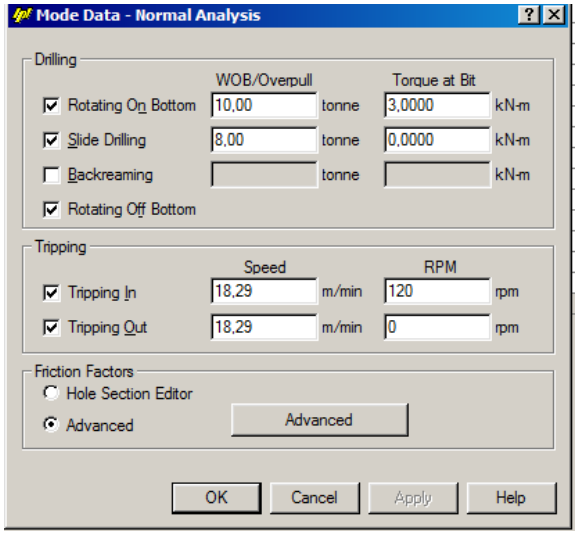

Figure C.9: Run parameters for 8 ½" x 9 ½ " string (Copy from WellPlan™).

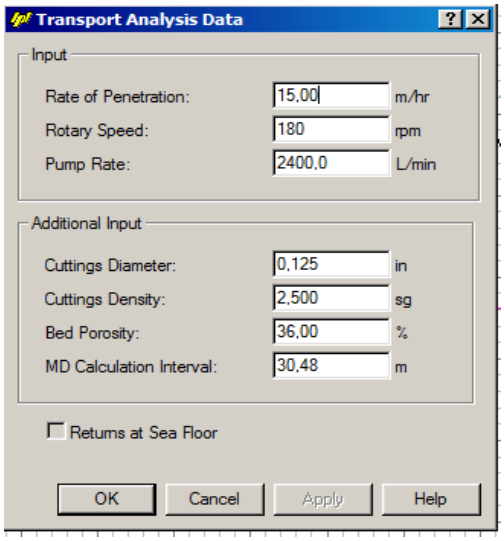

Figure C.10: Transport analysis data for 8 ½" x 9 ½ " hole (Copy from WellPlan™).

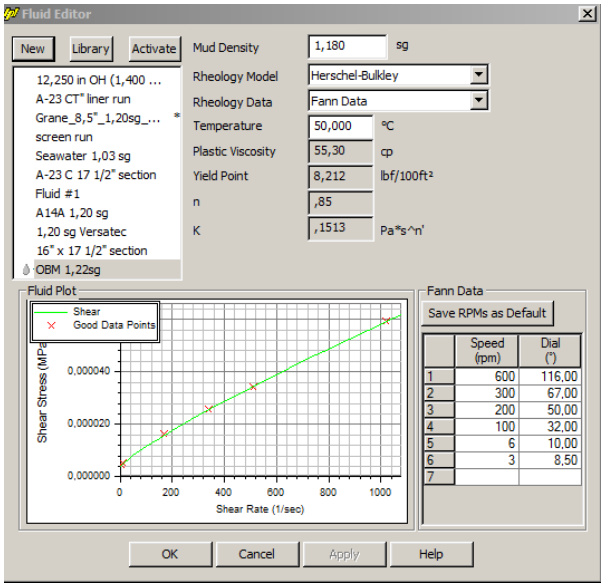

Figure C.11: Fluid data – 8 ½" x 9 ½ " hole (Copy from WellPlan™).

7” x 6 $^{5}/_{8}$” Liner– Conventional Pipe - WellPlan™ Setup

	Section Type	Measured Depth (m)	Length (m)	ID (in)	Drift (in)	Effective Hole Diameter (in)	Friction Factor	Linear Capacity (L/m)	Item Description
1	Casing	3969.00	3969.000	12.347	12.250	17.755	0.25	77.25	13 3/8 in, 72.000 ppf, L-80 (ACTIVE),
2	Casing	6380.00	2411.000	9.660	9.504	17.500	0.25	47.28	10 3/4 in, 60.700 ppf, L-80 (ACTIVE),
3	Open Hole	9390.00	3010.000	9.500		9.500	0.30	45.73	
4									

Table C.9: Hole section data running 7” x 6 5/8” Liner (Copy from WellPlan™).

	Section Type	Length (m)	Measured Depth (m)	OD (in)	ID (in)	Weight (ppf)	Item Description
1	Heavy Weight	390.870	390.87	6.625	4.500	71.39	Heavy Weight Drill Pipe, 6.625 in, 71.39 ppf, 1340 MOD, 6 5/8 FH
2	Drill Pipe	400.000	790.87	6.625	5.901	32.42	Drill Pipe, 6.625 in, 32.42 ppf, S-135_2 [SH], FH
3	Heavy Weight	1250.000	2040.87	5.500	3.625	51.16	Heavy Weight Drill Pipe, 5.500 in, 51.16 ppf, 1340 MOD, 5 1/2 FH
4	Heavy Weight	2300.000	4340.87	6.625	4.500	71.39	Heavy Weight Drill Pipe, 6.625 in, 71.39 ppf, 1340 MOD, 6 5/8 FH
5	Drill Pipe	1980.000	6320.87	6.625	5.901	32.42	Drill Pipe, 6.625 in, 32.42 ppf, S-135_2[SH], FH
6	Tubing	31.130	6352.00	7.000	6.184	29.00	Casing, 7.000 in, 29 ppf, L-80,
7	Tubing	1140.000	7492.00	6.625	5.920	24.00	Casing, 6.625 in, 24.00 ppf, L-80 [XH], Vam Top
8	Packer	11.000	7503.00	8.250	4.670	23.00	Casing External Packer, 8.250 in, 23.00 ppf, 4145H MOD [SH], Vam TOP
9	Sand Control Screen	600.000	8103.00	7.420	5.965	28.00	Mesh, 7.420 in, 28.00 ppf, 13-CR-L80, Vam Top
10	Packer	11.000	8114.00	8.250	4.670	23.00	Casing External Packer, 8.250 in, 23.00 ppf, 4145H MOD [SH], Vam TOP
11	Sand Control Screen	504.000	8618.00	6.625	5.965	28.06	Mesh, 6.625 in, 28.06 ppf, 13-CR-L80, Vam Top
12	Packer	11.000	8629.00	8.250	4.670	23.00	Casing External Packer, 8.250 in, 23.00 ppf, 4145H MOD [SH], Vam TOP
13	Sand Control Screen	504.000	9133.00	7.420	5.965	28.00	Mesh, 7.420 in, 28.00 ppf, 13-CR-L80, Vam Top
14	Packer	9.000	9142.00	8.250	4.670	23.00	Casing External Packer, 8.250 in, 23.00 ppf, 4145H MOD [SH], Vam TOP
15	Sand Control Screen	248.000	9390.00	7.420	5.965	28.00	Mesh, 7.420 in, 28.00 ppf, 13-CR-L80, Vam Top
16							

Table C.10: String and BHA specifications for 7” x 6 5/8” Liner (Copy from WellPlan™).

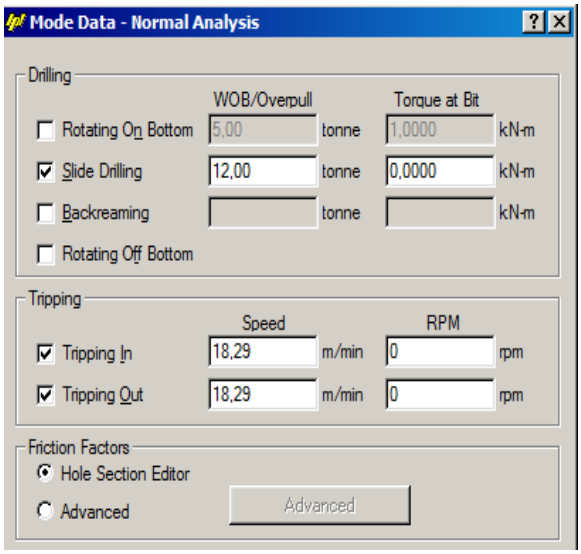

Figure C.12: Run parameters for 7” x 6 5/8” Liner (Copy from WellPlan™).

12 ¼” x 13 ½“ hole - Composite Drill Pipe - WellPlan™

	Section Type	Measured Depth (m)	Length (m)	ID (in)	Drift (in)	Effective Hole Diameter (in)	Friction Factor	Linear Capacity (L/m)	Item Description
1	Casing	3969,00	3969,000	12,347	12,258	17,500	0,20	77,28	13 3/8 in, 72 ppf, P-110 (XH),
2	Open Hole	6329,00	2360,000	13,500		13,500	0,30	92,35	10 3/4 in, 60.7 ppf, P-110,
3	Open Hole	6380,00	51,000	12,250		12,250	0,30	76,04	
4									

Table C.11: Hole section data for 12 ¼” x 13 ½“ hole (Copy from WellPlan™).

	Section Type	Length (m)	Measured Depth (m)	OD (in)	ID (in)	Weight (ppf)	Item Description
1	Drill Pipe	1309,640	1309,64	5,875	4,400	14,25	Drill Pipe 5,875 in, 14.2 ppf, Composite
2	Drill Pipe	4980,000	6289,64	5,875	4,400	14,25	Drill Pipe 5,875 in, 14.2 ppf, Composite
3	Heavy Weight	9,000	6298,64	6,625	4,500	73,50	Heavy Weight Drill Pipe Grant Prideco - Spiral, 6 5/8 in, 73.50 ppf
4	Sub	1,000	6299,64	5,400	2,160	45,24	Cross Over, 5,400 in, 67,32 kg/m, 4130-80, 4 1/2 REG
5	Heavy Weight	18,000	6317,64	5,000	3,000	49,99	Heavy Weight Drill Pipe, 5,000 in, 74,40 kg/m, 1340 MOD, NC 50
6	Jar	9,330	6326,97	6,500	2,750	143,00	Hydraulic Jar, 6,500 in, 212,81 kg/m, 4145H MOD, 4 1/2" IF
7	Stabilizer	2,000	6328,97	4,500	2,000	43,43	Integral Blade Stabilizer 6 3/4" FG, 4 1/2 x2 in
8	Heavy Weight	9,000	6337,97	5,000	3,000	49,99	Heavy Weight Drill Pipe, 5,000 in, 74,40 kg/m, 1340 MOD, NC 50
9	Stabilizer	2,000	6339,97	4,500	2,000	48,11	Integral Blade Stabilizer 6 3/4" FG, 4 1/2 x1 1/2 in
10	Sub	0,800	6340,77	7,000	2,812	110,00	Non-Mag Crossover Sub 6 3/4" Stop Sub, 6 3/4" in
11	MWD	7,300	6348,07	6,750	2,813	113,51	Logging While Drilling TesTrak, 6 3/4 in
12	Sub	2,100	6350,17	6,875	2,813	105,00	Non-Mag Crossover Sub, 6,875 in, 156,26 kg/m, SS07, NC 50 x 6 3/4" T2
13	MWD	2,380	6352,55	6,750	2,264	167,84	Logging While Drilling, 6,750 in, 249,77 kg/m, SS07, 8 1/4" T2
14	MWD	3,020	6355,57	6,750	1,875	175,18	Logging While Drilling, 6,750 in, 260,70 kg/m, SS07, 6 3/4" T2
15	Sub	2,100	6357,67	6,960	2,340	78,91	Non-Mag Crossover Sub, 6,960 in, 117,43 kg/m, 1340 MOD, 5 1/2 REG
16	MWD	4,950	6362,62	6,750	2,281	160,17	Pulser Sub, 6,750 in, 238,36 kg/m, SS07, 6 3/4" T2
17	Stabilizer	1,310	6363,93	6,750	2,250	84,00	Non-Mag Integral Blabe Stabilizer, 6,750 in, 84,00 ppf, SS07 (XH), 6 3/4" T2
18	MWD	5,000	6368,93	6,750	2,281	178,04	MWD Tool, 6,750 in, 264,95 kg/m, SS07, 6 3/4" T2
19	MWD	2,200	6371,13	6,750	2,281	168,43	MWD Tool, 6,750 in, 250,65 kg/m, SS07, 6 3/4" T2
20	Stabilizer	1,700	6372,83	6,750	2,299	117,29	Non-Mag Integral Blabe Stabilizer, 6,750 in, 117,29 ppf, SS07 (XH), 6 3/4" T2
21	MWD	6,590	6379,42	9,625	2,375	192,18	MWD Tool, 9,625 in, 192,18 ppf, 15-15LC MOD (1) [SH], 7 5/8" Reg
22	Bit	0,580	6380,00	12,250		739,17	Polycrystalline Diamond Bit, 1,210 in²
23							

Table C.12: String and BHA specifications for 12 ¼" x 13 ½" hole (Copy from WellPlan™).

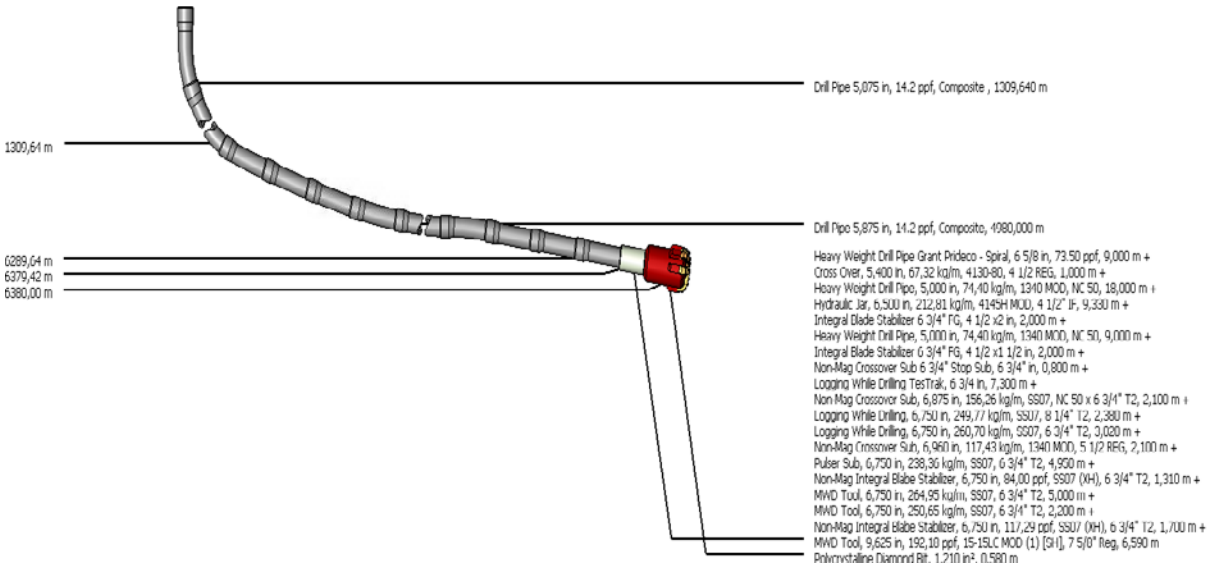

Figure C.13: String and BHA specifications for 12 ¼" x 13 ½" hole (Copy from WellPlan™).

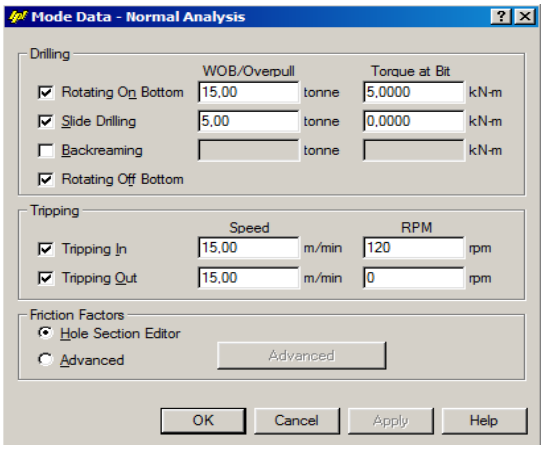

Figure C.14: Run parameters for 12 ¼" x 13 ½" string (Copy from WellPlan™).

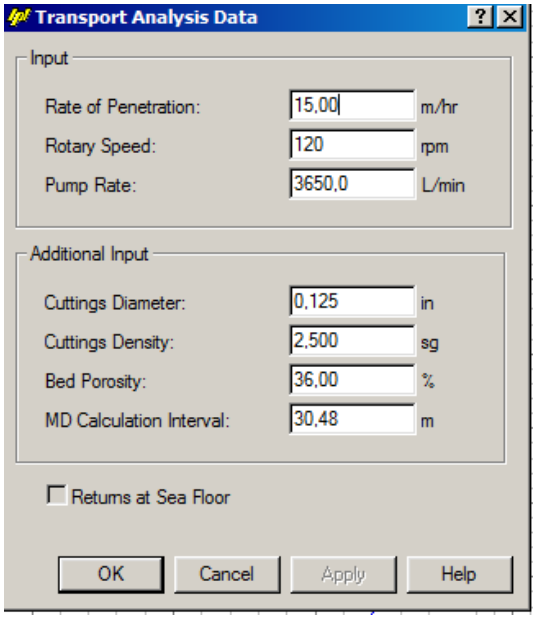

Figure C.15: Transport analysis data for 12 ¼" x 13 ½" hole (Copy from WellPlan™).

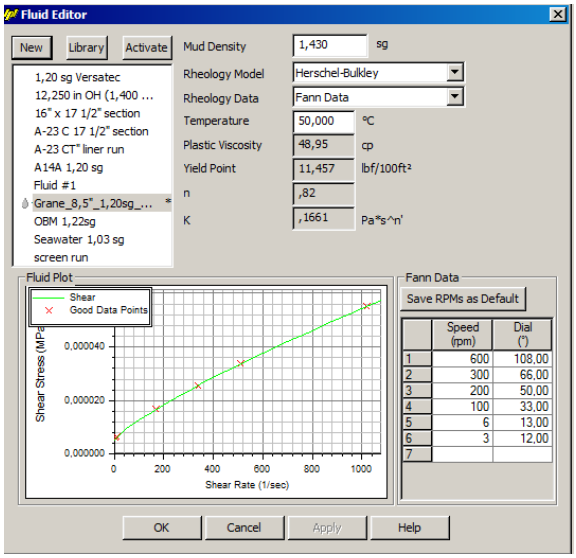

Figure C.16: Fluid data – 12 ¼" x 13 ½" hole (Copy from WellPlan™).

10 ¾ " Liner - Composite Drill Pipe - WellPlan™ Setup

	Section Type	Measured Depth (m)	Length (m)	ID (in)	Drift (in)	Effective Hole Diameter (in)	Friction Factor	Linear Capacity (L/m)	Item Description
1	Casing	3969,00	3969,000	12,347	12,250	17,500	0,20	77,25	13 3/8 in, 72,000 ppf, P-110, 13 3/8" Vam T
2	Open Hole	6329,00	2360,000	13,500		13,500	0,30	92,35	13,5 in
3	Open Hole	6380,00	51,000	12,250		12,250	0,30	76,04	
4									

Table C.13: Hole section data running 10 ¾" Liner (Copy from WellPlan™).

	Section Type	Length (m)	Measured Depth (m)	OD (in)	ID (in)	Weight (ppf)	Item Description
1	Drill Pipe	3104,000	3104,00	5,875	4,400	14,25	Drill Pipe 5,875 in, 14.2 ppf, Composite
2	Drill Pipe	765,000	3869,00	5,875	4,400	14,25	Drill Pipe 5,875 in, 14.2 ppf, Composite
3	Casing	2511,000	6380,00	10,750	9,660	60,70	10 3/4 in, 60.700 ppf, P-110 (ACTIVE), Vam TOP
4							

Table C.14: String and BHA specifications for 10 ¾” Liner (Copy from WellPlan™).

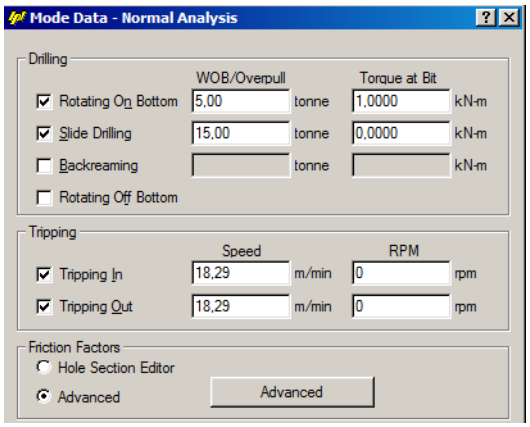

Figure C.17: Run parameters for 10 ¾” Liner (Copy from WellPlan™).

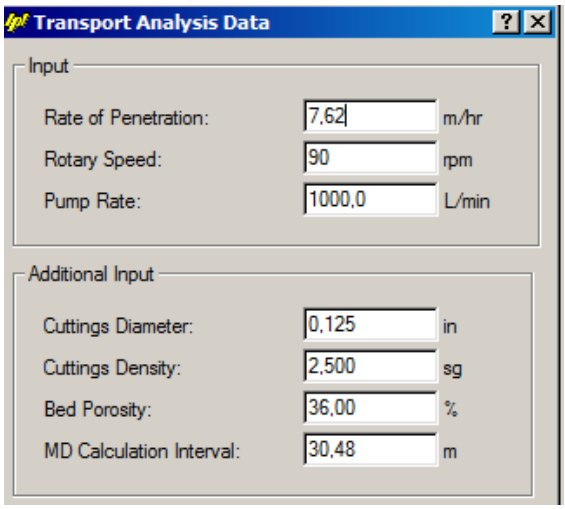

Figure C.18: Transport analysis data for 10 ¾” Liner (Copy from WellPlan™).

8 ½” x 9 ½” hole - Composite Drill Pipe - WellPlan™ Setup

	Section Type	Measured Depth (m)	Length (m)	ID (in)	Drift (in)	Effective Hole Diameter (in)	Friction Factor	Linear Capacity (L/m)	Item Description
1	Casing	3969,00	3969,000	12,347	12,258	17,500	0,20	77,28	13 3/8 in, 72 ppf, P-110 (XH),
2	Casing	6380,00	2411,000	9,660	9,504	13,500	0,25	47,28	10 3/4 in, 60.7 ppf, P-110,
3	Open Hole	9350,00	2970,000	9,500		9,500	0,30	45,73	
4	Open Hole	9400,00	50,000	8,500		8,500	0,30	36,61	
5									

Table C.15: Hole section data for 8 ½” x 9 ½” hole (Copy from WellPlan™).

	Section Type	Length (m)	Measured Depth (m)	OD (in)	ID (in)	Weight (ppf)	Item Description
1	Drill Pipe	3914,210	3914,21	5,875	4,400	14,25	Drill Pipe 5,875 in, 14.2 ppf, Composite
2	Drill Pipe	5400,000	9314,21	5,875	4,400	14,25	Drill Pipe 5,875 in, 14.2 ppf, Composite
3	Heavy Weight	9,000	9323,21	5,000	3,000	49,99	Heavy Weight Drill Pipe, 5,000 in, 74,40 kg/m, 1340 MOD, NC 50
4	Sub	1,000	9324,21	5,400	2,160	45,24	Cross Over, 5,400 in, 67,32 kg/m, 4130-80, 4 1/2 REG
5	Heavy Weight	18,000	9342,21	5,000	3,000	49,99	Heavy Weight Drill Pipe, 5,000 in, 74,40 kg/m, 1340 MOD, NC 50
6	Jar	9,330	9351,54	6,500	2,750	143,00	Hydraulic Jar, 6,500 in, 212,81 kg/m, 4145H MOD, 4 1/2" IF
7	Stabilizer	2,000	9353,54	4,500	2,000	43,43	Integral Blade Stabilizer 6 3/4" FG, 4 1/2 x2 in
8	Heavy Weight	9,000	9362,54	5,000	3,000	49,99	Heavy Weight Drill Pipe, 5,000 in, 74,40 kg/m, 1340 MOD, NC 50
9	Stabilizer	2,000	9364,54	4,500	2,000	48,11	Integral Blade Stabilizer 6 3/4" FG, 4 1/2 x1 1/2 in
10	Sub	0,800	9365,34	7,000	2,812	110,00	Non-Mag Crossover Sub 6 3/4" Stop Sub, 6 3/4" in
11	MWD	7,300	9372,64	6,750	2,813	113,51	Logging While Drilling TesTrak, 6 3/4 in
12	Sub	2,100	9374,74	6,875	2,813	105,00	Non-Mag Crossover Sub, 6,875 in, 156,26 kg/m, SS07, NC 50 x 6 3/4" T2
13	MWD	2,380	9377,12	6,750	2,264	167,84	Logging While Drilling, 6,750 in, 249,77 kg/m, SS07, 8 1/4" T2
14	MWD	3,020	9380,14	6,750	1,875	175,18	Logging While Drilling, 6,750 in, 260,70 kg/m, SS07, 6 3/4" T2
15	Sub	2,100	9382,24	6,960	2,340	78,91	Non-Mag Crossover Sub, 6,960 in, 117,43 kg/m, 1340 MOD, 5 1/2 REG
16	MWD	4,950	9387,19	6,750	2,281	160,17	Pulser Sub, 6,750 in, 238,36 kg/m, SS07, 6 3/4" T2
17	Stabilizer	1,310	9388,50	6,750	2,250	84,00	Non-Mag Integral Blabe Stabilizer, 6,750 in, 84,00 ppf, SS07 (XH), 6 3/4" T2
18	MWD	5,000	9393,50	6,750	2,281	178,04	MWD Tool, 6,750 in, 264,95 kg/m, SS07, 6 3/4" T2
19	MWD	2,200	9395,70	6,750	2,281	168,43	MWD Tool, 6,750 in, 250,65 kg/m, SS07, 6 3/4" T2
20	Stabilizer	1,700	9397,40	6,750	2,299	117,29	Non-Mag Integral Blabe Stabilizer, 6,750 in, 117,29 ppf, SS07 (XH), 6 3/4" T2
21	Stabilizer	2,200	9399,60	6,750	3,000	246,65	Adjustable Stabilizer, 6,750 in, 246,65 ppf, 1340 MOD (XH), 6 3/4" T2
22	Bit	0,400	9400,00	8,500		200,00	, 0x11, 0,778 in²
23							

Table C.16: String and BHA specifications for 8 ½" x 9 ½" hole (Copy from WellPlan™).

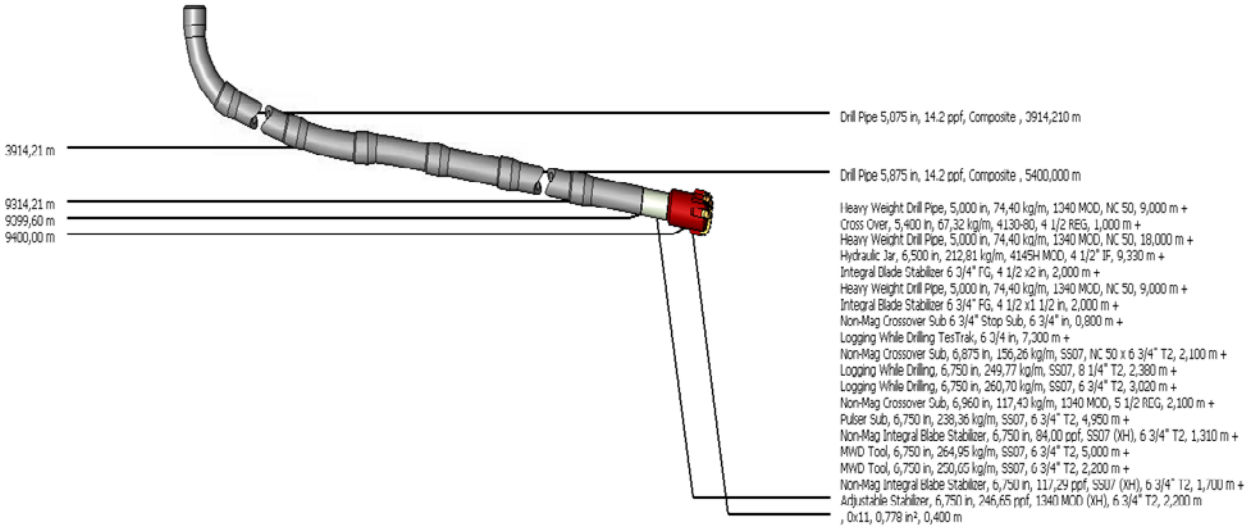

Figure C.19: String and BHA specifications for 8 ½" x 9 ½" hole (Copy from WellPlan™).

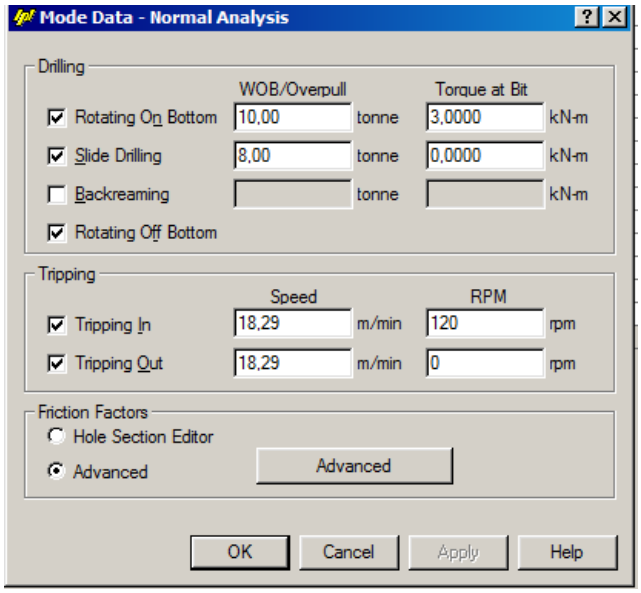

Figure C.20: Run parameters for 8 ½" x 9 ½" string (Copy from WellPlan™).

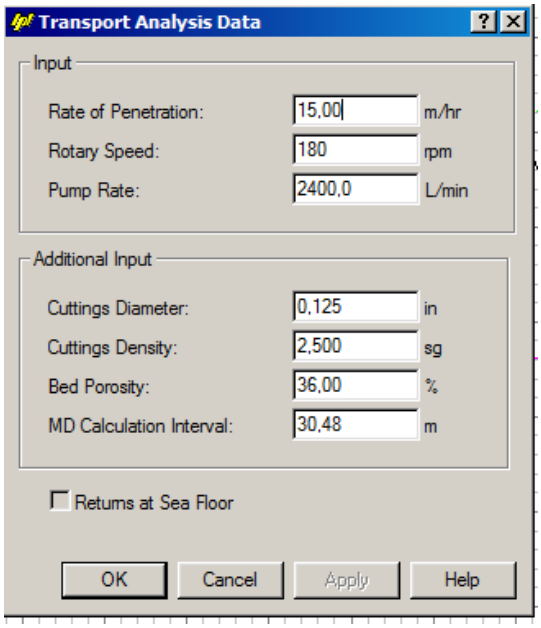

Figure C.21: Transport analysis data for 8 ½" x 9 ½" hole (Copy from WellPlan™).

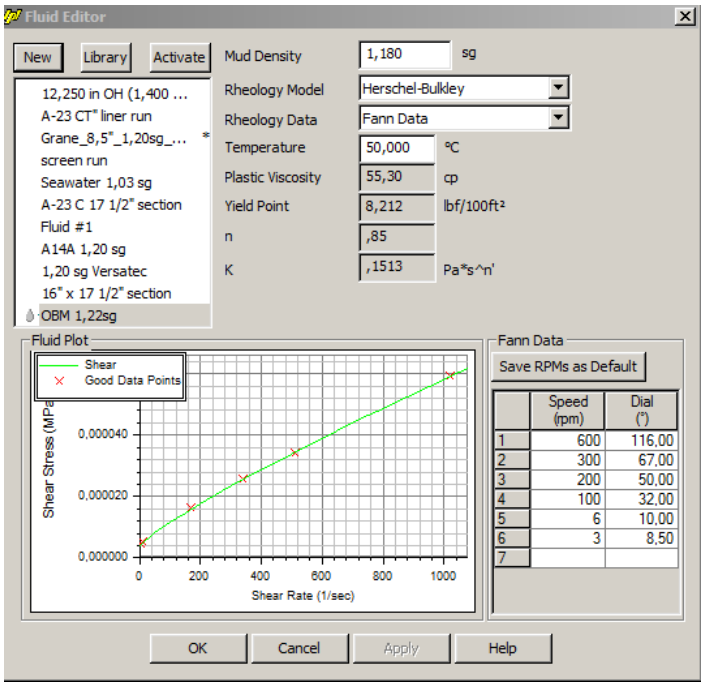

Figure C.22: Fluid data – 8 ½" x 9 ½" hole (Copy from WellPlan™).

6 5/8" Liner – Composite Drill Pipe - WellPlan™ Setup

	Section Type	Measured Depth (m)	Length (m)	ID (in)	Drift (in)	Effective Hole Diameter (in)	Friction Factor	Linear Capacity (L/m)	Item Description
1	Casing	3969.00	3969.000	12.347	12.250	17.755	0.25	77.25	13 3/8 in, 72,000 ppf, L-80 (ACTIVE),
2	Casing	6380.00	2411.000	9.660	9.504	17.500	0.25	47.28	10 3/4 in, 60,700 ppf, L-80 (ACTIVE),
3	Open Hole	9390.00	3010.000	9.500		9.500	0.30	45.73	
4									

Table C.17: Hole section data running 7" x 6 5/8" Liner (Copy from WellPlan™).

	Section Type	Length (m)	Measured Depth (m)	OD (in)	ID (in)	Weight (ppf)	Item Description
1	Drill Pipe	6320,870	6320,87	5,875	4,400	14,25	Drill Pipe 5,875 in, 14,2 ppf, Composite
2	Tubing	31,130	6352,00	7,000	6,184	29,00	Casing, 7,000 in, 29 ppf, L-80,
3	Tubing	1140,000	7492,00	6,625	5,920	24,00	Casing, 6,625 in, 24,00 ppf, L-80 [XH], Vam Top
4	Packer	11,000	7503,00	8,250	4,670	23,00	Casing External Packer, 8,250 in, 23,00 ppf, 4145H MOD [SH], Vam TOP
5	Sand Control Screen	600,000	8103,00	7,420	5,965	28,00	Mesh, 7,420 in, 28,00 ppf, 13-CR-L80, Vam Top
6	Packer	11,000	8114,00	8,250	4,670	23,00	Casing External Packer, 8,250 in, 23,00 ppf, 4145H MOD [SH], Vam TOP
7	Sand Control Screen	504,000	8618,00	6,625	5,965	28,06	Mesh, 6,625 in, 28,06 ppf, 13-CR-L80, Vam Top
8	Packer	11,000	8629,00	8,250	4,670	23,00	Casing External Packer, 8,250 in, 23,00 ppf, 4145H MOD [SH], Vam TOP
9	Sand Control Screen	504,000	9133,00	7,420	5,965	28,00	Mesh, 7,420 in, 28,00 ppf, 13-CR-L80, Vam Top
10	Packer	9,000	9142,00	8,250	4,670	23,00	Casing External Packer, 8,250 in, 23,00 ppf, 4145H MOD [SH], Vam TOP
11	Sand Control Screen	248,000	9390,00	7,420	5,965	28,00	Mesh, 7,420 in, 28,00 ppf, 13-CR-L80, Vam Top
12							

Table C.18: String and BHA specifications for 7” x 6 5/8” (Copy from WellPlan™).

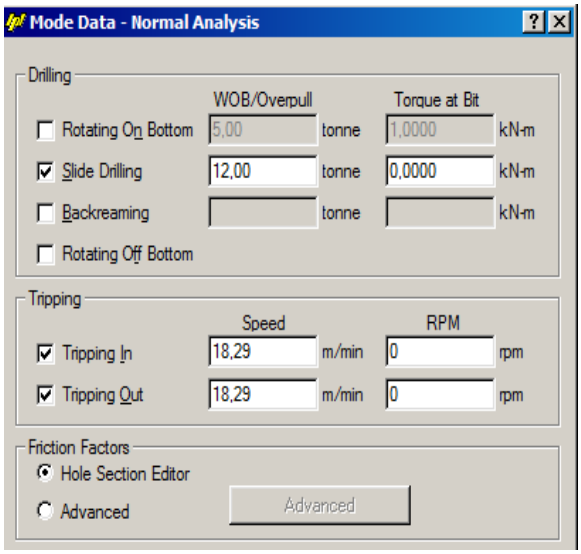

Figure C.23: Run parameters for 7” x 6 5/8” Liner (Copy from WellPlan™).

Appendix D – Rig equipment

Pumps: 3 x Continental Emsco FB-1600

Maximum work pressure (bar/psi	345/5000
Maximum discharge flow	2724 L/min
Stroke	12"
Maximum strokes	120 stroke/min
Input power requirement	1600 HP
Fluid line size	5,5" -7"
Discharge outlet	5", 5000 psi API

Table D.1: Technical data for the Continental Emsco pumps used on Brage.

Mud tank	
Mud storage tanks A-B-C	108-108-66 m^3
Reserve Pits 1-2-3-4	50-52-52-52 m^3
Active pit	42 m^3
Draw work - WIRTH	
Capacity	350 ton
Wire size	1 ½”
Maximum static hook load	4450 kN
Maximum line speed	20,3 m/sec
Top drive - AKER MH	
Capacity	650 ton
Revolutions per minute	245 rpm
Hydraulic pressure	345 bar
Maximum torque	83 kNm
BOP: Cameron	
ID	18 3/4"
Operating pressure (bar/psi)	345/5000
Weight	60 ton

Drill Pipe Specs

	Nominal					Body			Connection		Connection Torsional Yield (kN-m)	Tool Joint Lenght (m)	Linear Capacity (L/m)	Makeup Torque (kN-m)
	Diameter	Weight	Grade	Connection	Class	OD (in)	ID (in)	Weight (ppf)	OD (in)	ID (in)				
Conventional API Drill Pipe	**6 5/8**	**27.70**	**S**	**FH**	**P**	**6.625**	**5.902**	**31.54**	**8.000**	**4.250**	**119.1181**	**0.483**	**14.05**	**71.4706**
Conventional API Drill Pipe	**5 1/2**	**21.90**	**S**	**FH**	**P**	**5.500**	**4.778**	**26.33**	**6.938**	**3.000**	**80.0977**	**0.457**	**11.09**	**48.0583**
5 7/8" Composite Pipe	**5 7/8**	**14.20**	**Carbon Composite**	**XT57**	**1**	**5.875**	**4.290**	**14.25**	**7.000**	**2.950**	**85.000**	**0.800**	**9.33**	**48.000**

Table D.2: Pipe data for the drill pipes used in the Wellplan™ simulations

Appendix E – Simulation results

Drilling 12 ¼” x 13 ½” hole – Conventional Pipe

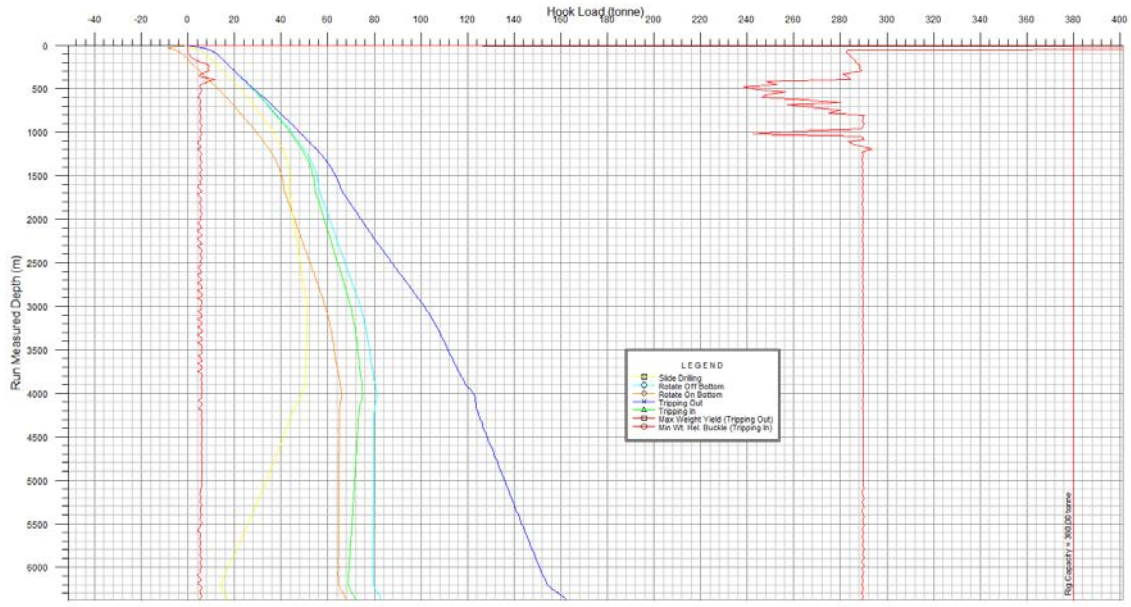

Figure E.1: Hook load drilling 12 ¼” x 13 ½” hole (Copy from WellPlan™).

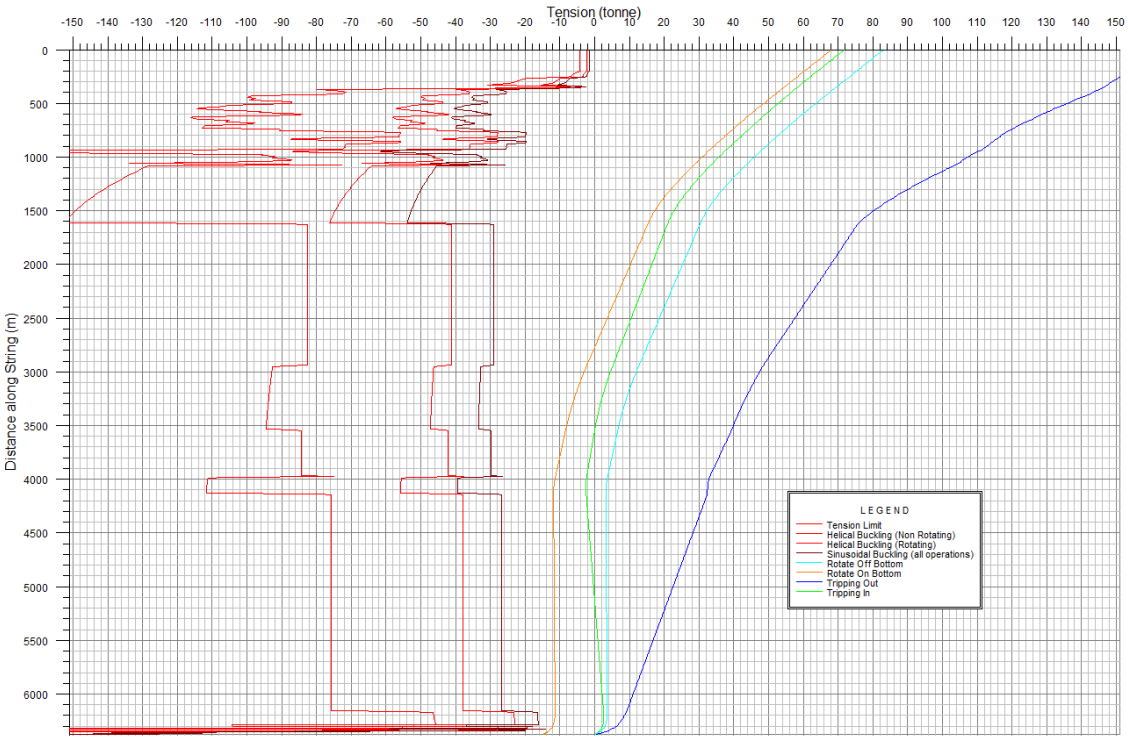

Figure E.2: Tension load drilling 12 ¼” x 13 ½” hole (Copy from WellPlan™).

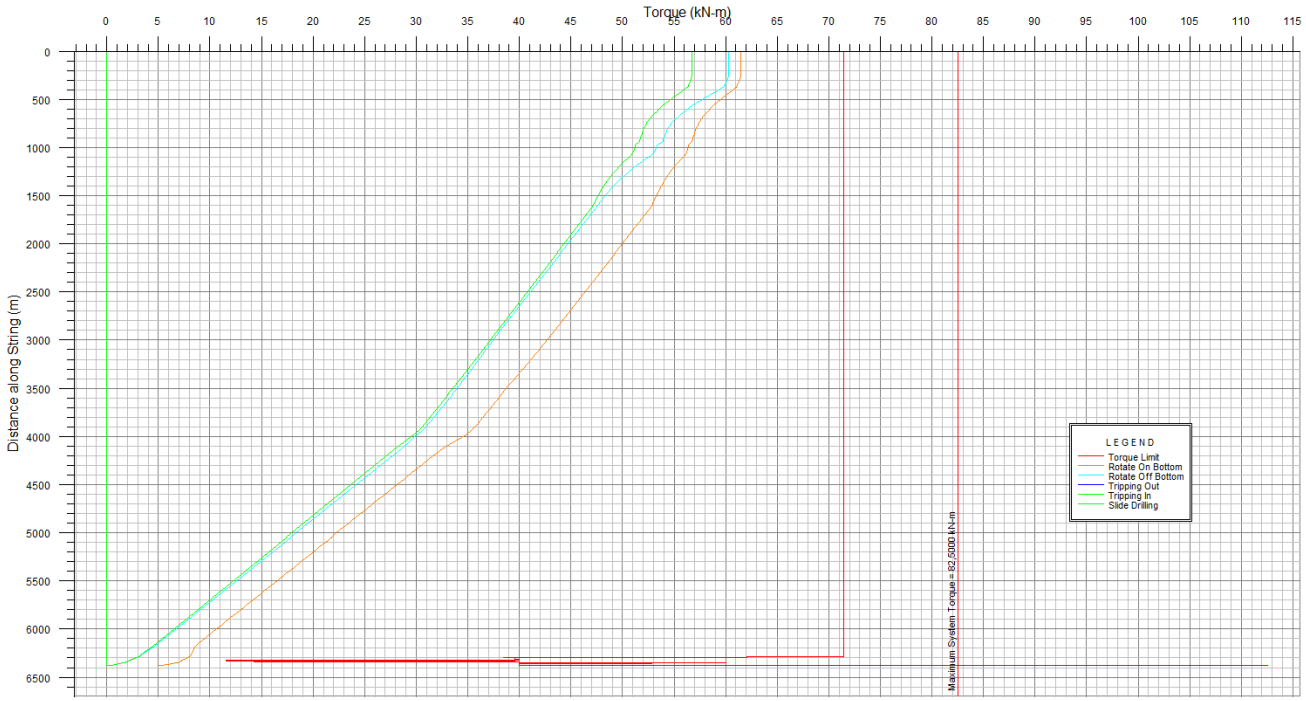

Figure E.3: Torque drilling 12 ¼" x 13 ½" hole (Copy from WellPlan™).

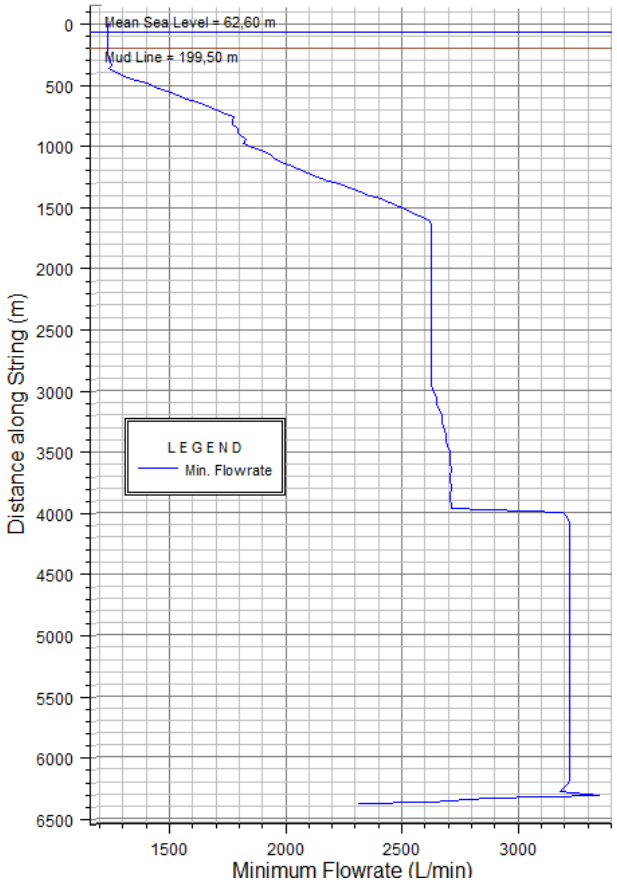

Figure E.4: Minimum flow rate drilling 12 ¼" x 13 ½" hole (Copy from WellPlan™).

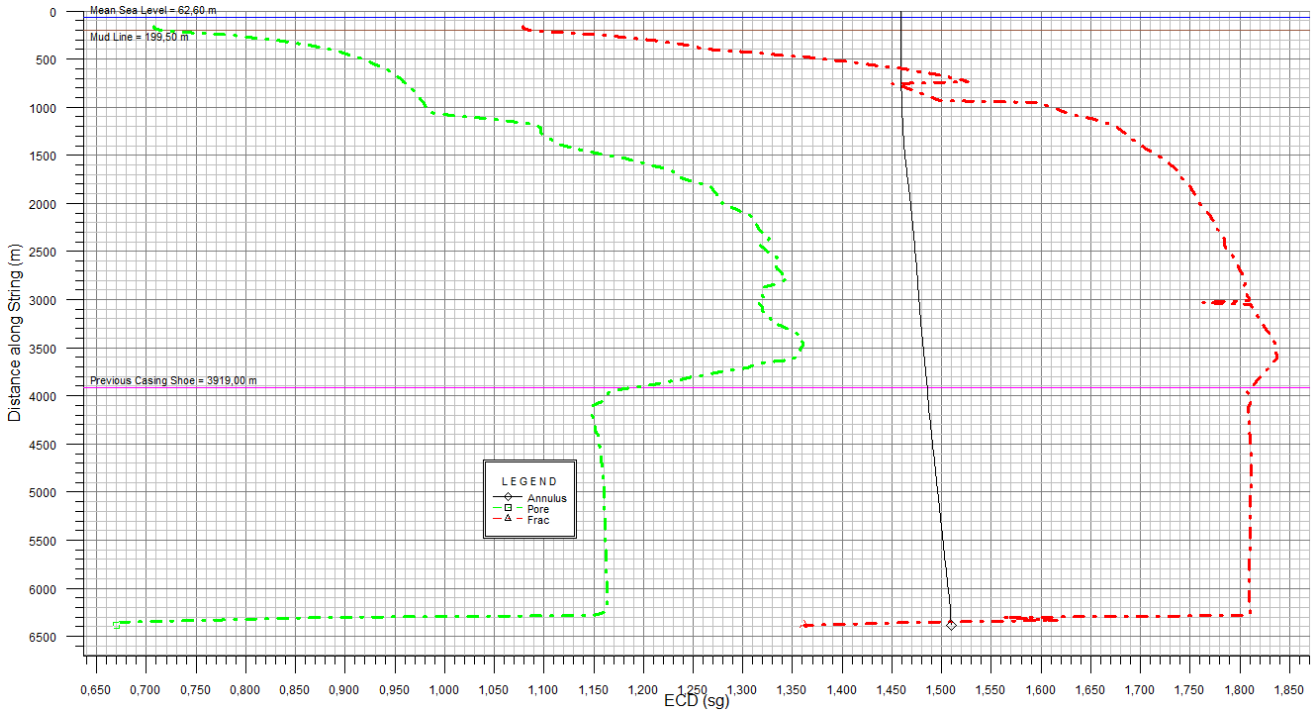

Figure E.5: ECD vs depth 12 ¼" x 13 ½" hole (Copy from WellPlan™).

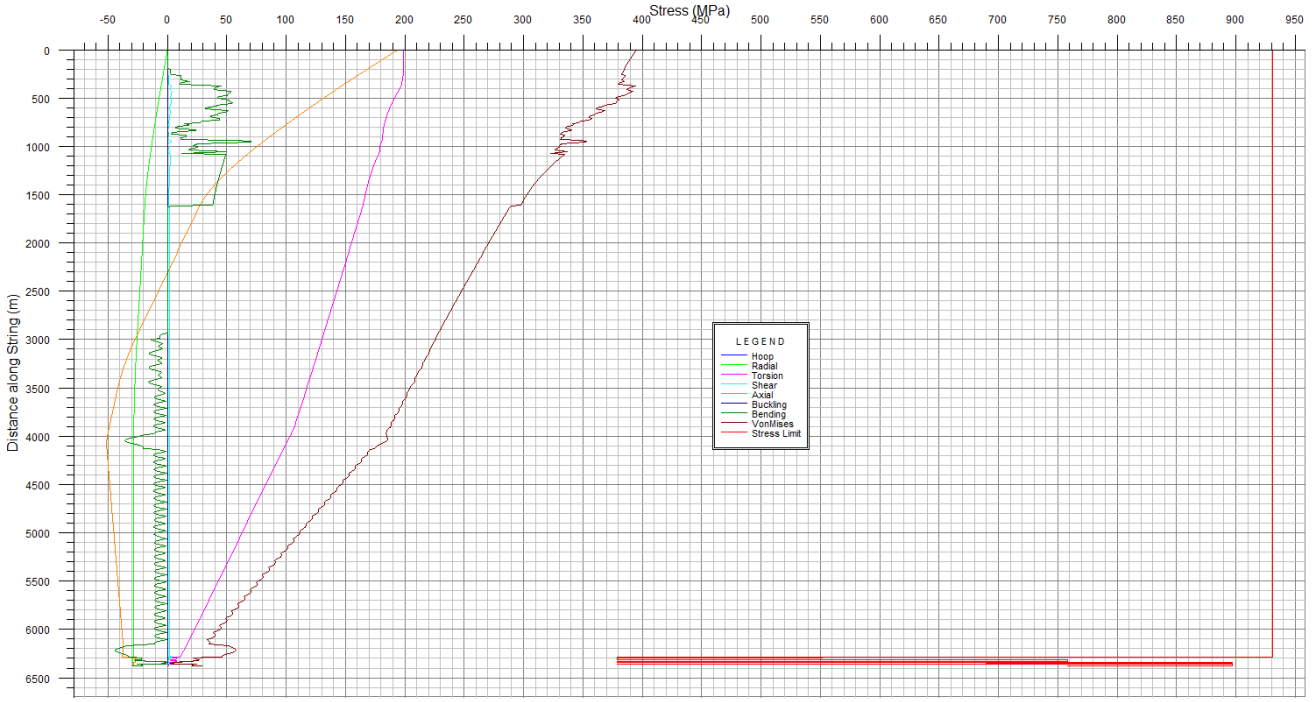

Figure E.6: Stress graph tripping in 12 ¼" x 13 ½" hole (Copy from WellPlan™).

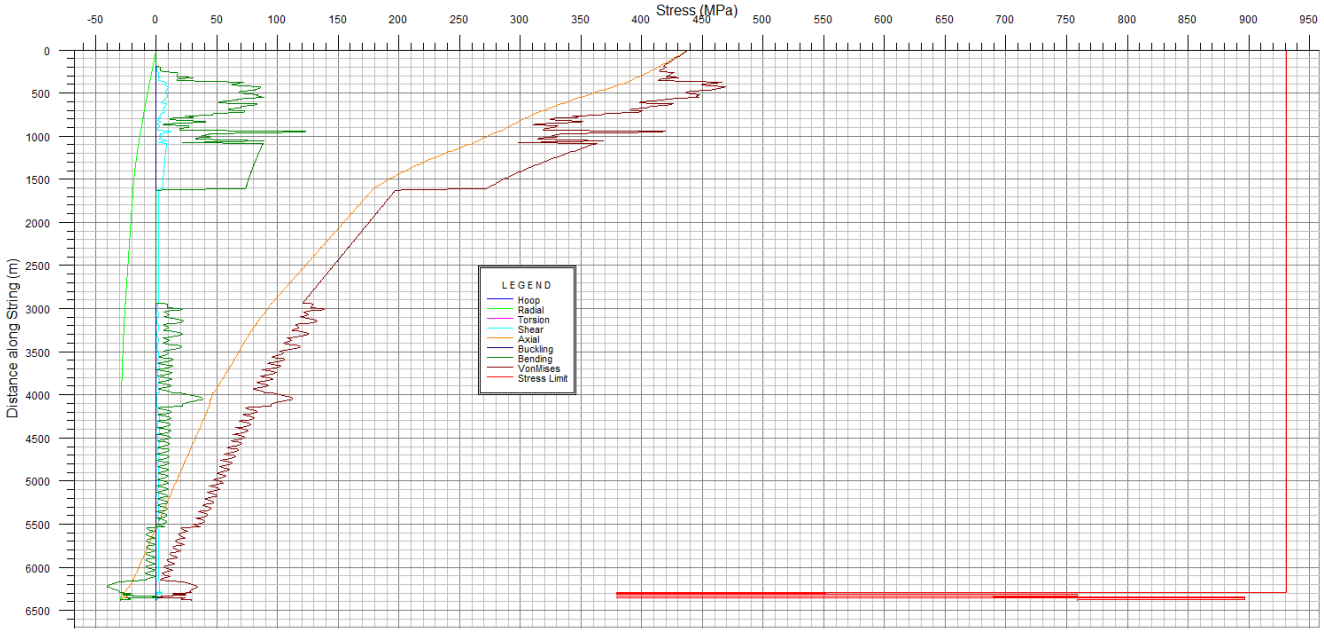

Figure E.7: Stress graph tripping out 12 ¼" x 13 ½" hole (Copy from WellPlan™).

Installing 10 ¾" Liner – Conventional Pipe

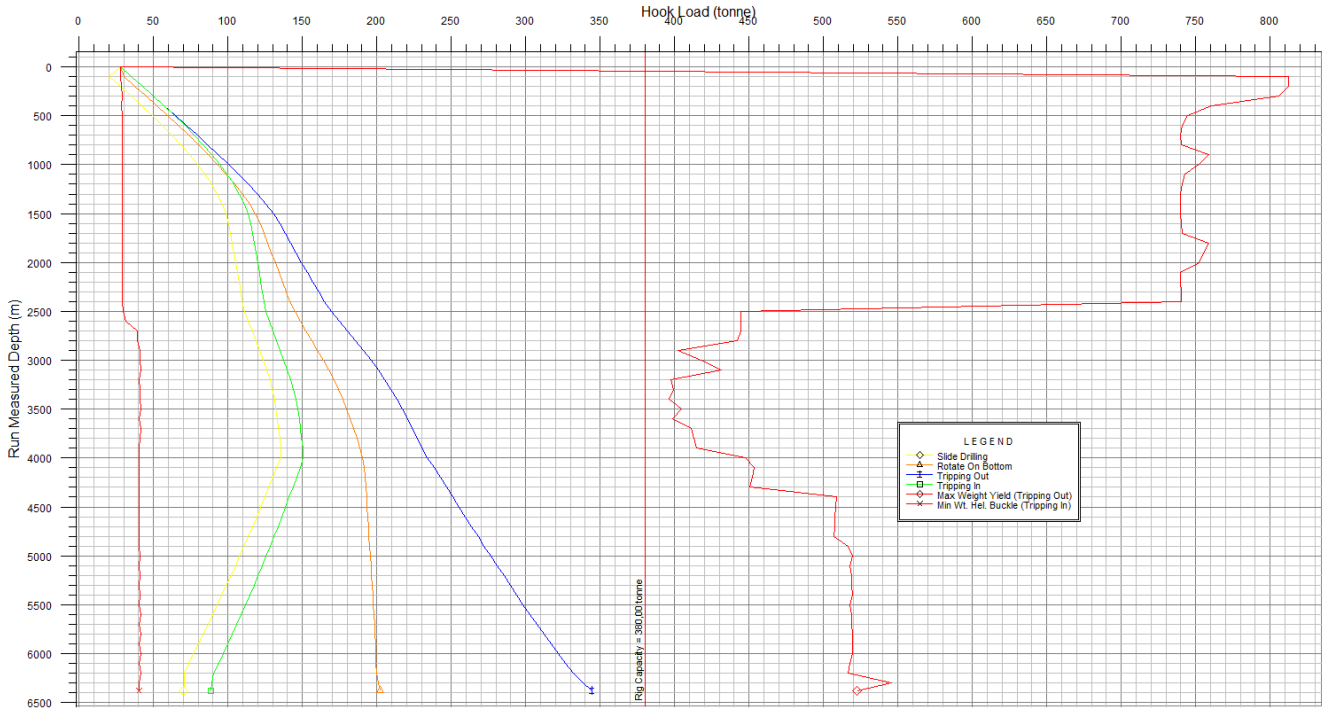

Figure E.8: Hook load 10 ¾" liner (Copy from WellPlan™).

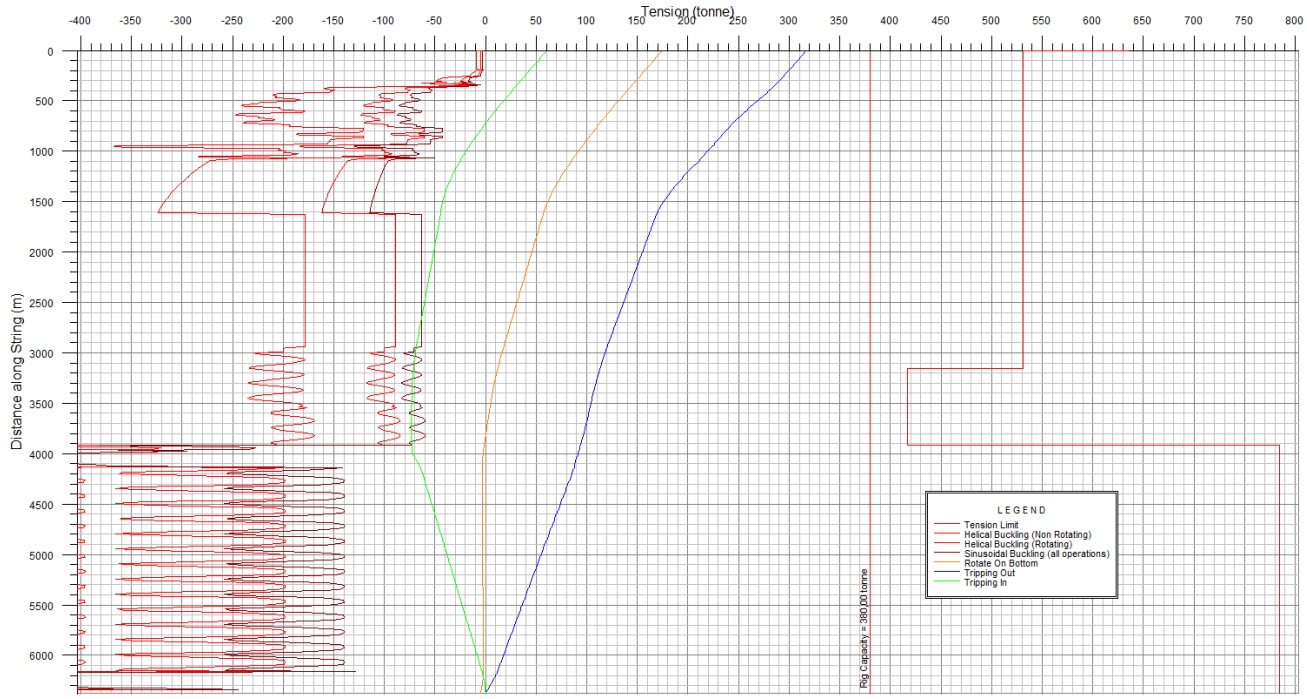

Figure E.9: Tension load 10 ¾" liner (Copy from WellPlan™).

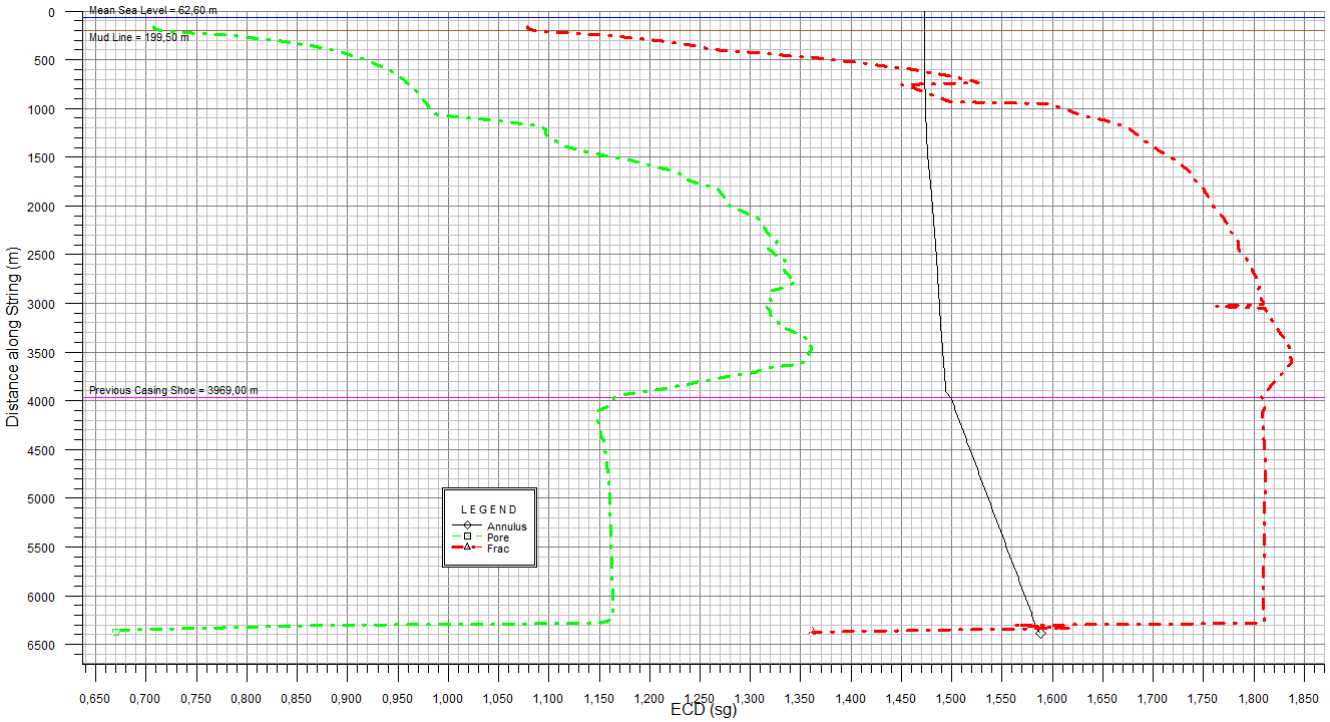

Figure E.10: ECD vs depth 10 ¾" liner (Copy from WellPlan™).

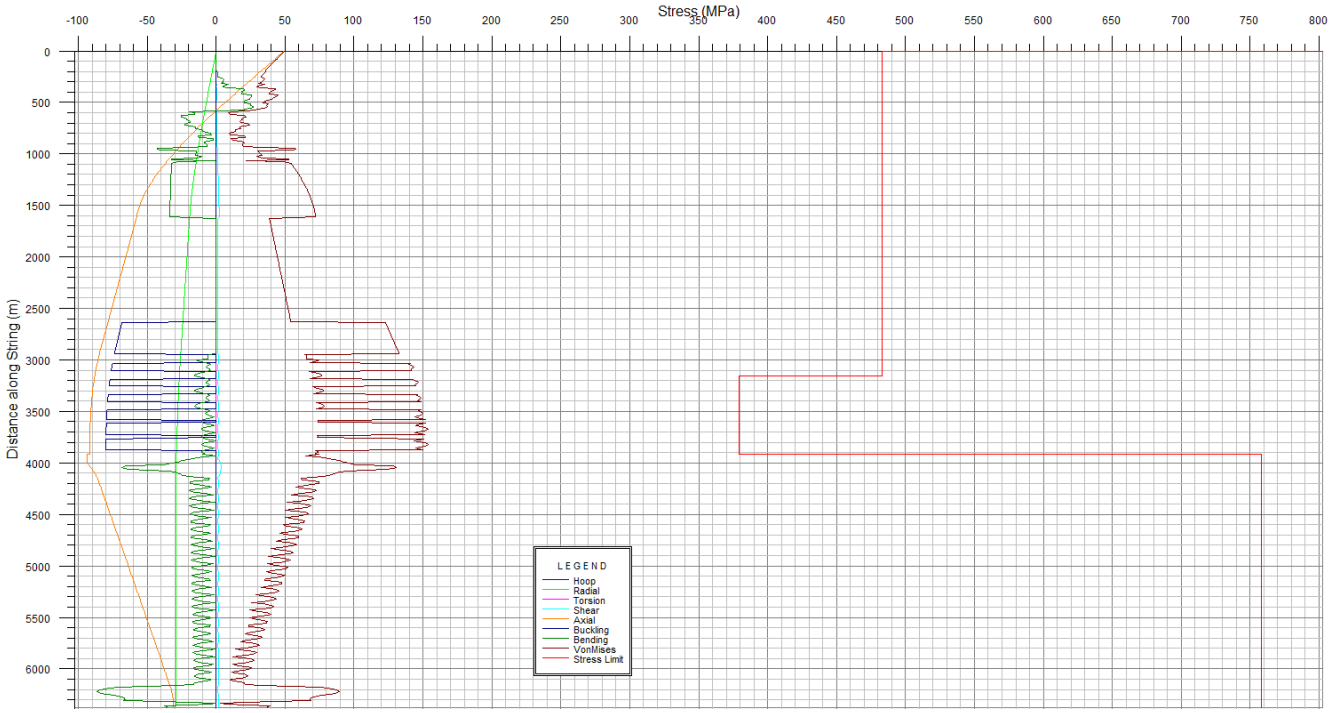

Figure E.11: Stress graph tripping in with 10 ¾" Liner (Copy from WellPlan™).

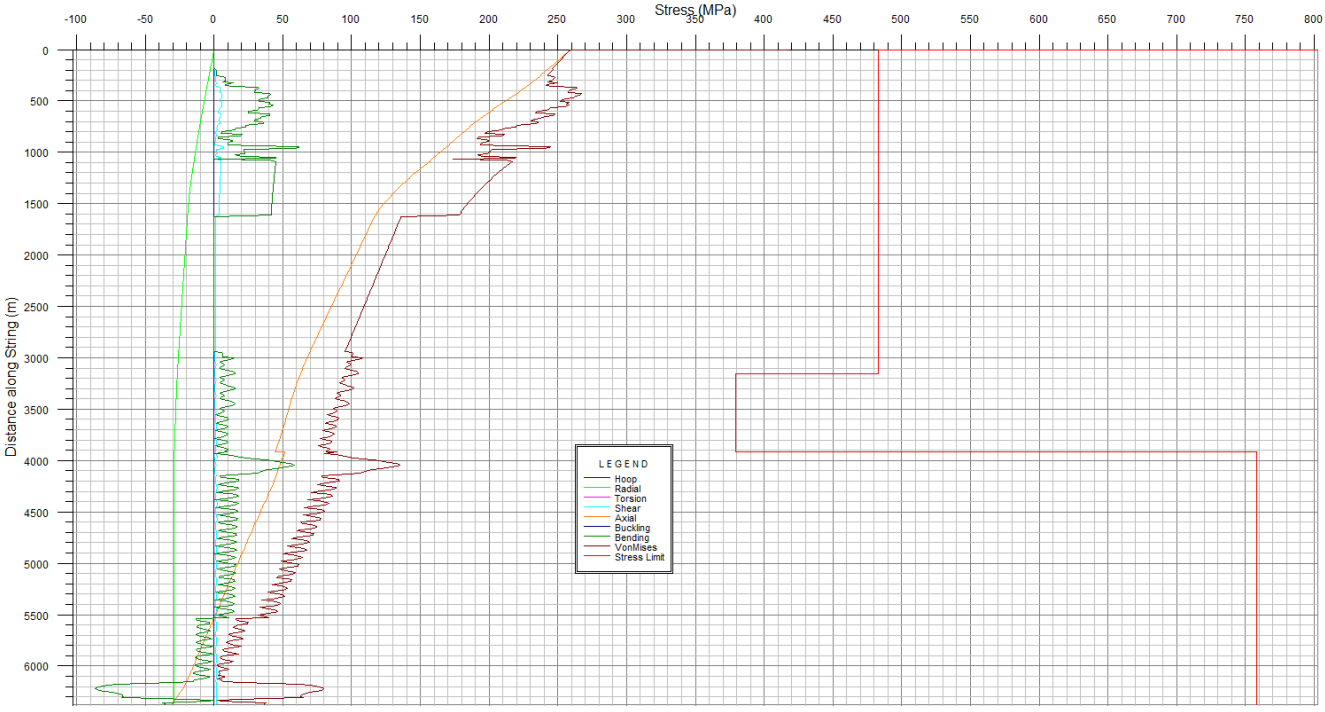

Figure E.12: Stress graph tripping out with 10 ¾" Liner (Copy from WellPlan™).

Drilling 8 ½" x 9 ½" hole – Conventional Pipe

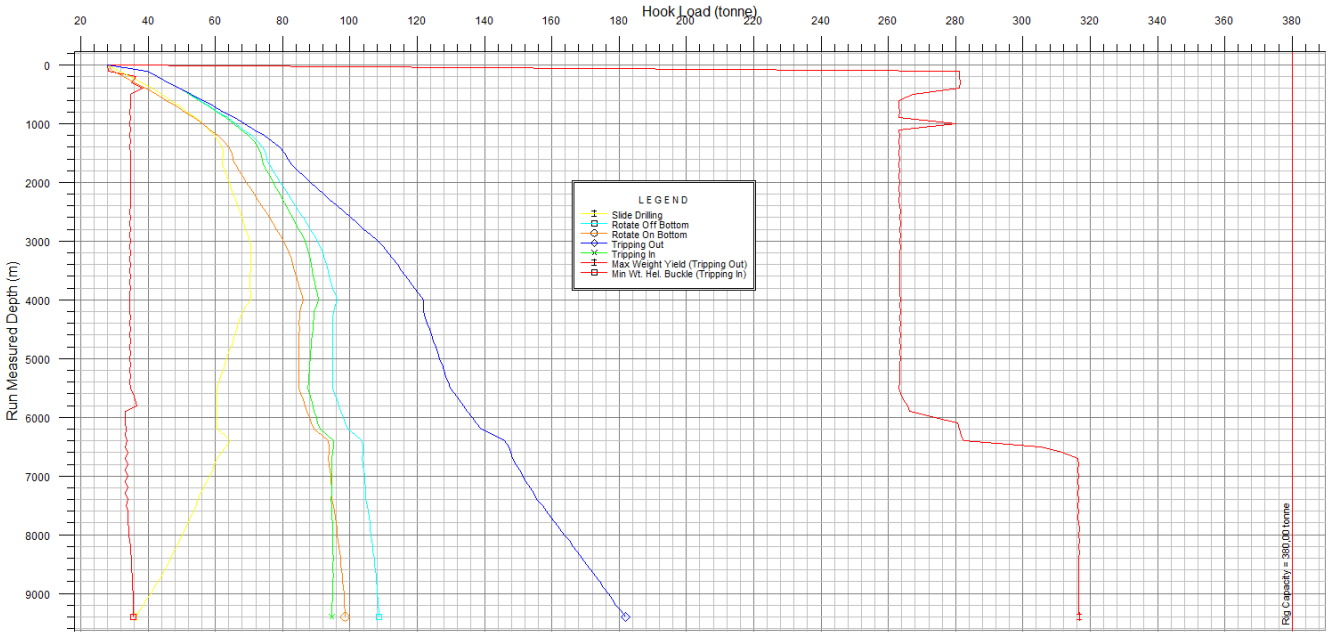

Figure E.13: Hook load drilling 8 ½" x 9 ½" hole (Copy from WellPlan™).

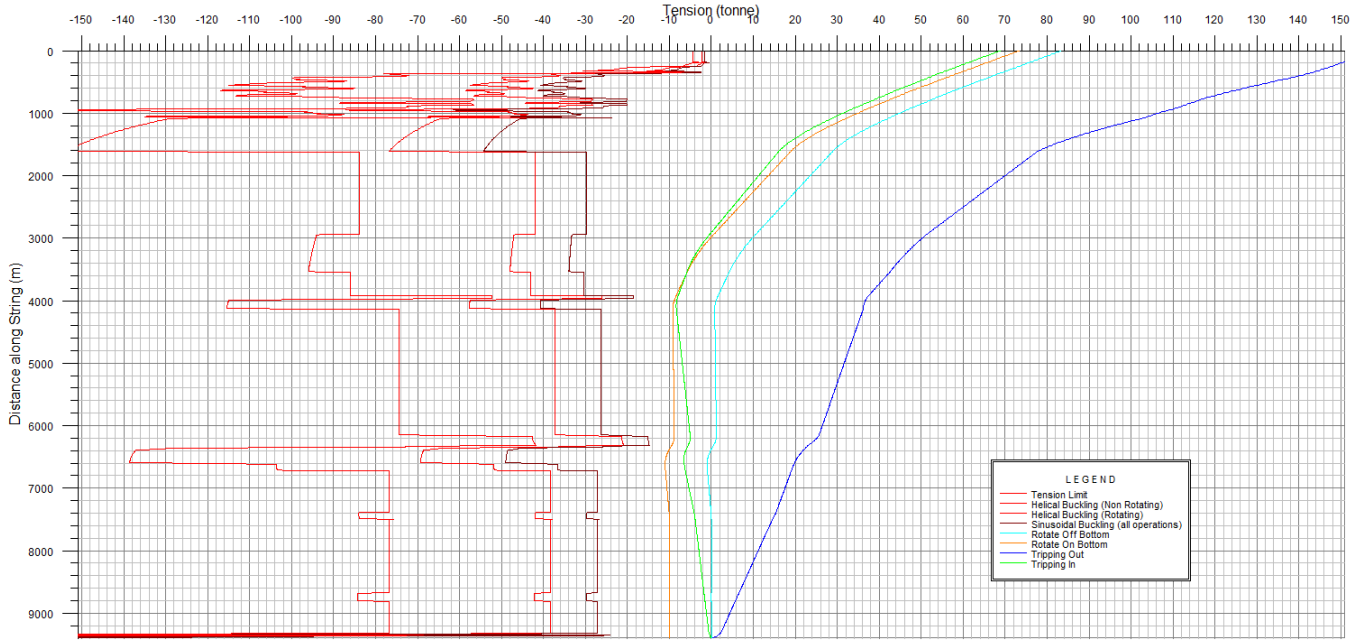

Figure E.14: Tension load drilling 8 ½" x 9 ½" hole (Copy from WellPlan™).

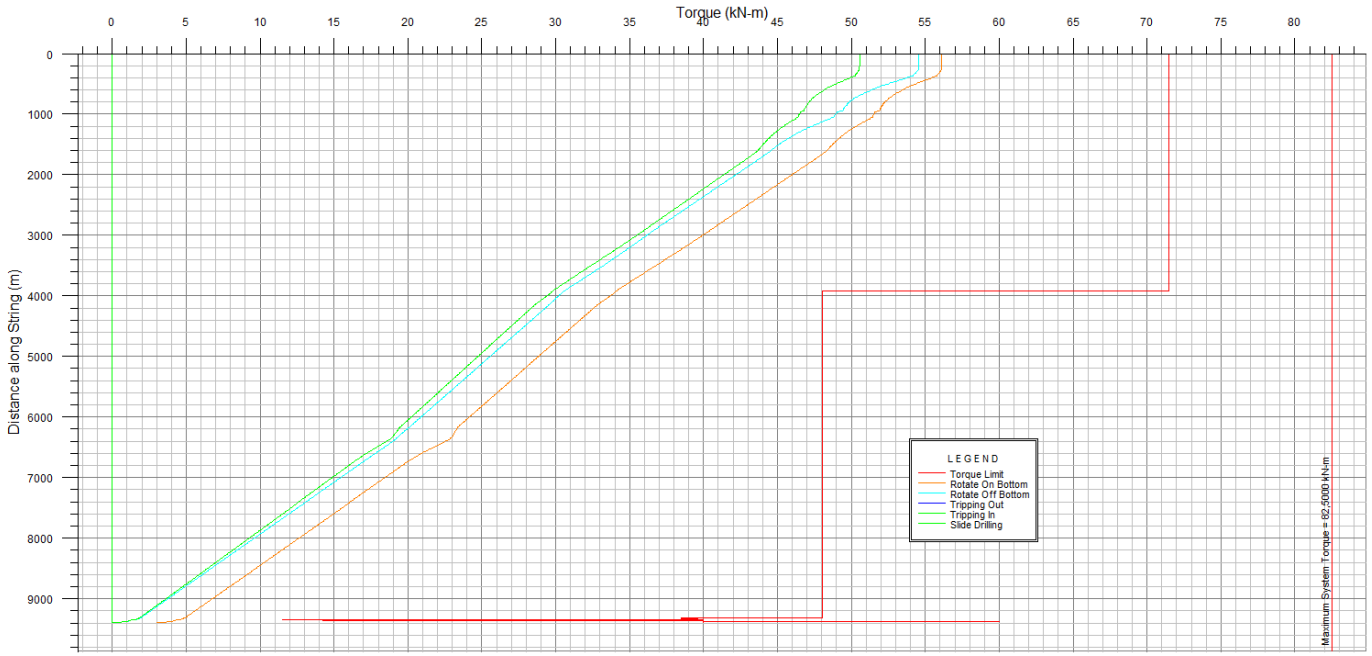

Figure E.15: Torque drilling 8 ½" x 9 ½" hole (Copy from WellPlan™).

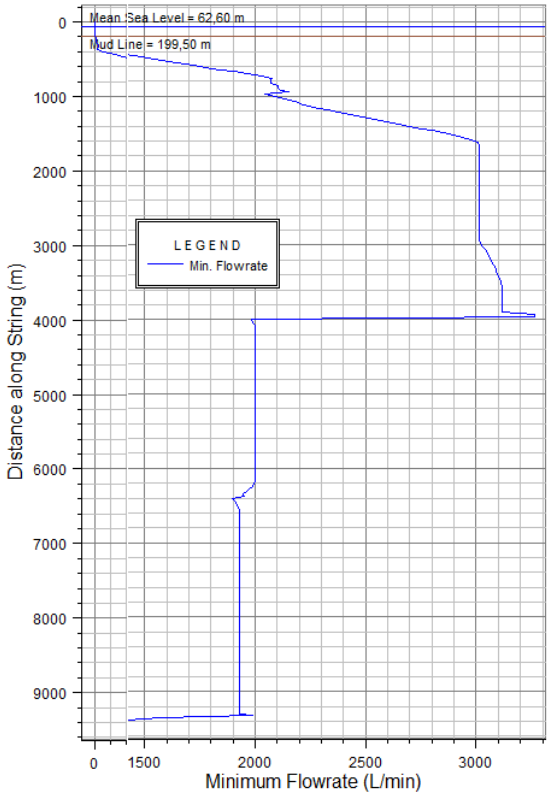

Figure E.16: Minimum flow rate drilling 8 ½" x 9 ½" hole (Copy from WellPlan™).

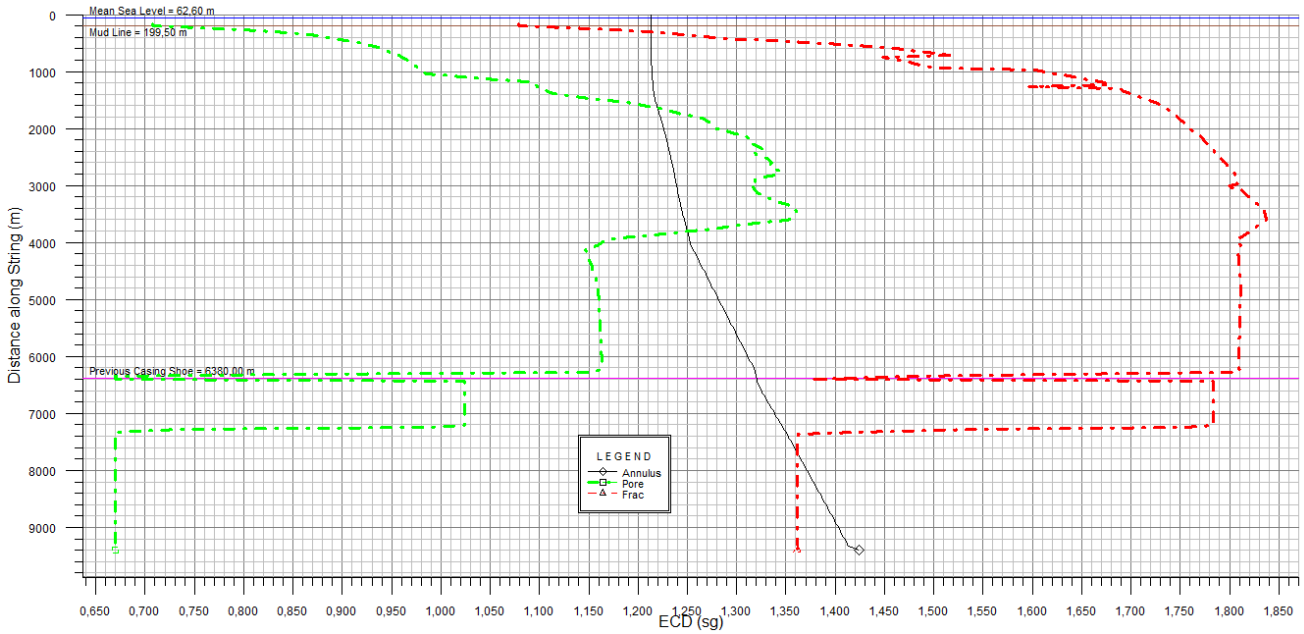

Figure E.17: ECD vs depth 8 ½" x 9 ½" hole (Copy from WellPlan™).

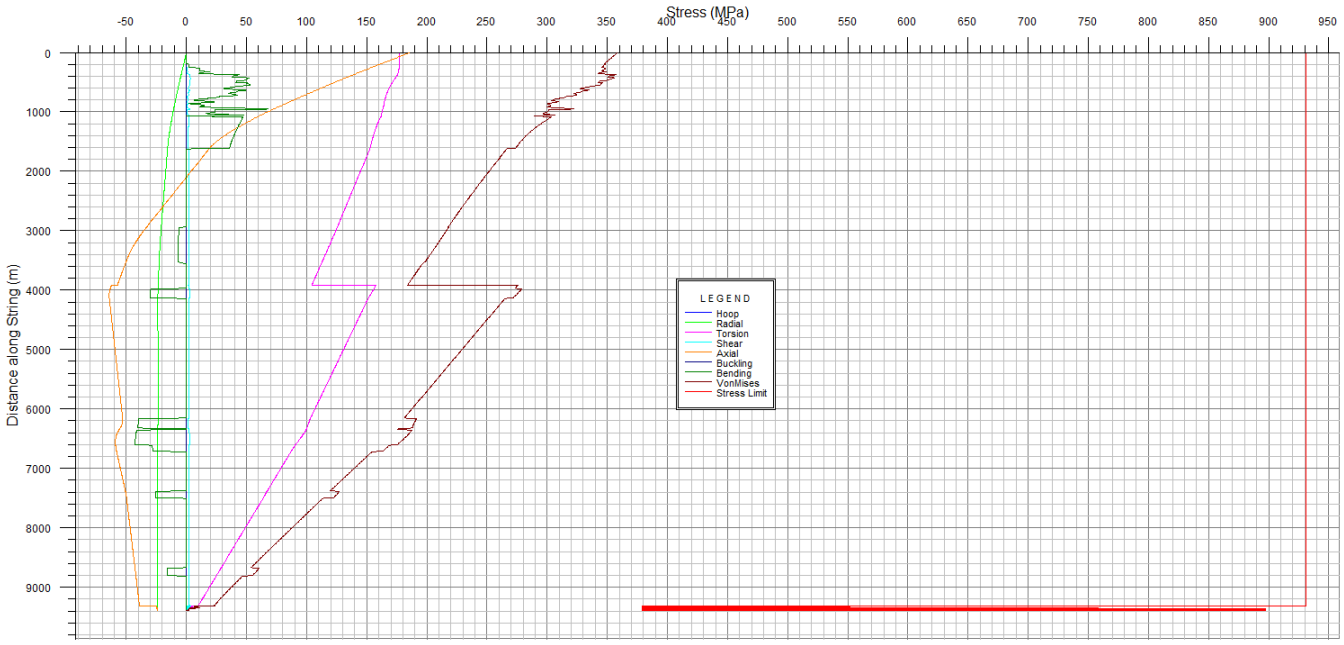

Figure E.18: Stress graph tripping in 8 ½" x 9 ½" hole (Copy from WellPlan™).

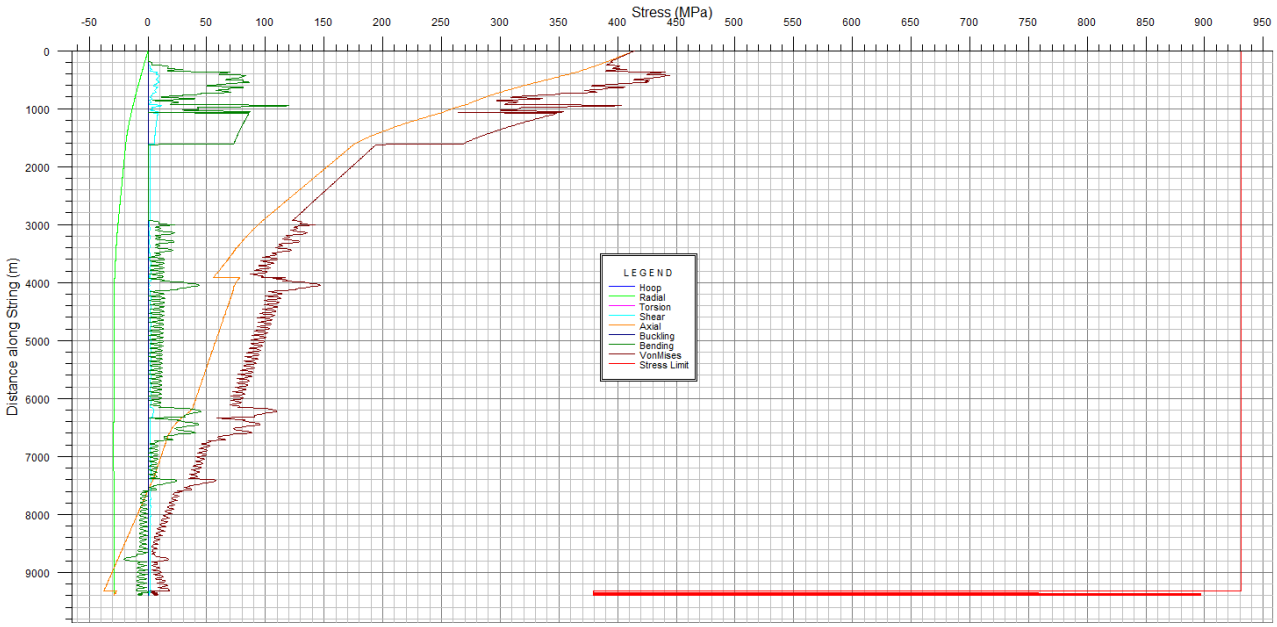

Figure E.19: Stress graph tripping out 8 ½” x 9 ½” hole (Copy from WellPlan™).

Installing 7” x 6 5/8” Liner - Conventional Pipe

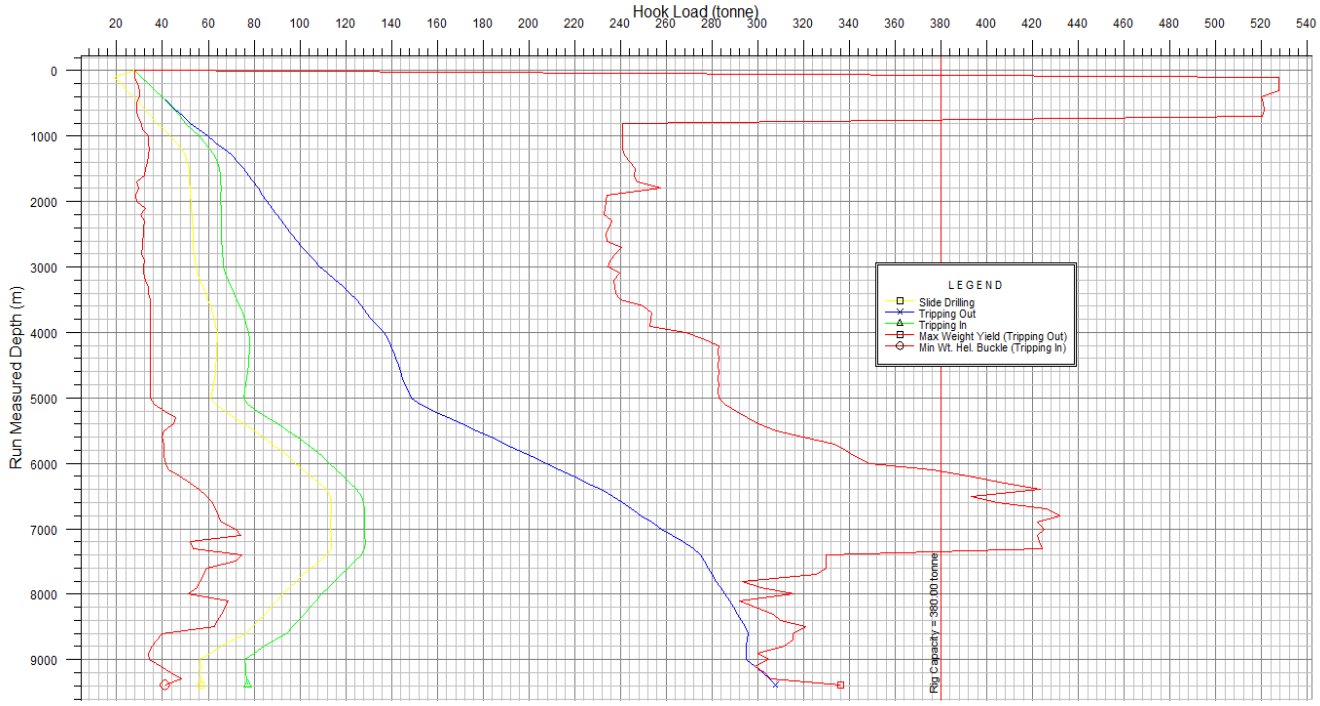

Figure E.20: Hook load 7” x 6 5/8” screen (Copy from WellPlan™).

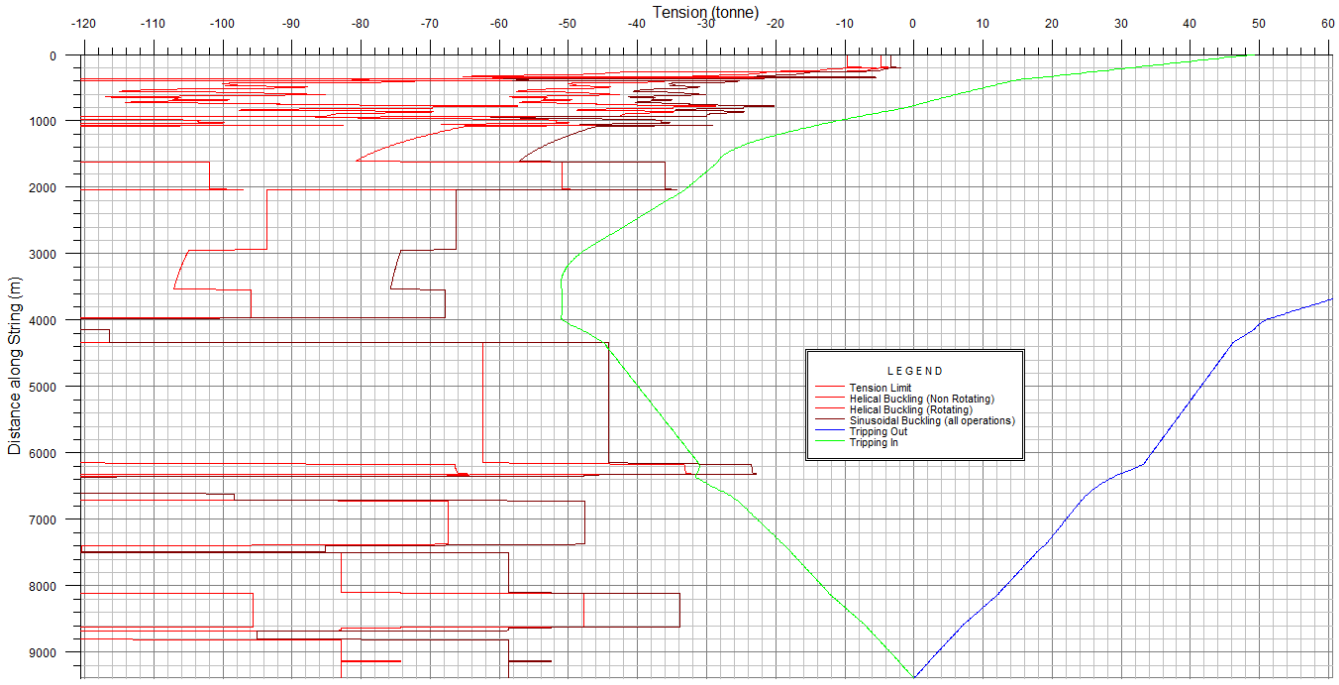

Figure E.21: Tension load 7” x 6 5/8” screen (Copy from WellPlan™).

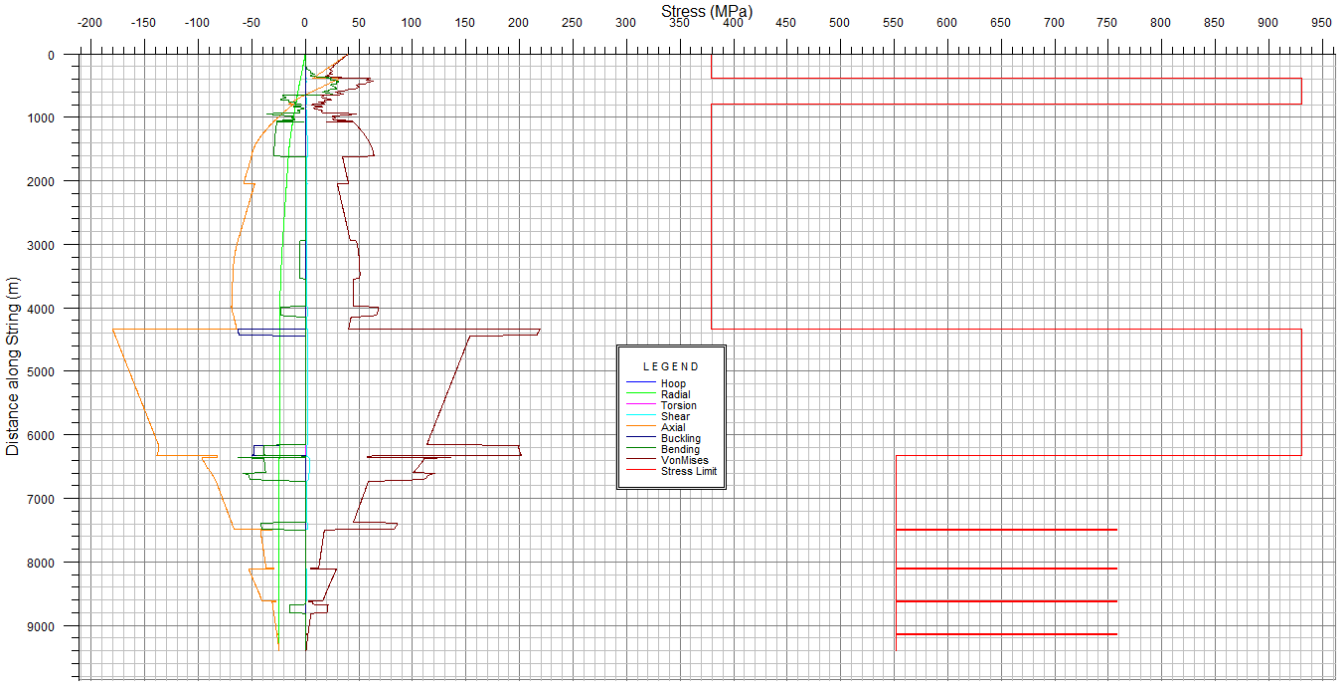

Figure E.22: Stress graph tripping in with 7” x 6 5/8” screen (Copy from WellPlan™).

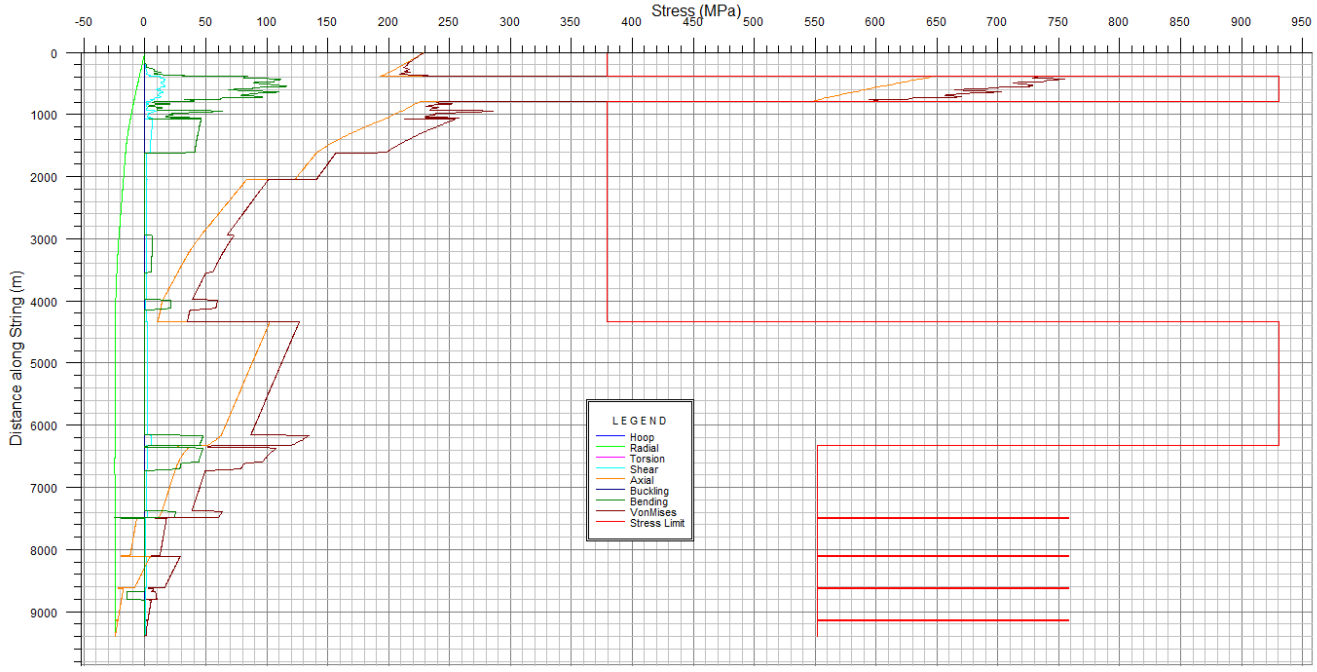

Figure E.23: Stress graph tripping out with 7” x 6 5/8” screen (Copy from WellPlan™).

Drilling 12 ¼" x 13 ½" hole – Composite Drill Pipe

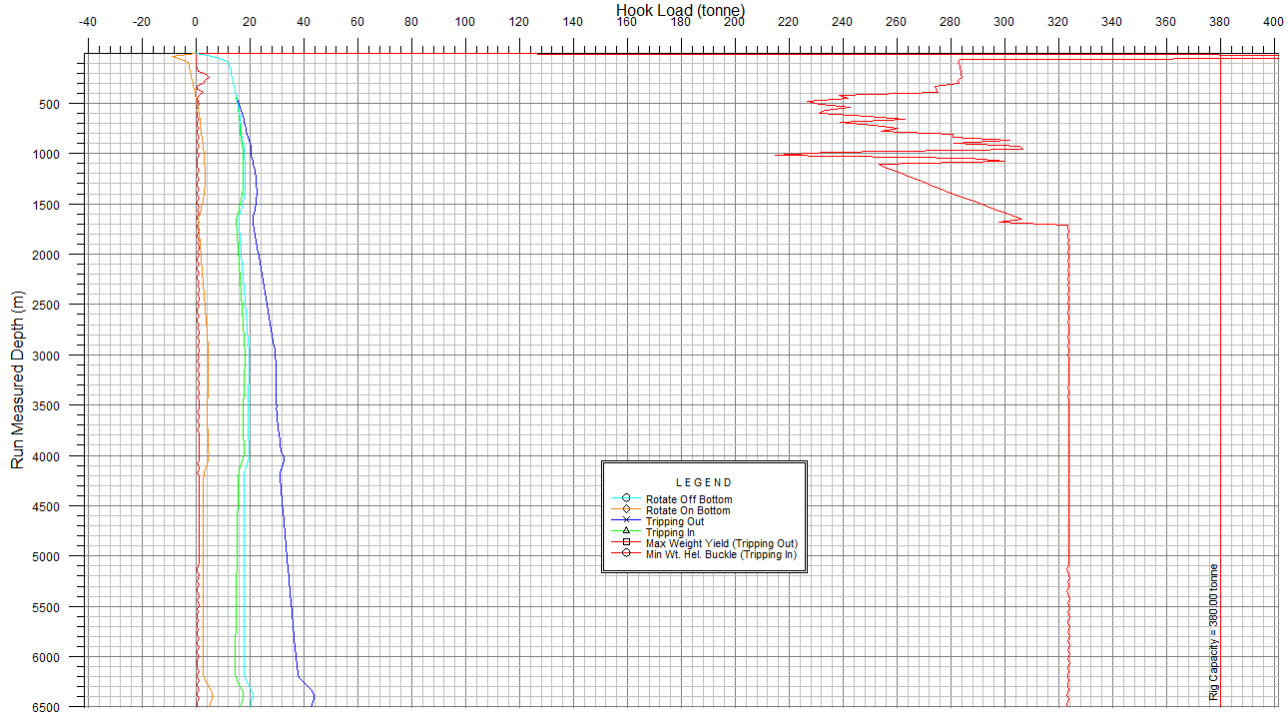

Figure E.24: Hook load drilling 12 ¼" x 13 ½" hole (Copy from WellPlan™).

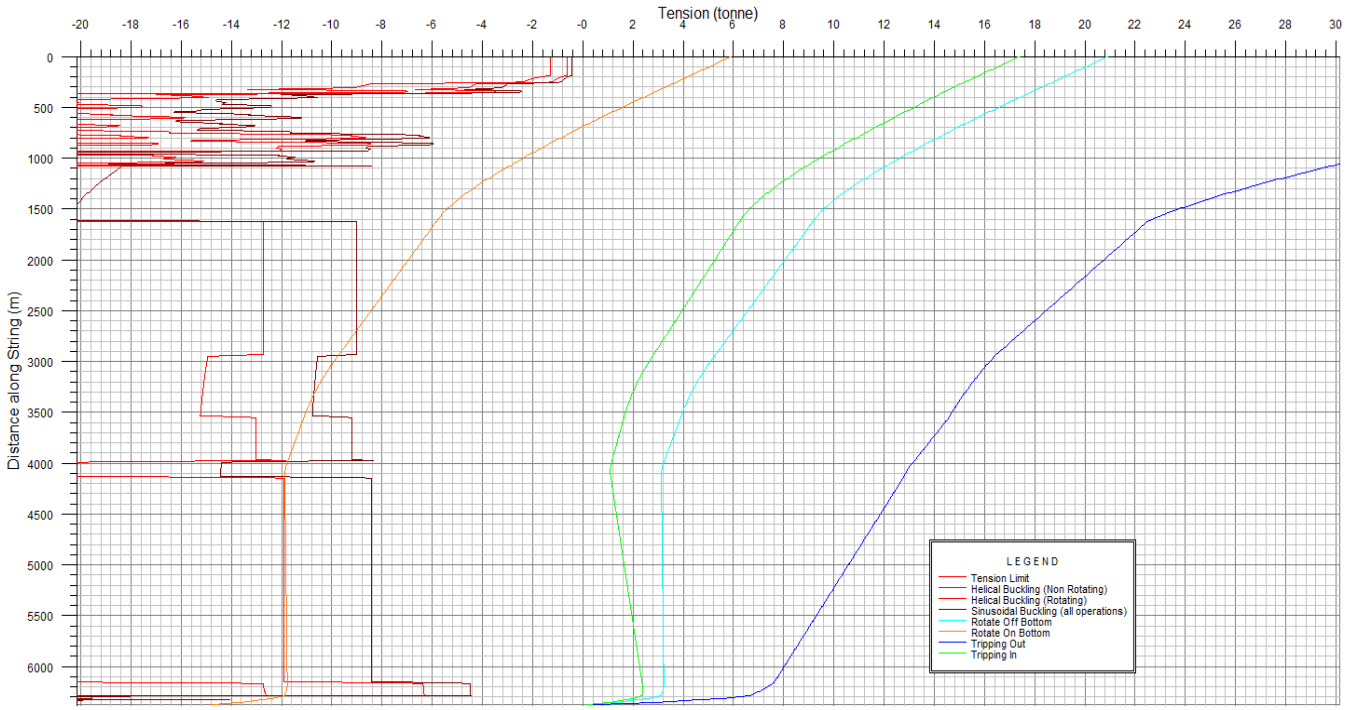

Figure E.25: Tension load drilling 12 ¼" x 13 ½" hole (Copy from WellPlan™).

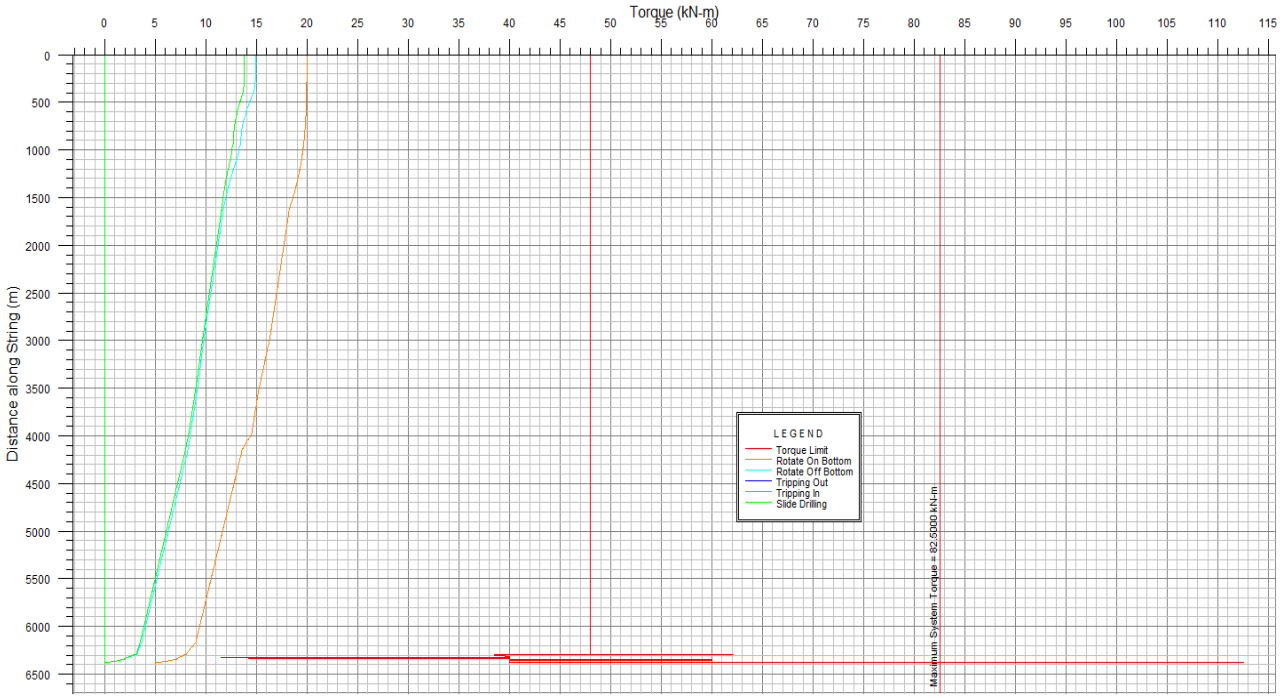

Figure E.26: Torque drilling 12 ¼" x 13 ½" hole (Copy from WellPlan™).

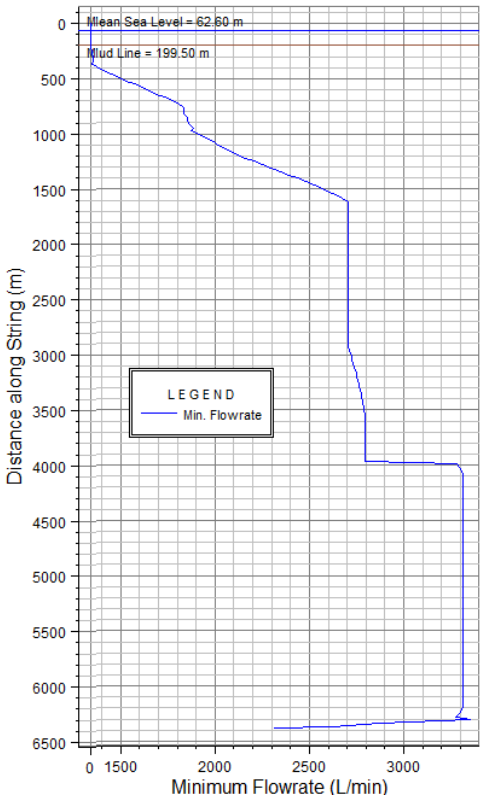

Figure E.27: Minimum flow rate drilling 12 ¼" x 13 ½" hole (Copy from WellPlan™).

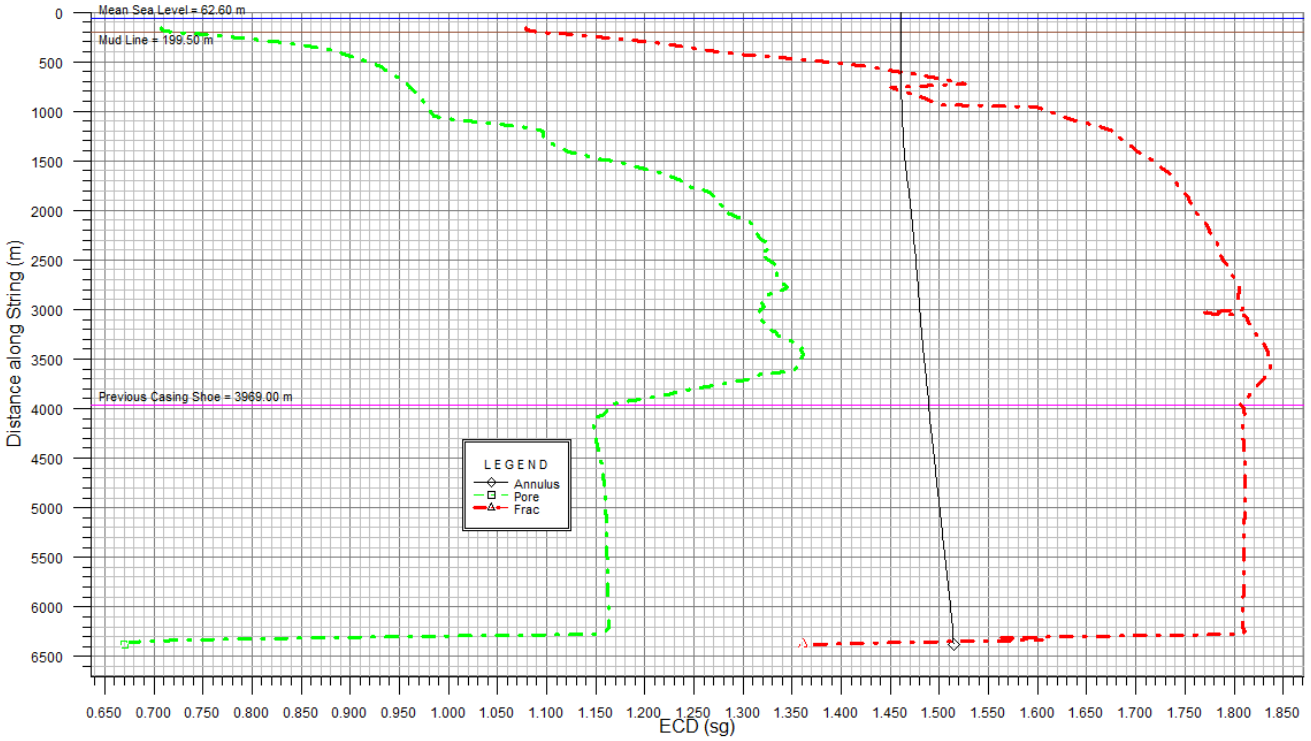

Figure E.28: ECD vs depth 12 ¼" x 13 ½" hole (Copy from WellPlan™).

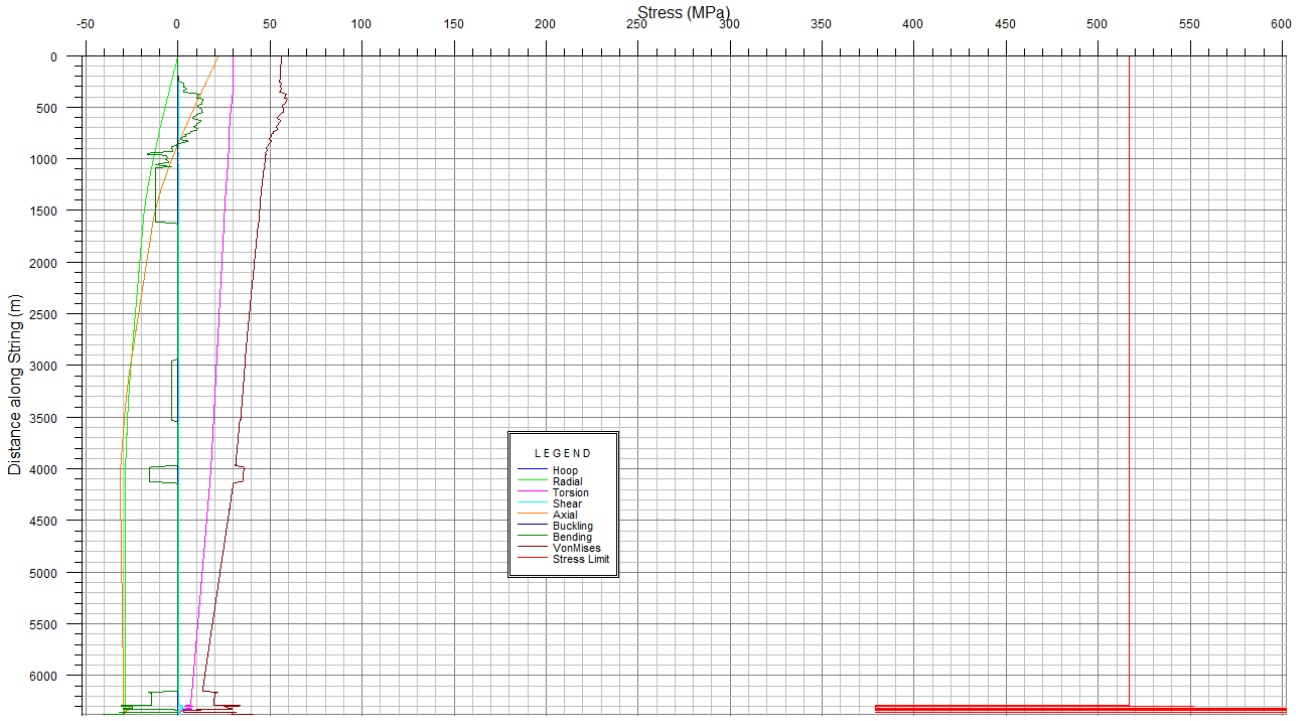

Figure E.29: Stress graph tripping in 12 ¼" x 13 ½" hole (Copy from WellPlan™).

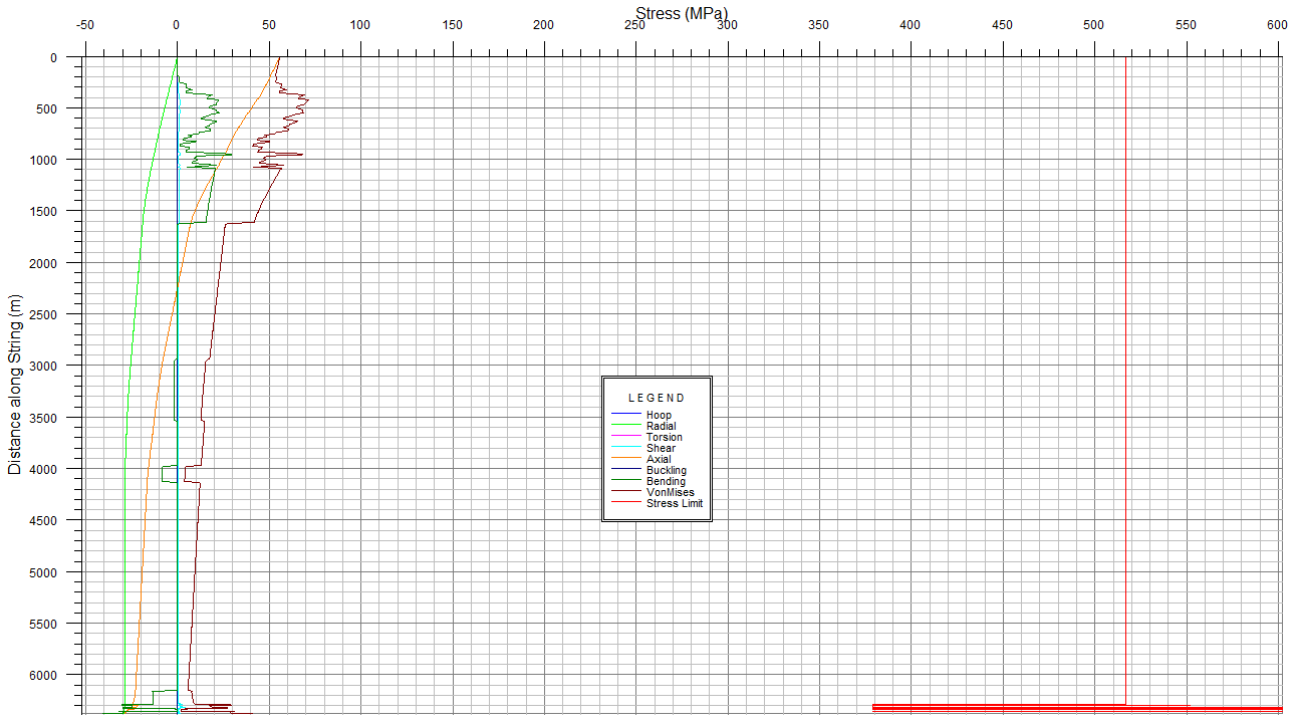

Figure E.30: Stress graph tripping out 12 ¼" x 13 ½" hole (Copy from WellPlan™).

Installing 10 ¾" Liner – Composite Drill Pipe

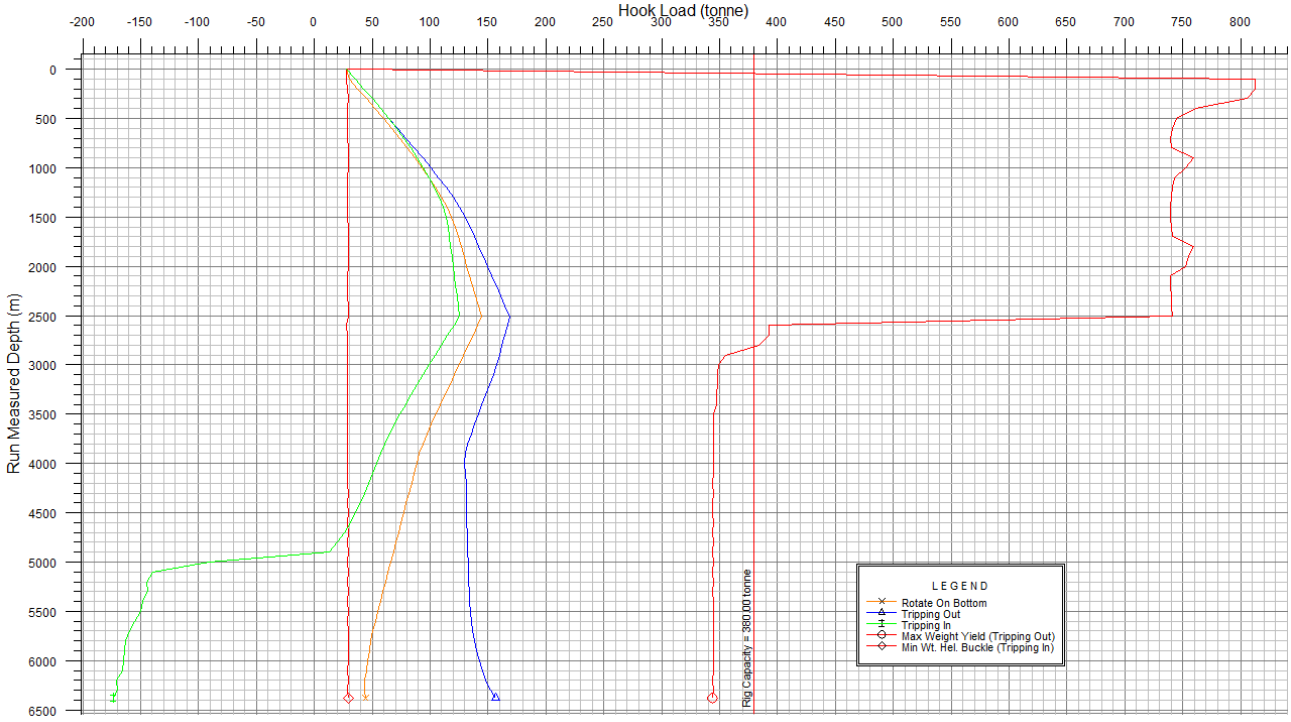

Figure E.31: Hook load 10 ¾" liner (Copy from WellPlan™).

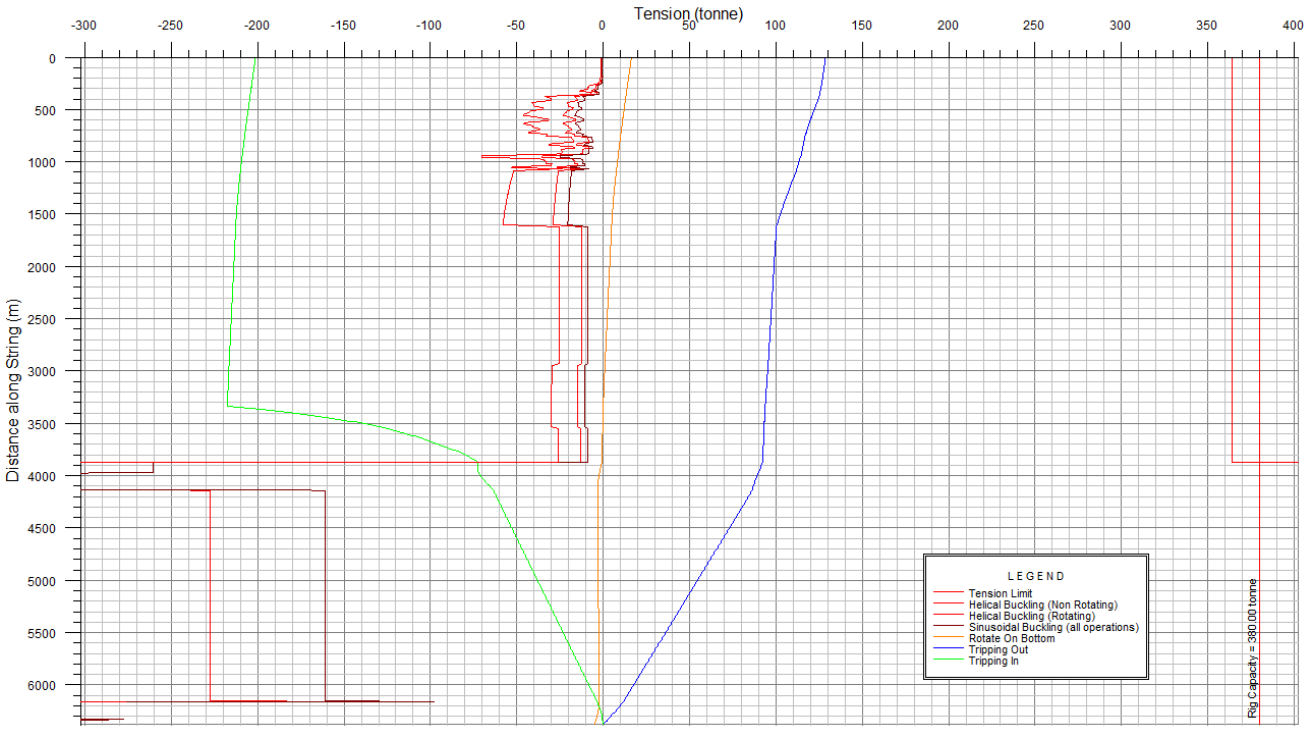

Figure E.32: Tension load 10 ¾" liner (Copy from WellPlan™).

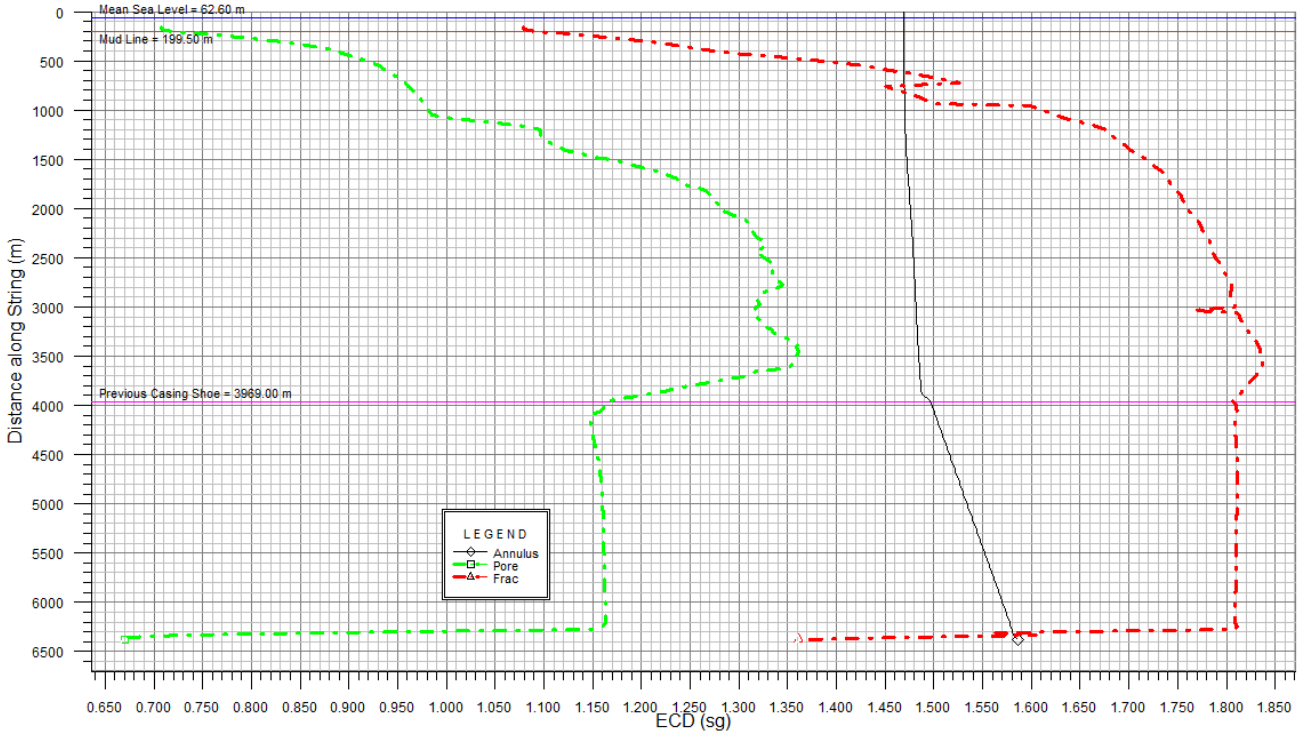

Figure E.33: ECD vs depth 10 ¾" liner (Copy from WellPlan™).

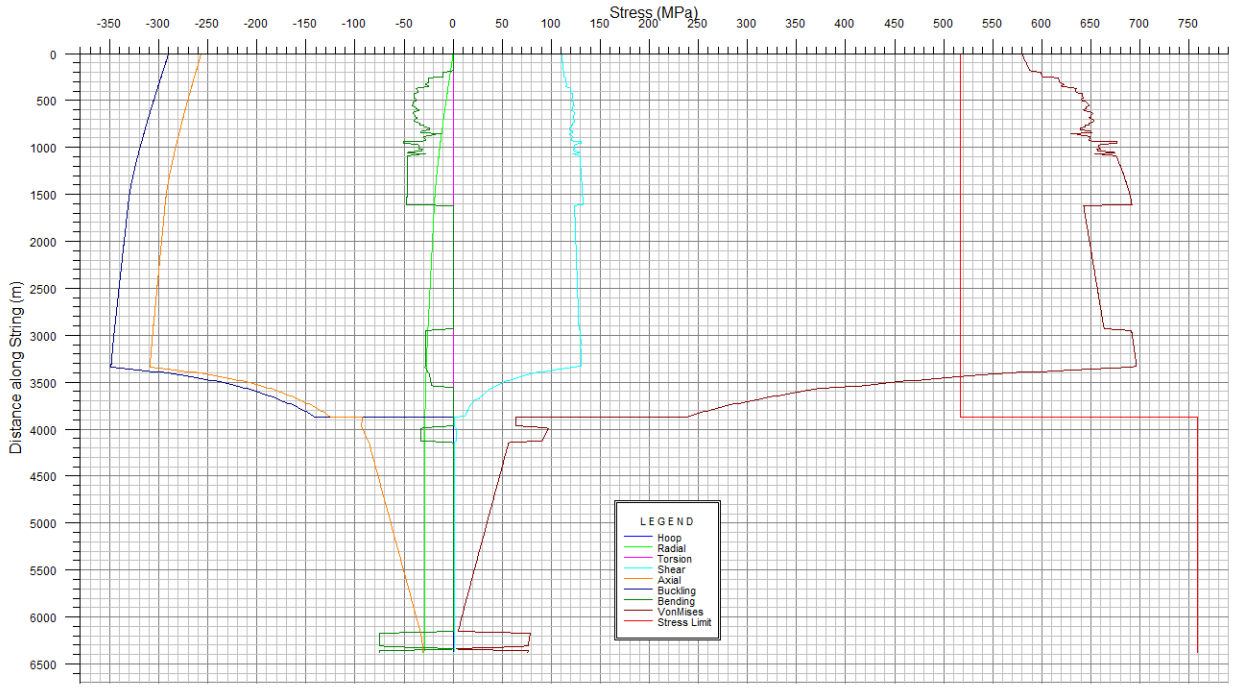

Figure E.34: Stress graph tripping in with 10 ¾" Liner (Copy from WellPlan™).

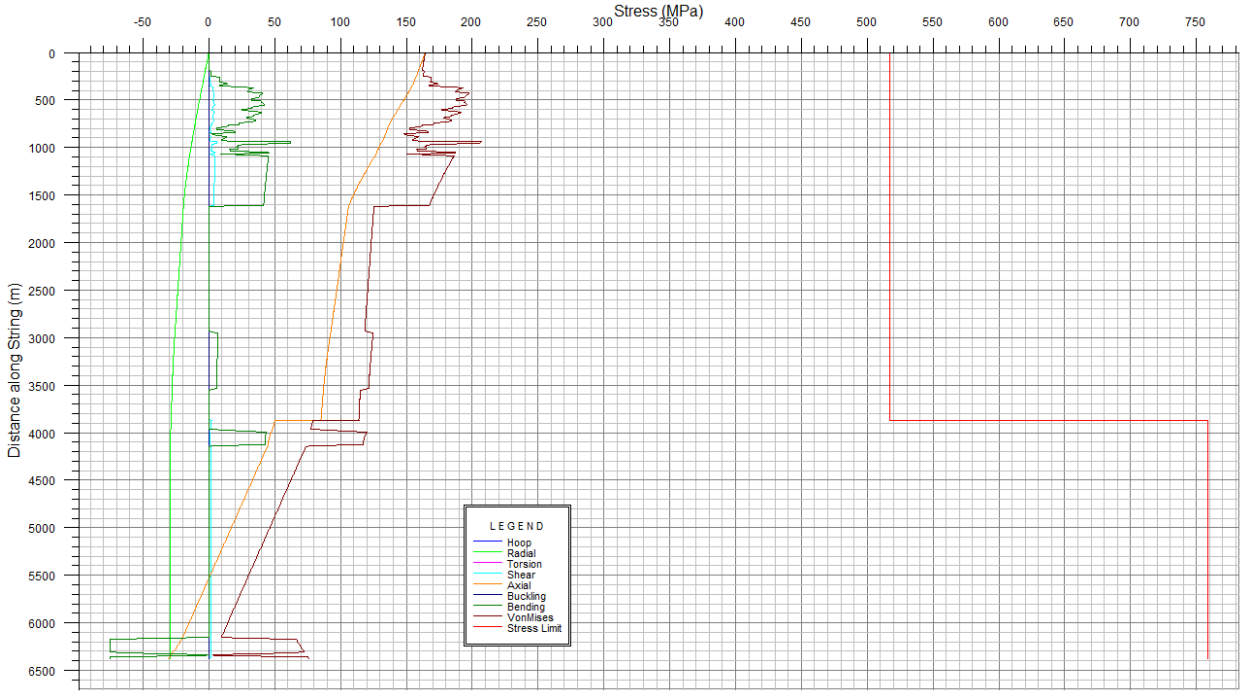

Figure E.35: Stress graph tripping out with 10 ¾" Liner (Copy from WellPlan™).

Drilling 8 ½" x 9 ½" hole – Composite Drill Pipe

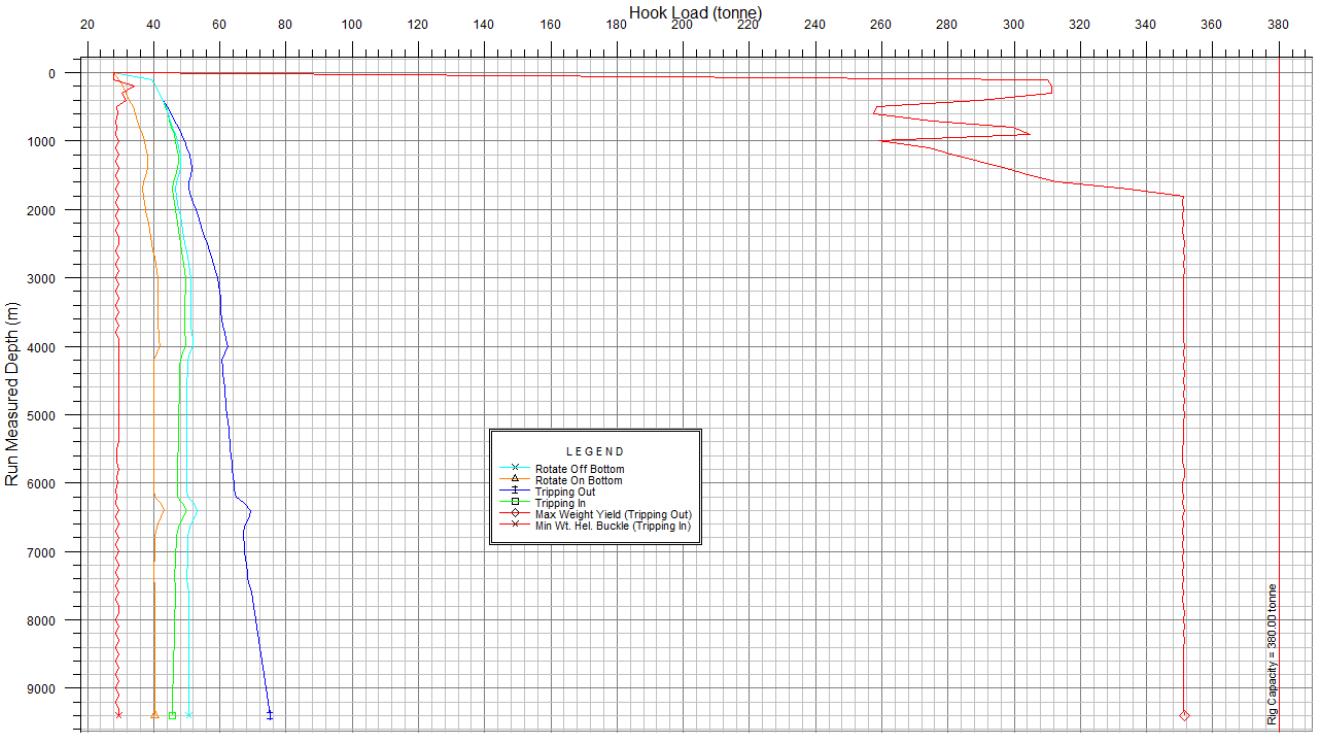

Figure E.36: Hook load drilling 8 ½" x 9 ½" hole (Copy from WellPlan™).

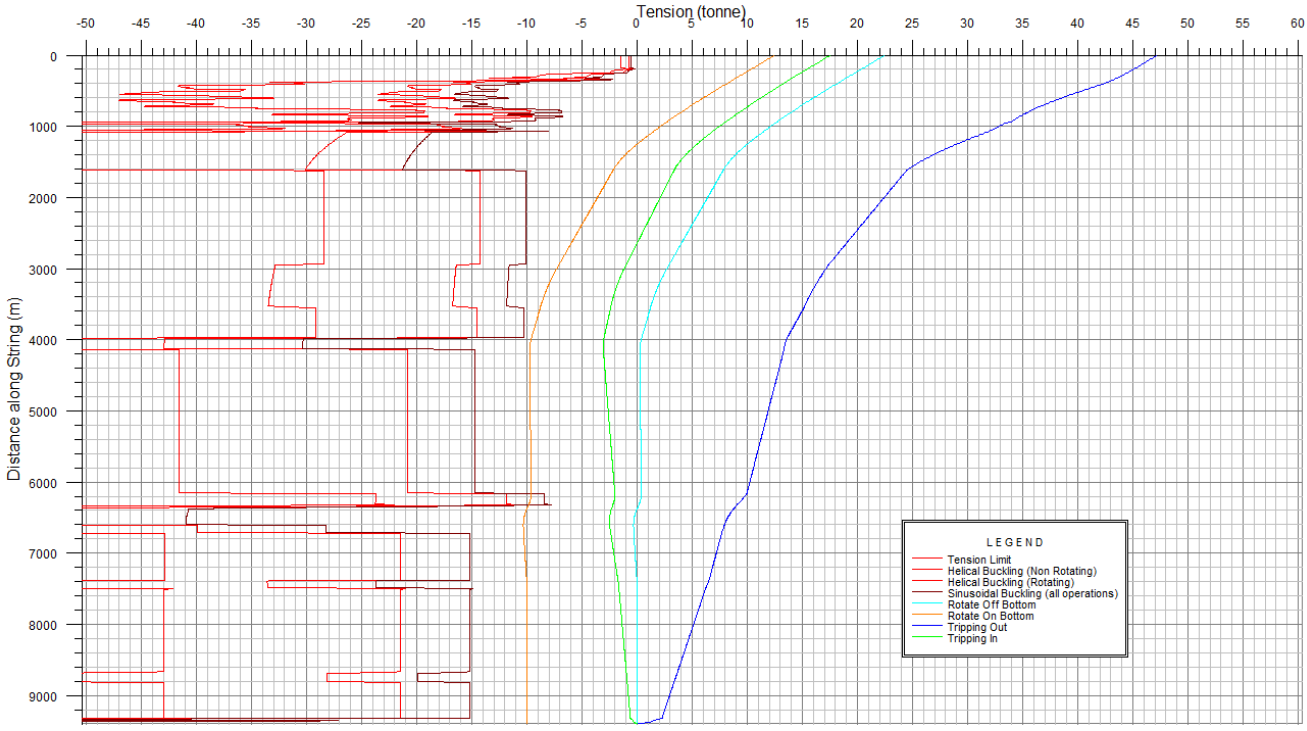

Figure E.37: Tension load drilling 8 ½" x 9 ½" hole (Copy from WellPlan™).

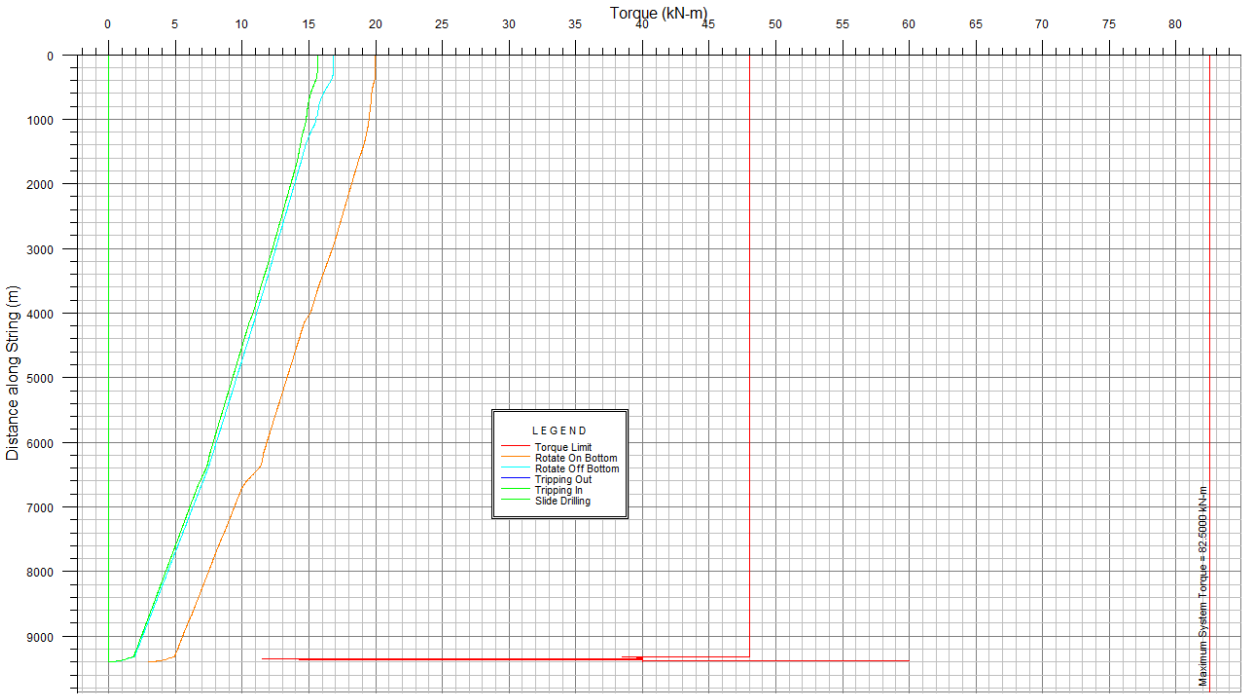

Figure E.38: Torque drilling 8 ½" x 9 ½" hole (Copy from WellPlan™).

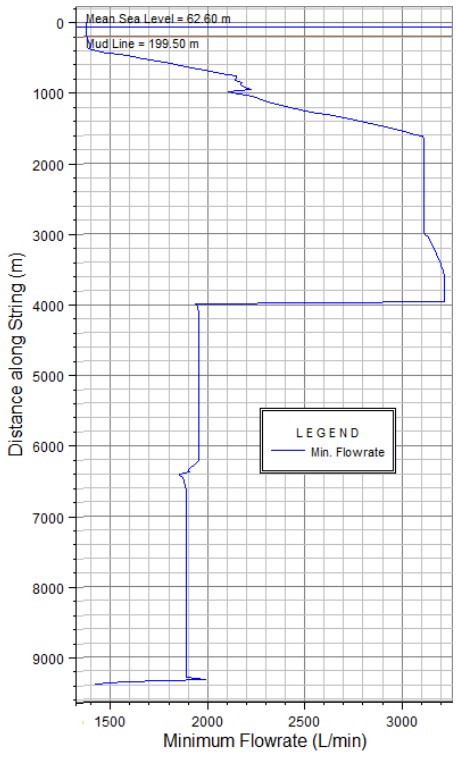

Figure E.39: Minimum flow rate drilling 8 ½" x 9 ½" hole (Copy from WellPlan™)

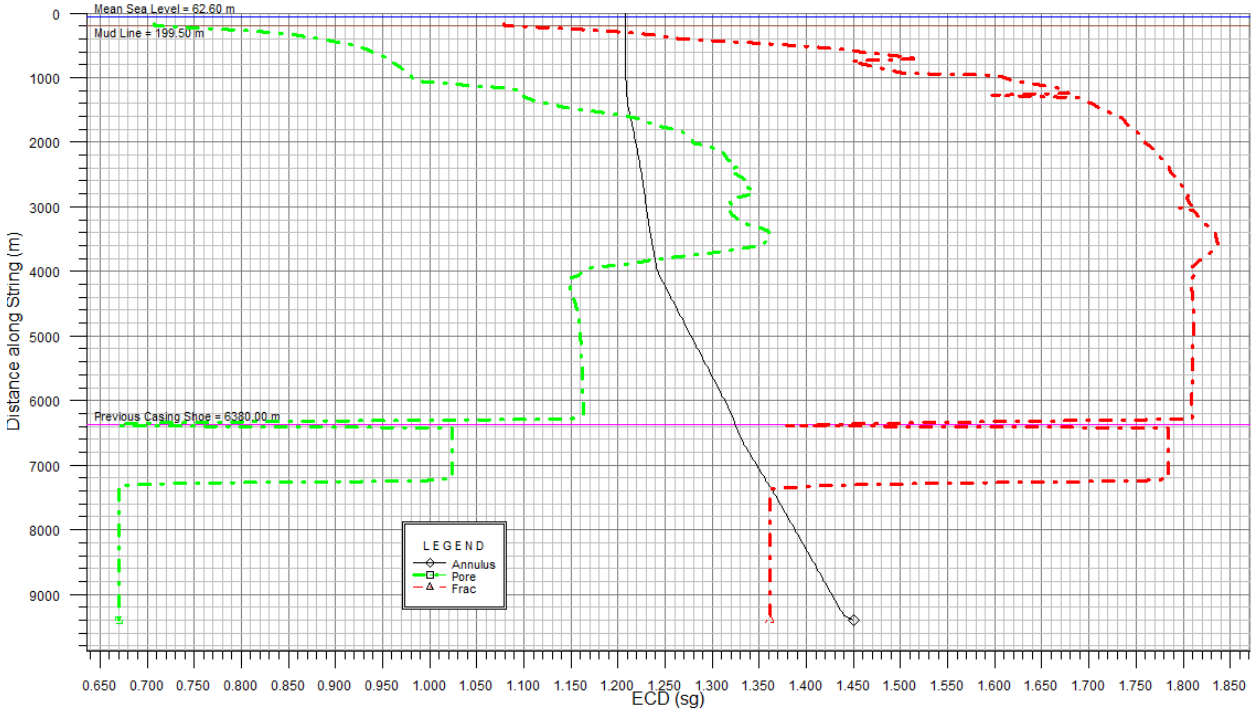

Figure E.40: ECD vs depth 8 ½" x 9 ½" hole (Copy from WellPlan™).

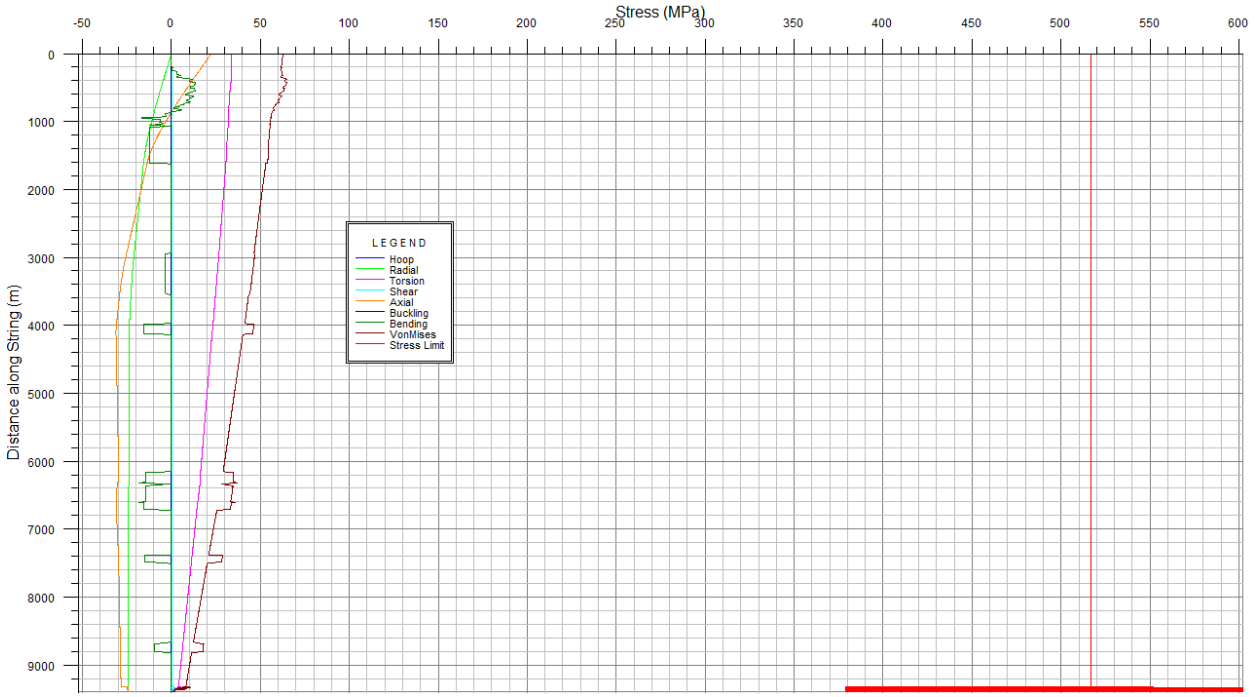

Figure E.41: Stress graph tripping in 8 ½" x 9 ½" hole (Copy from WellPlan™).

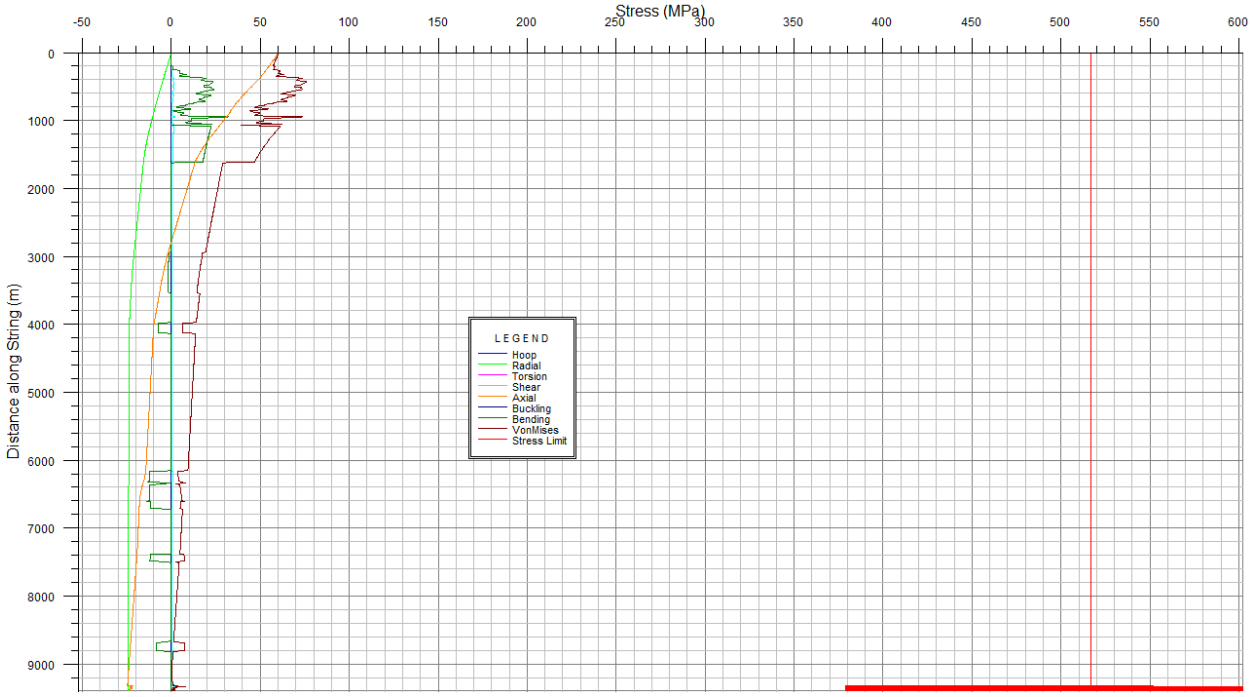

Figure E.42: Stress graph tripping out 8 ½" x 9 ½" hole (Copy from WellPlan™).

Installing 7" x 6 5/8" Liner - Composite Drill Pipe

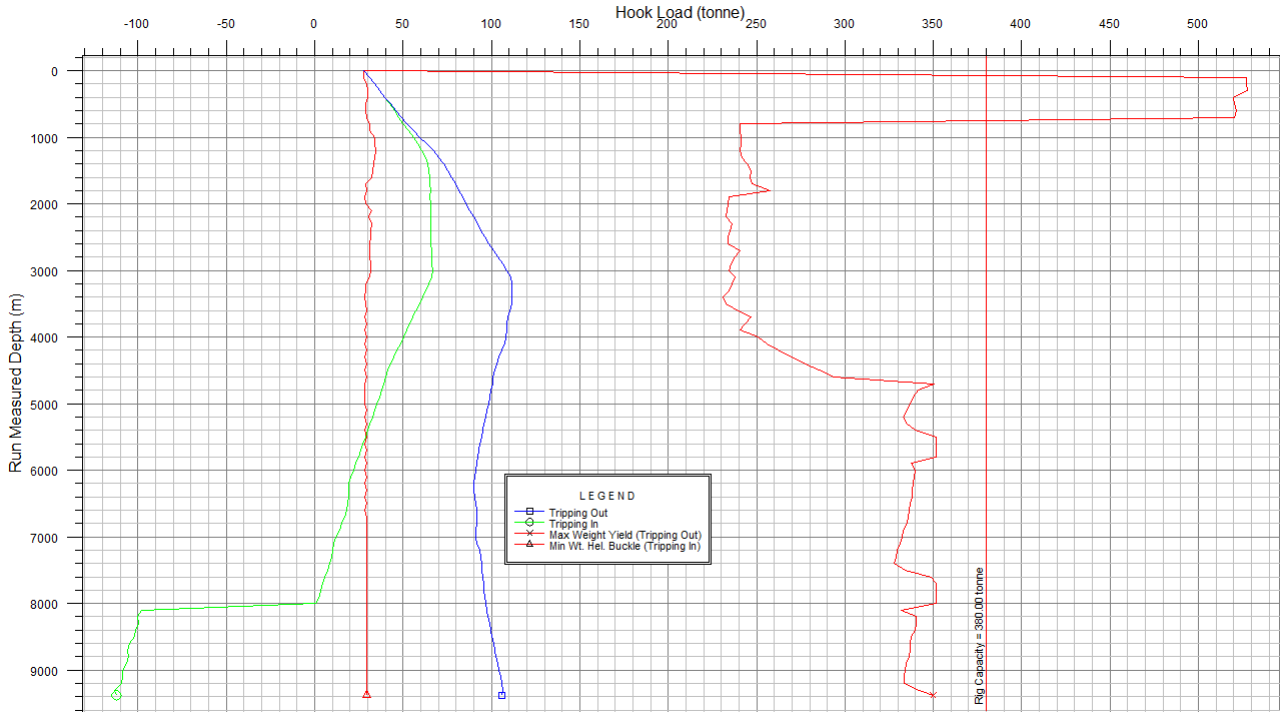

Figure E.43: Hook load 7" x 6 5/8" screen (Copy from WellPlan™).

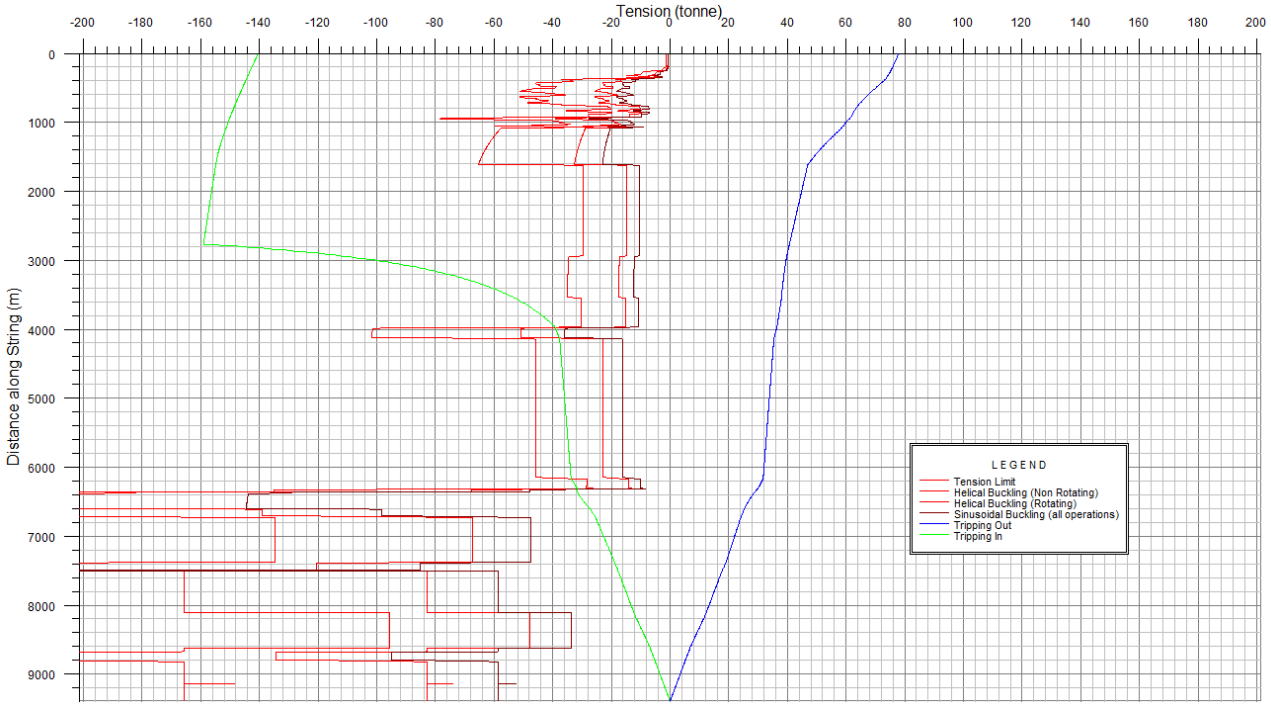

Figure E.44: Tension load 7” x 6 5/8” screen (Copy from WellPlan™).

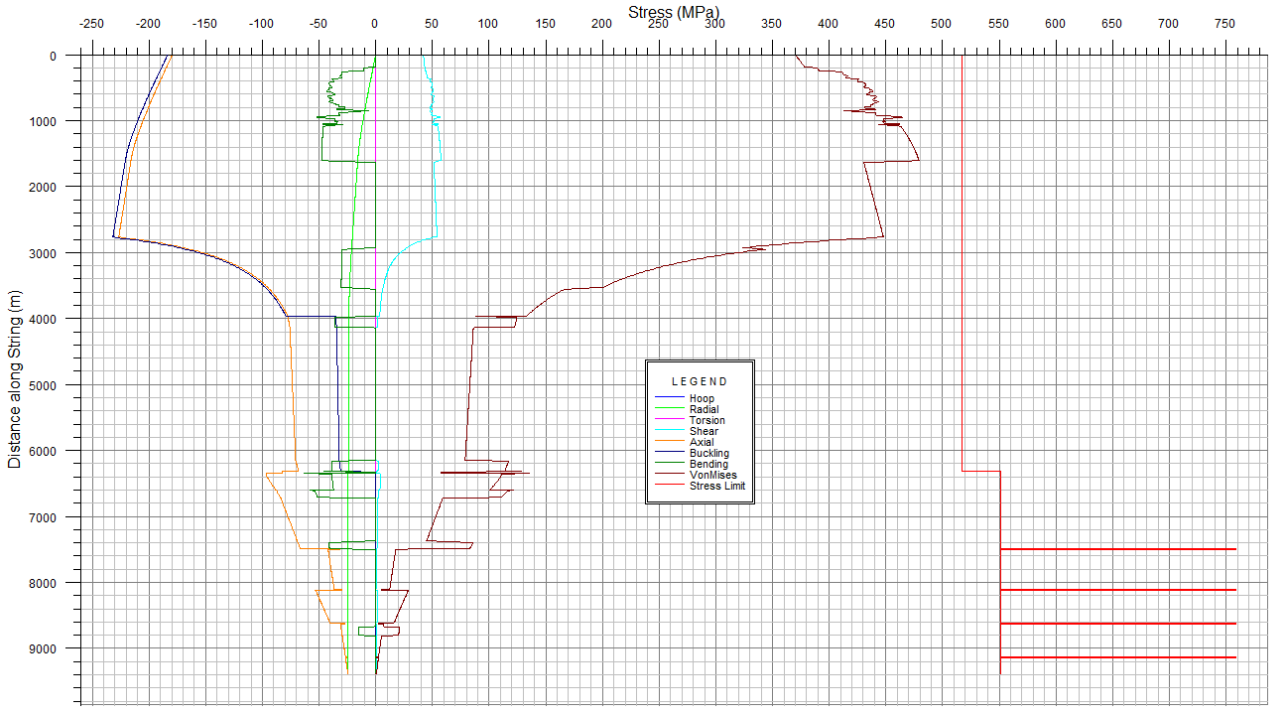

Figure E.45: Stress graph tripping in with 7” x 6 5/8” screen (Copy from WellPlan™).

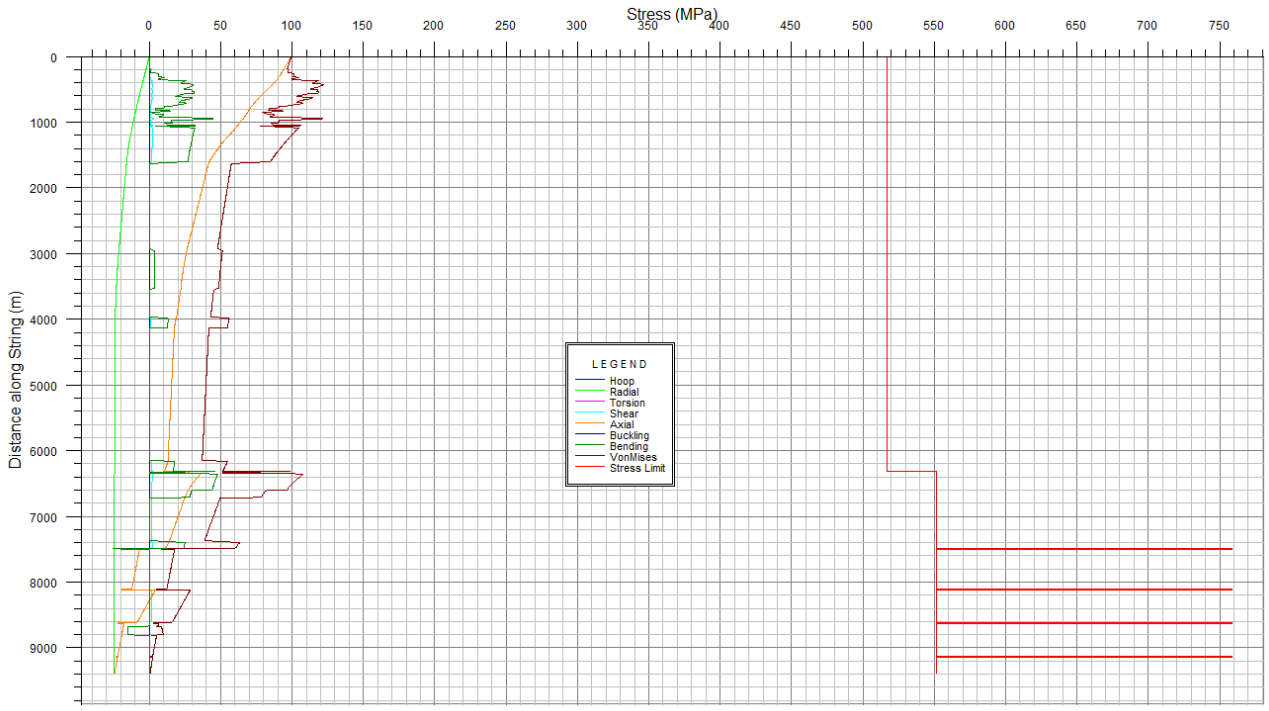

Figure E.46: Stress graph tripping out with 7” x 6 5/8” screen (Copy from WellPlan™).

Appendix F – Software

Wellplan™

Landmark's Wellplan™ software provides drilling and completion engineers a set of software tools that helps them create optimal well designs. Wellplan™ has a set of software tools that can be used to perform analysis, well planning, modelling and well operations. Using sophisticated engineering science and modelling, Wellplan™ helps engineers to analyze and improve well designs, reduce drilling problem and drill wells more efficiently (Landmark A).
In this thesis Wellplan™ was used for load analysis, torque and drag modelling, stress analysis and hydraulic modelling.